A Theoretical Study of Spectral Properties of Gamma-Ray Pulsars

Wang Yu

Co-workers: KS Cheng & Jumpei Takata

OUTLINE

- 1. Brief introduction of the magnetic pair creation controlled outer gap model
- 2. Two-layer model and the fitting of the phase-averaged spectra of the gamma-ray pulsars
- 3. Application of a 3-D model to fit the energy dependent light curves of Vela Pulsar

1. Introduction of magnetic pair creation controlled outer gap model

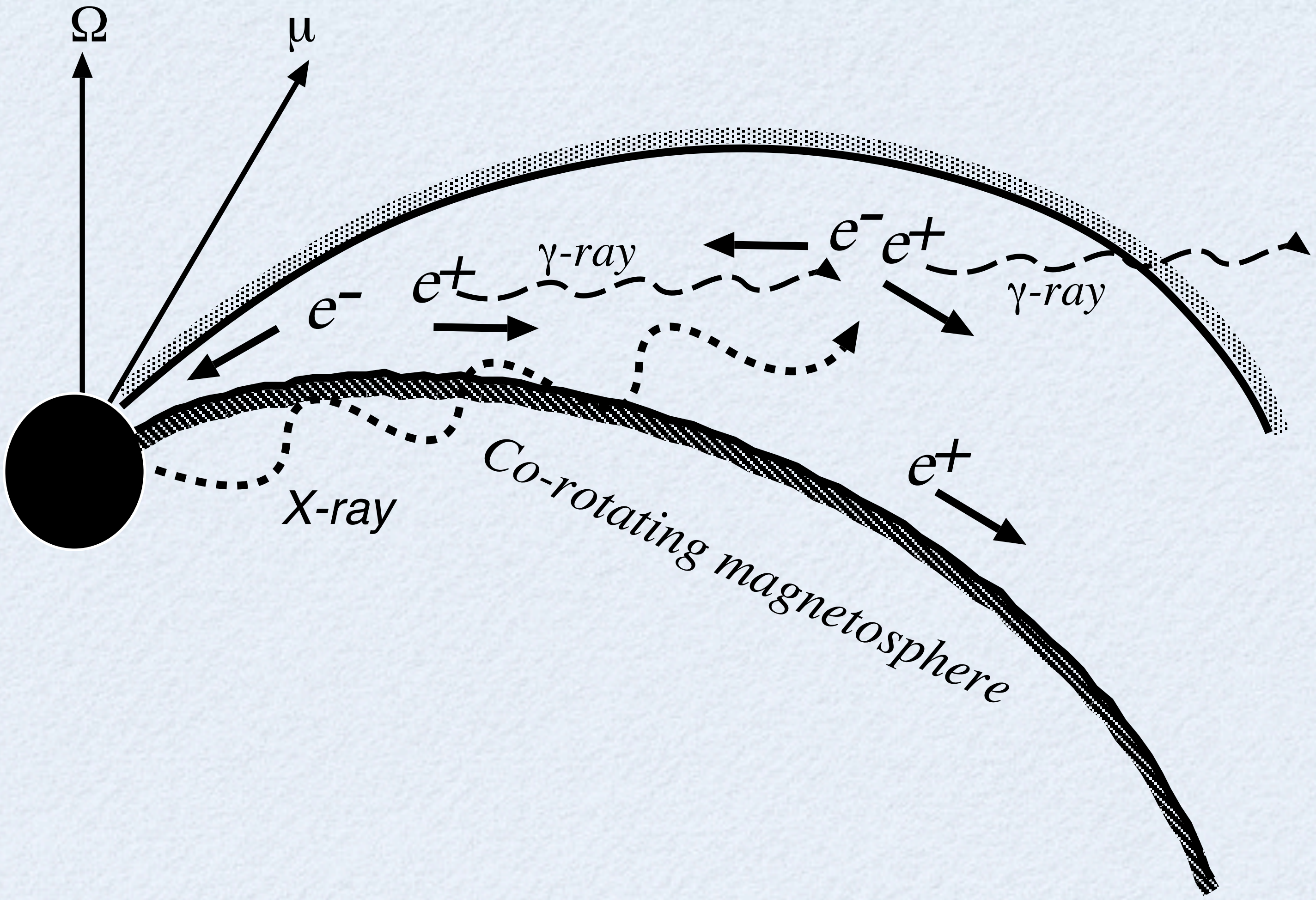

Magnetic pair creation:

$$\gamma + B \rightarrow e^{+} + e^{-}$$

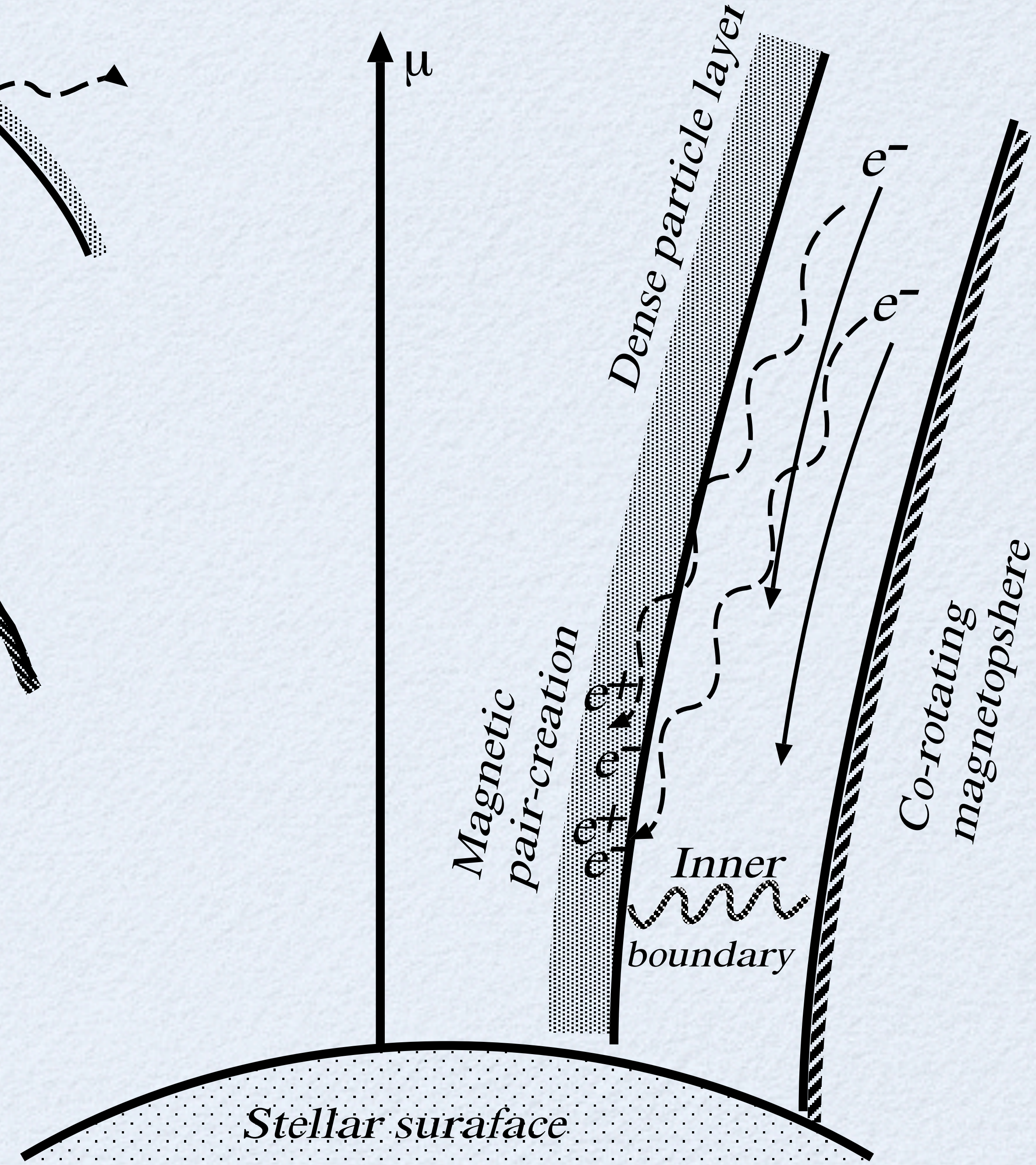

(Takata, Wang & Cheng, 2010)

1. Introduction of magnetic pair creation controlled outer gap model

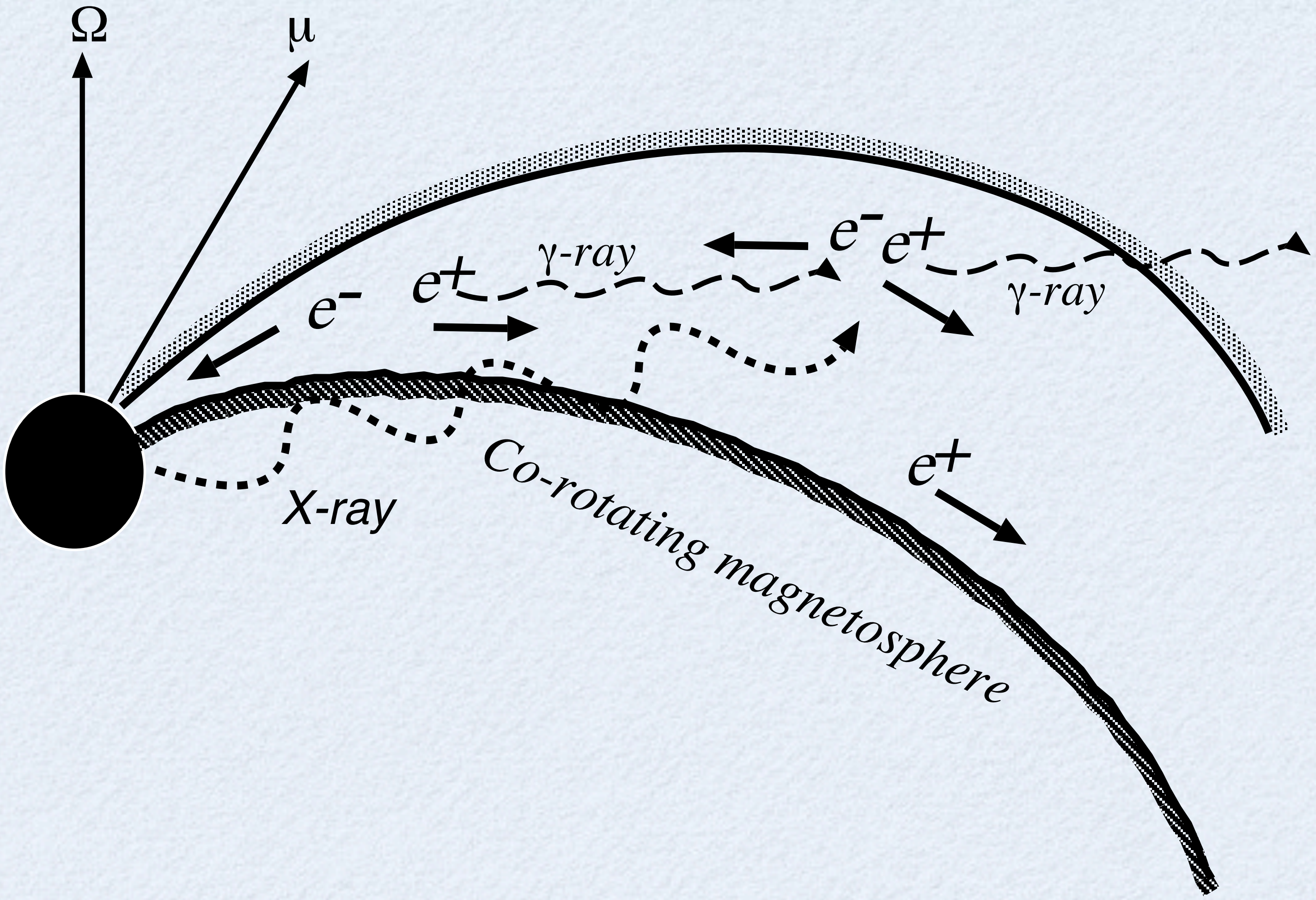

Magnetic pair creation:

$$\gamma + B \rightarrow e^{+} + e^{-}$$

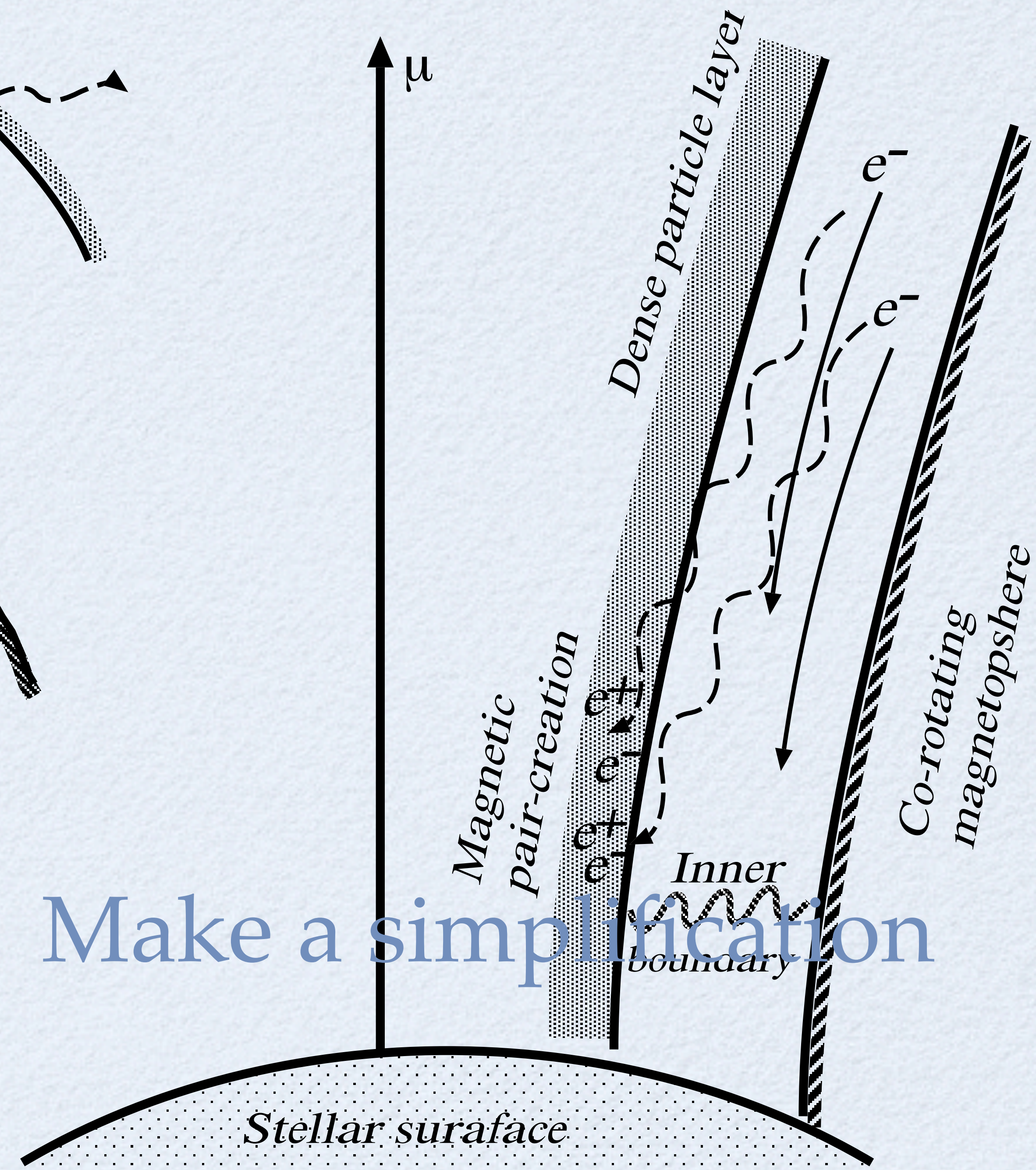

Make a simplification

(Takata, Wang & Cheng, 2010)

2. 2-Layer Model

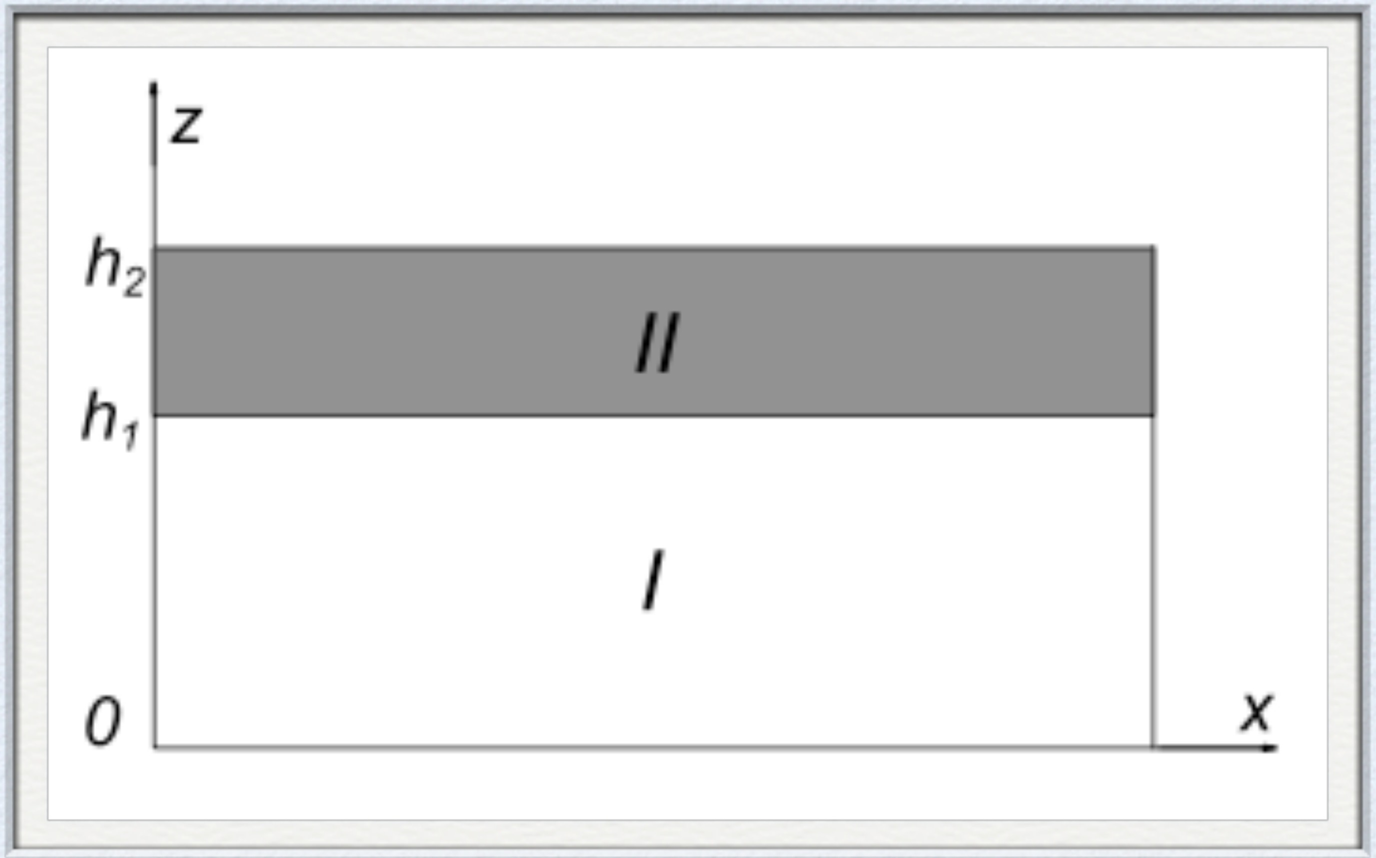

2. 2-Layer Model

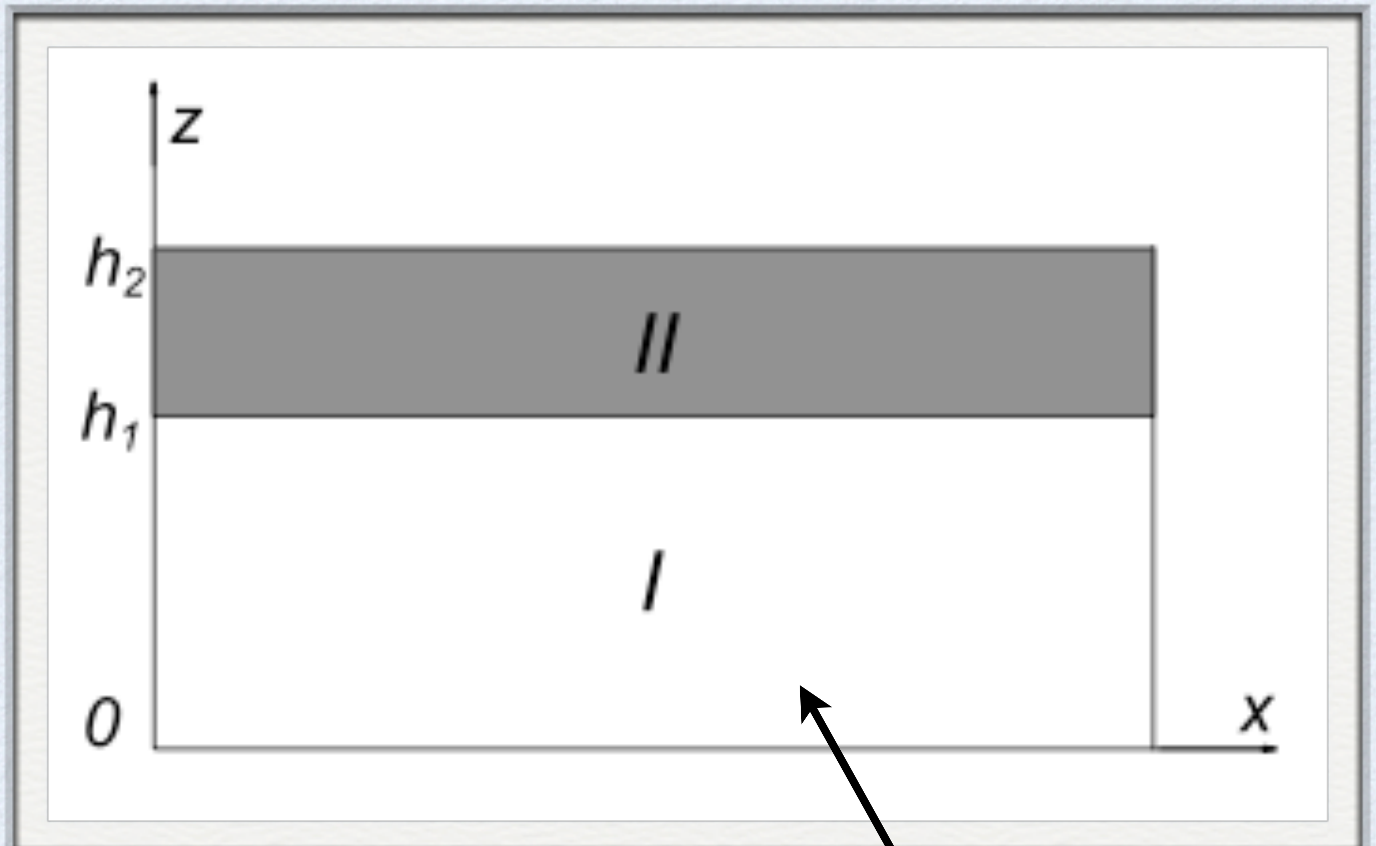

Main acceleration region

2. 2-Layer Model

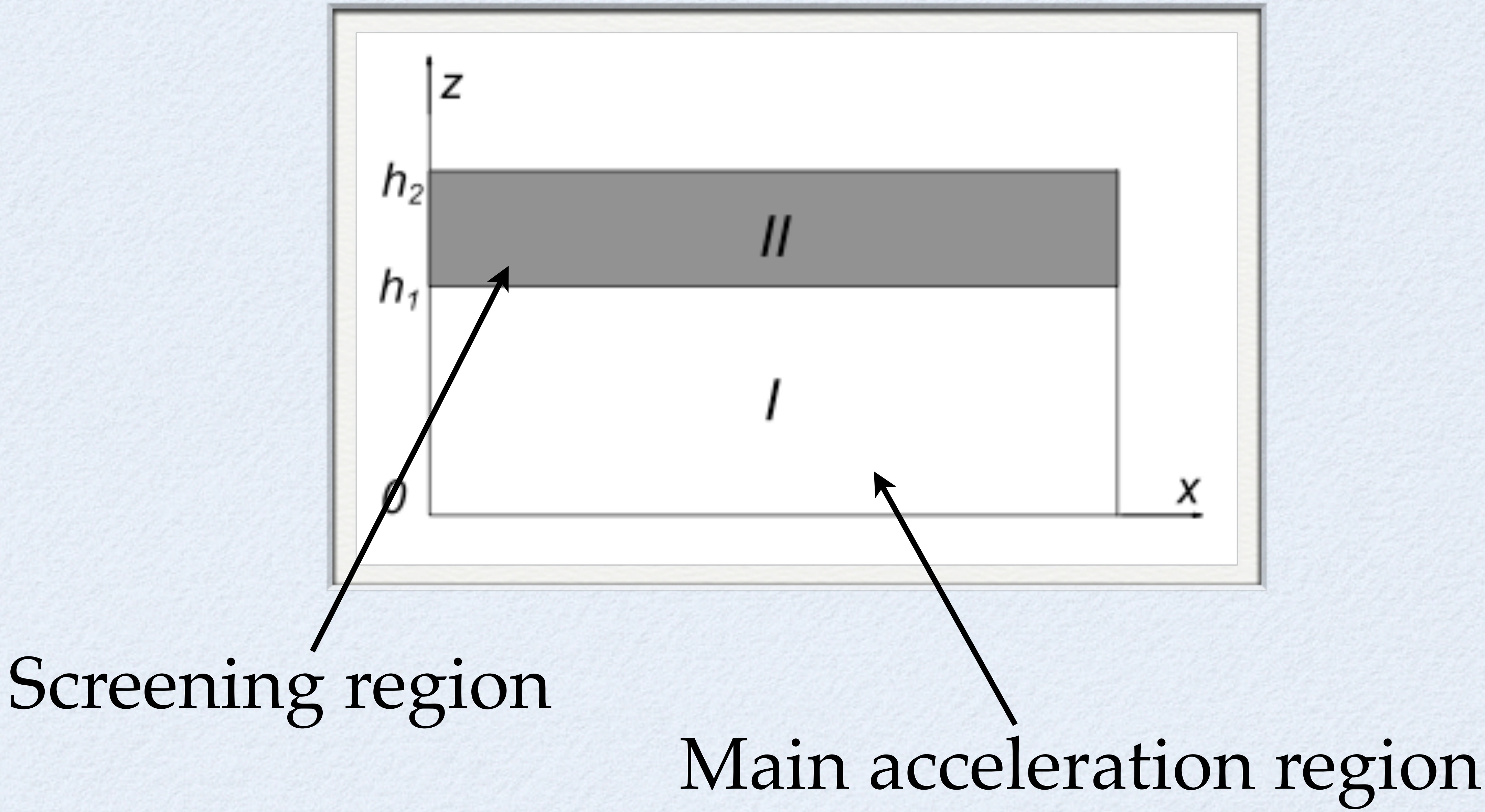

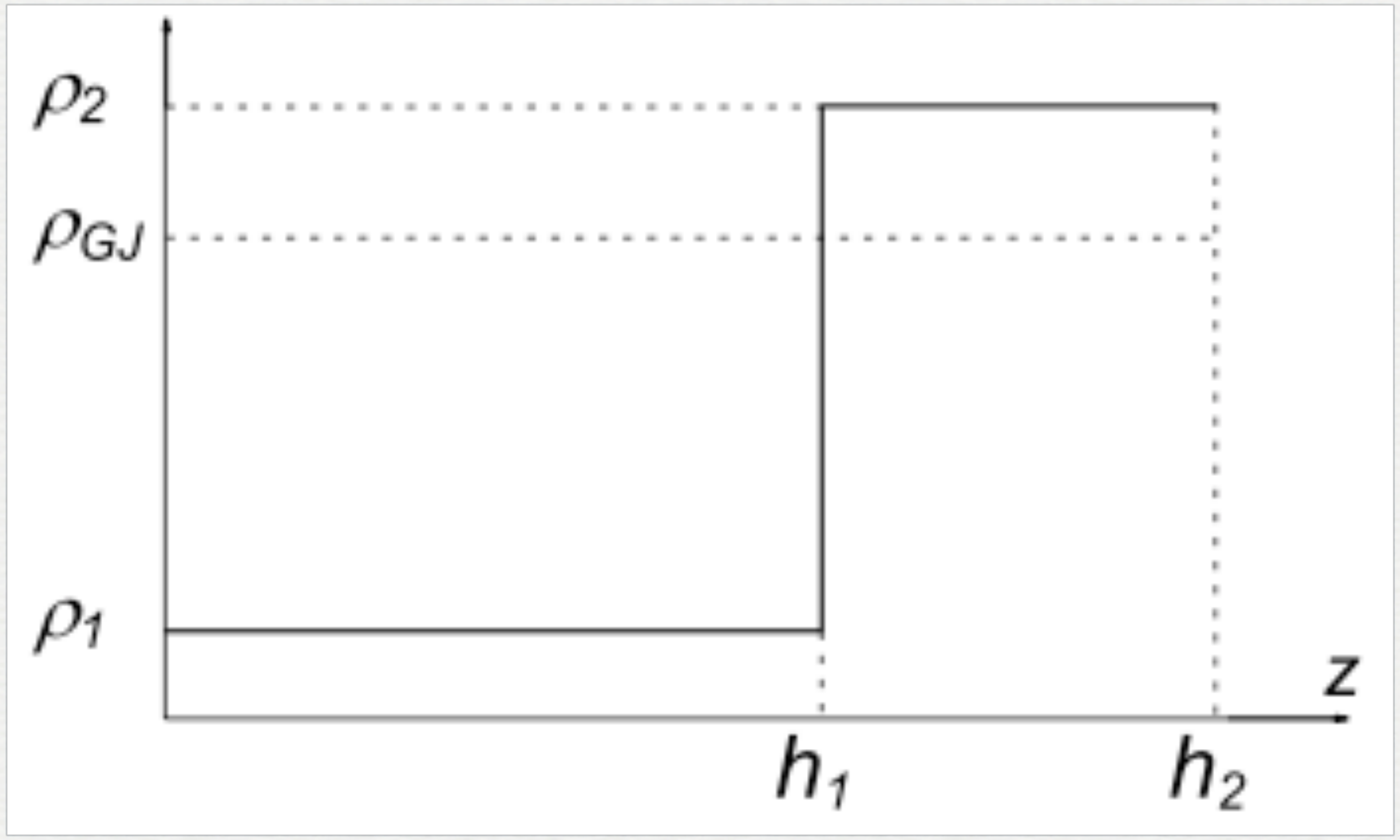

ρ_2
ρ_{GJ}
ρ_1
z
h_1
h_2

Poisson equation of Φ' in the simple 2-dimensional geometry

Poisson equation of Φ' in the simple 2-dimensional geometry

$$\left(\frac{\partial^2}{\partial x^2} + \frac{\partial^2}{\partial z^2}\right)\Phi' = -4\pi(\rho - \rho_{GJ})$$

Poisson equation of Φ' in the simple 2-dimensional geometry

$$\left(\frac{\partial^2}{\partial x^2}+\frac{\partial^2}{\partial z^2}\right)\Phi' = -4\pi(\rho-\rho_{GJ})$$

$$\rho-\rho_{GJ}\sim g(z)\rho_{GJ}(x)$$

Poisson equation of Φ' in the simple 2-dimensional geometry

$$\left(\frac{\partial^2}{\partial x^2} + \frac{\partial^2}{\partial z^2}\right)\Phi' = -4\pi(\rho - \rho_{GJ})$$

$$\rho - \rho_{GJ} \sim g(z)\rho_{GJ}(x) \longrightarrow \frac{\partial^2}{\partial z^2}\Phi'(x,z) = -4\pi\rho_{GJ}(x)g(z)$$

Poisson equation of Φ′ in the simple 2-dimensional geometry

$$\left(\frac{\partial^2}{\partial x^2}+\frac{\partial^2}{\partial z^2}\right)\Phi' = -4\pi(\rho-\rho_{GJ})$$

$$\rho-\rho_{GJ}\sim g(z)\rho_{GJ}(x) \longrightarrow \frac{\partial^2}{\partial z^2}\Phi'(x,z) = -4\pi\rho_{GJ}(x)g(z)$$

$$\Phi'(x,z)=\rho_{GJ}(x)\Phi'(z)$$

Poisson equation of Φ' in the simple 2-dimensional geometry

$$\left(\frac{\partial^2}{\partial x^2} + \frac{\partial^2}{\partial z^2}\right)\Phi' = -4\pi(\rho - \rho_{GJ})$$

$$\rho - \rho_{GJ} \sim g(z)\rho_{GJ}(x) \longrightarrow \frac{\partial^2}{\partial z^2}\Phi'(x,z) = -4\pi\rho_{GJ}(x)g(z)$$

$$\Phi'(x,z) = \rho_{GJ}(x)\Phi'(z) \longrightarrow \frac{\partial^2}{\partial z^2}\Phi'(z) = -4\pi g(z)$$

Poisson equation of Φ′ in the simple 2-dimensional geometry

$$\left(\frac{\partial^2}{\partial x^2}+\frac{\partial^2}{\partial z^2}\right)\Phi' = -4\pi(\rho-\rho_{GJ})$$

$$\rho-\rho_{GJ} \sim g(z)\rho_{GJ}(x) \longrightarrow \frac{\partial^2}{\partial z^2}\Phi'(x,z) = -4\pi\rho_{GJ}(x)g(z)$$

$$\Phi'(x,z) = \rho_{GJ}(x)\Phi'(z) \longrightarrow \frac{\partial^2}{\partial z^2}\Phi'(z) = -4\pi g(z)$$

$$\left\langle\frac{\rho-\rho_{GJ}}{\rho_{GJ}}\right\rangle = g(z) = \begin{cases} -g_1, & \text{if} \quad 0\le z\le h_1 \\ g_2, & \text{if} \quad h_1 < z \le h_2 \end{cases}$$

Boundary conditions

Boundary conditions

$\Phi'z(z=0)=0$, $\Phi'z(z=h2)=0$ and imposing
the continuity of the potential field $\Phi'z$ and $\partial\Phi'z/\partial z$ at the height h_1

Boundary conditions

$\Phi'z(z = 0) = 0$, $\Phi'z(z = h2) = 0$ and imposing
the continuity of the potential field $\Phi'z$ and $\partial\Phi'z/\partial z$ at the height h_1

$E\perp(z=h2)=0$,

Solution

$$\Phi'(z) = \begin{cases} \frac{4\pi g_1 z^2}{2} + C_1 z, & \text{for} \quad 0 \le z \le h_1 \\ -\frac{4\pi g_2 z^2}{2} + D_1 z + D_2, & \text{for} \quad h_1 \le z \le h_2 \end{cases},$$

$$C_1 = \frac{2\pi[h_1(h_1 - 2h_2)g_1 + (h_1 - h_2)^2 g_2]}{h_2}$$

$$D_1 = \frac{2\pi[h_2^2 g_2 + h_1^2(g_1 + g_2)]}{h_2}$$

$$D_2 = -2\pi h_1^2(g_1 + g_2)$$

$$(\frac{h_2}{h_1})^2 = 1 + g_1/g_2$$

$$E_{||}(z) = -\frac{\partial}{\partial x}\Phi'(x,z) \sim -\Phi'_z(z)\frac{\partial \rho_{GJ}(x)}{\partial x} \sim \frac{\Omega B(R_{lc})}{2\pi s c}\Phi'_z(z)$$

$$E_{||}(z) = -\frac{\partial}{\partial x}\Phi'(x,z) \sim -\Phi'_z(z)\frac{\partial \rho_{GJ}(x)}{\partial x} \sim \frac{\Omega B(R_{lc})}{2\pi s c}\Phi'_z(z)$$

$$eE_{||}(z)c = l_{cur}(z)$$

$$E_{||}(z) = -\frac{\partial}{\partial x}\Phi'(x,z) \sim -\Phi'_z(z)\frac{\partial \rho_{GJ}(x)}{\partial x} \sim \frac{\Omega B(R_{lc})}{2\pi s c}\Phi'_z(z)$$

$$eE_{||}(z)c = l_{cur}(z)$$

$$l_{cur}(z) = 2e^2 c\gamma_e^4(z)/3s^2$$

is the power of the curvature radiation

$$E_{||}(z) = -\frac{\partial}{\partial x}\Phi'(x,z) \sim -\Phi'_z(z)\frac{\partial \rho_{GJ}(x)}{\partial x} \sim \frac{\Omega B(R_{lc})}{2\pi s c}\Phi'_z(z)$$

$$eE_{||}(z)c = l_{cur}(z)$$

$$l_{cur}(z) = 2e^2 c\gamma_e^4(z)/3s^2$$

is the power of the curvature radiation

$$\gamma_e(z) = \left[\frac{3}{2}\frac{s^2}{e}E_{||}(z)\right]^{1/4}$$

The shape of the spectrum can be determined by the current in the main acceleration region, the size of the main acceleration, and the thickness of the gap.

The effect of $1 - g_1, h_1/h_2, f$ on the shape of the spectrum

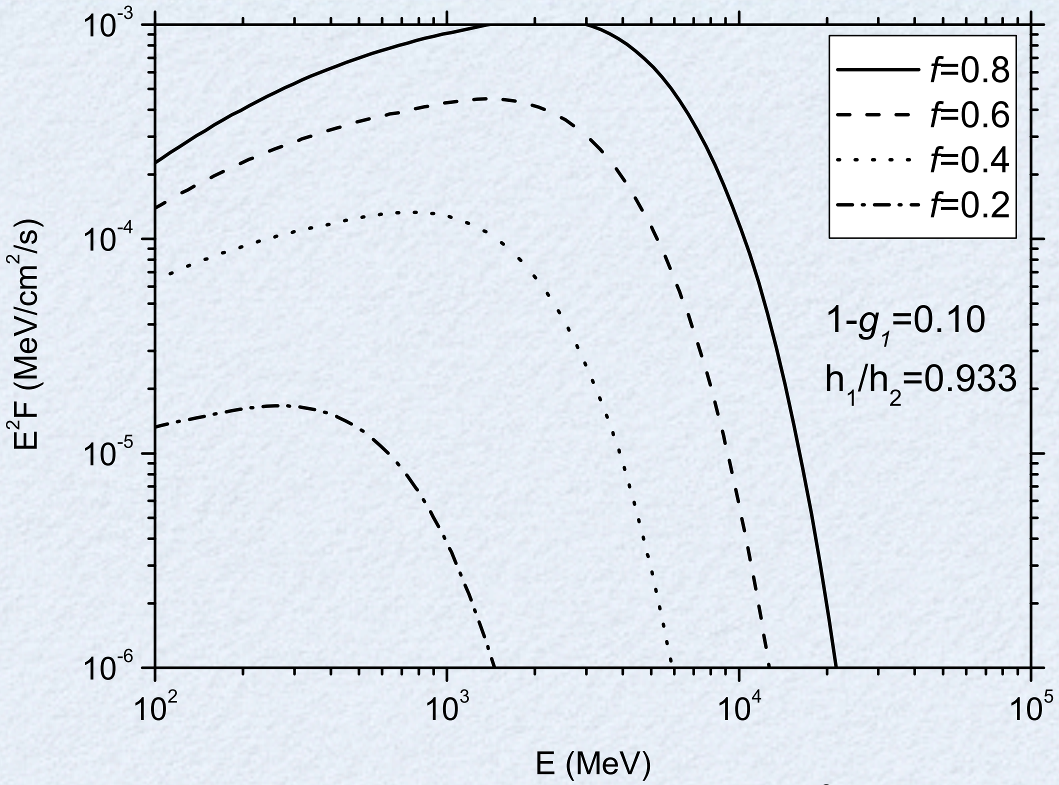

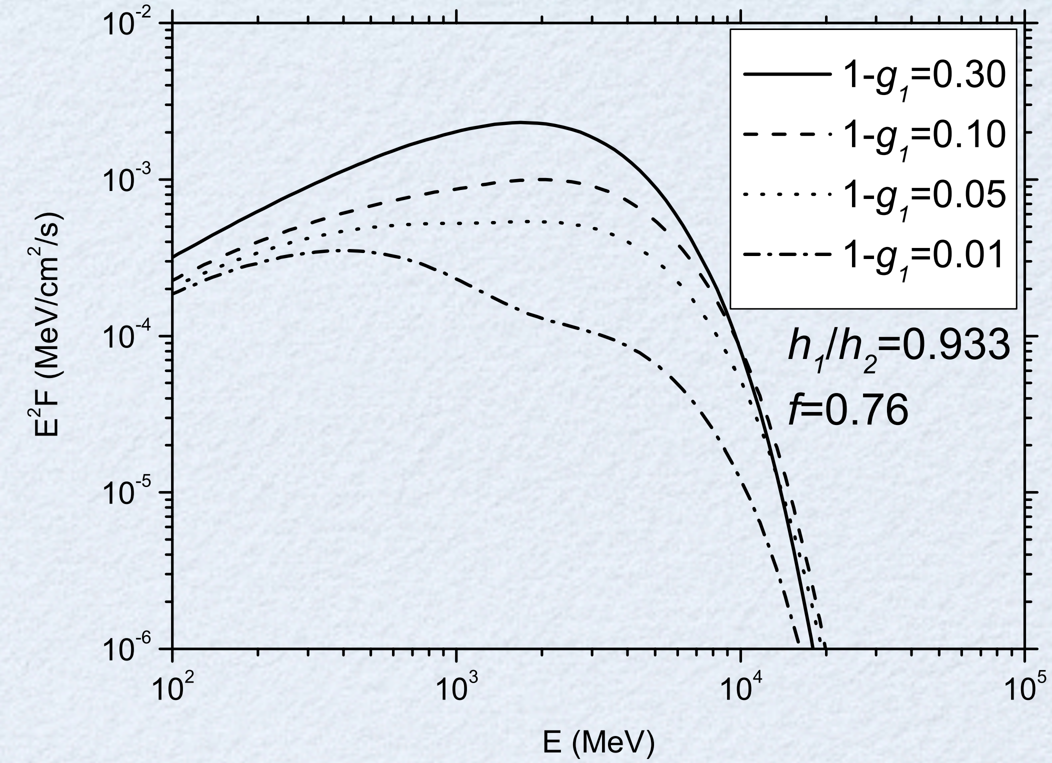

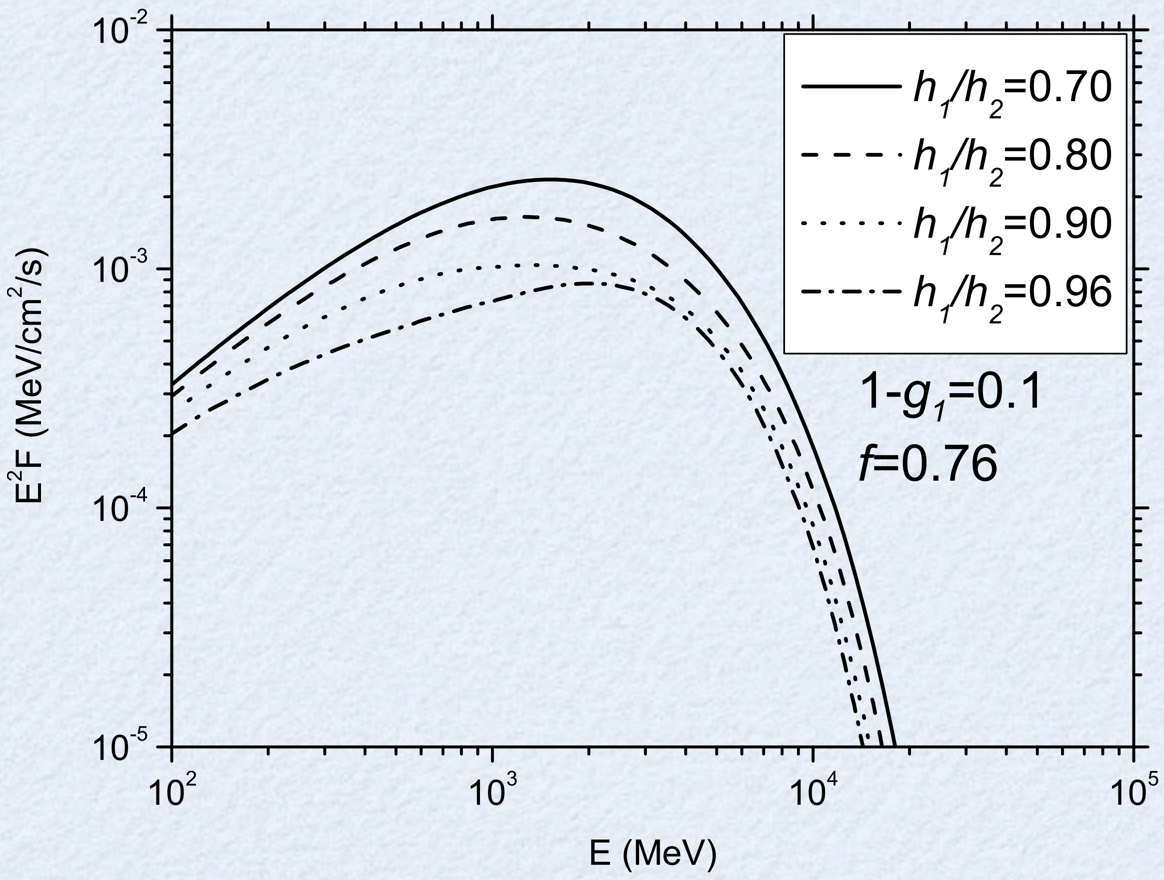

model result

1. canonical pulsars

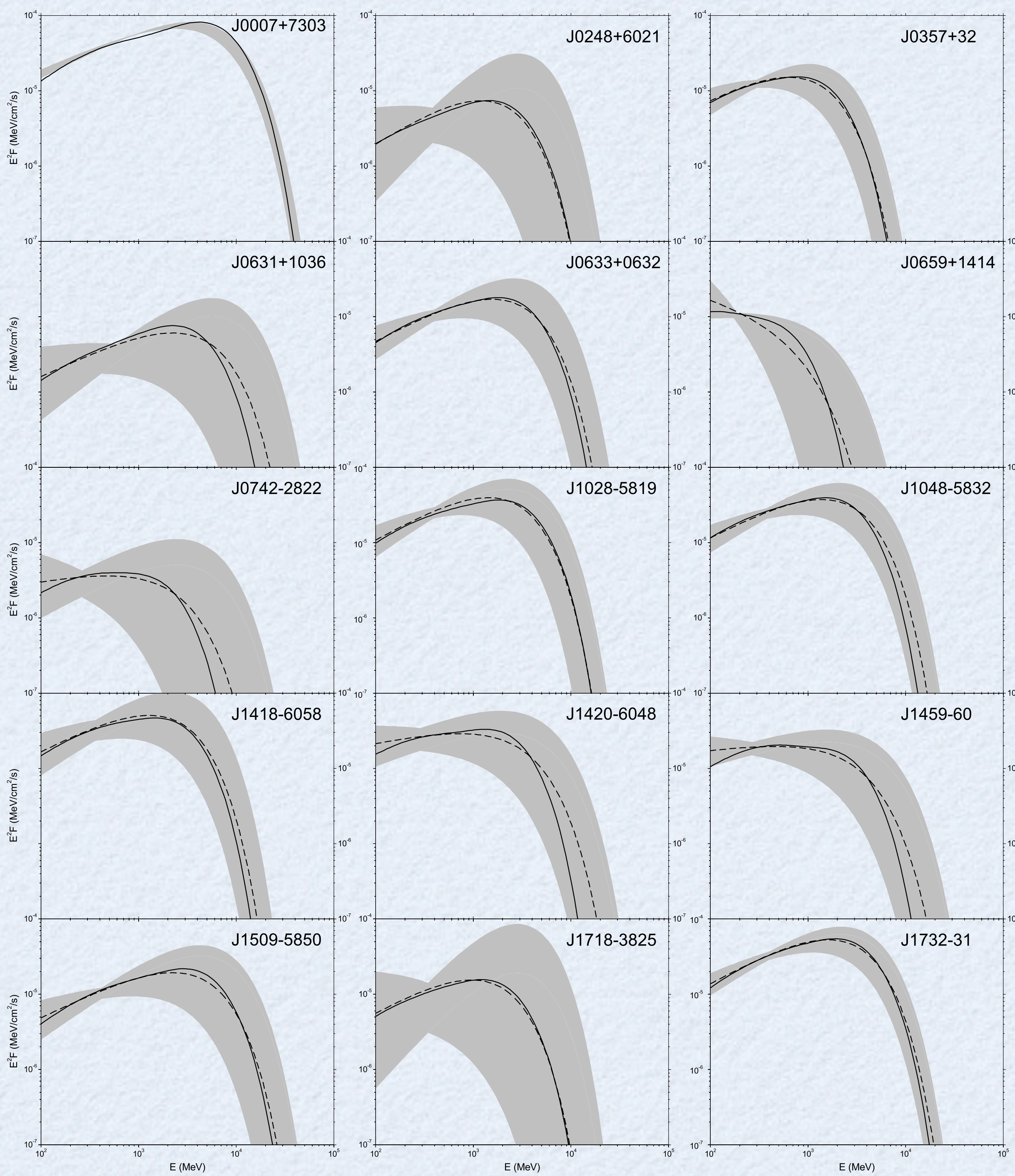

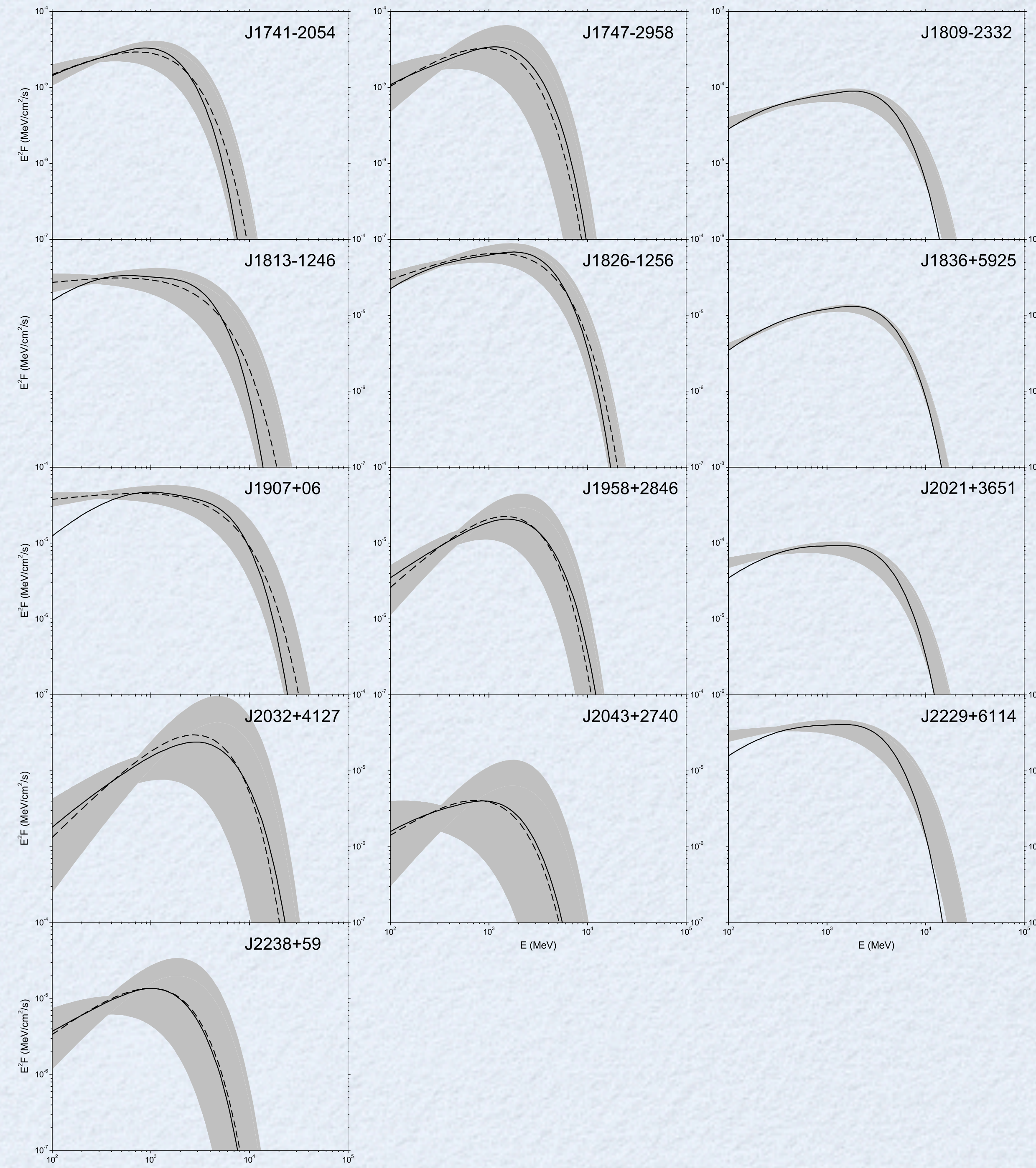

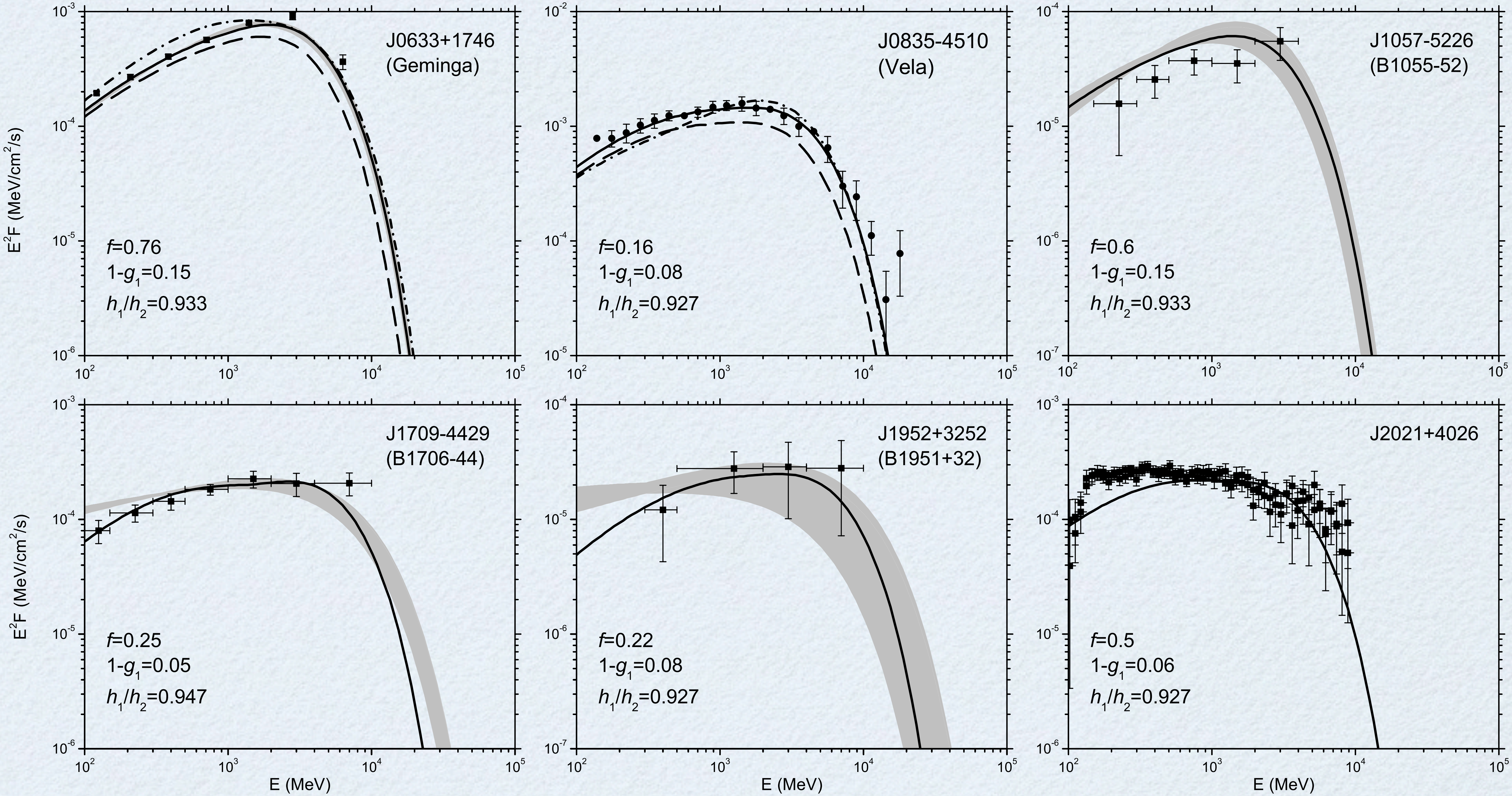

J0633+1746
(Geminga)
f=0.76
1-g1=0.15
h1/h2=0.933
J0835-4510
(Vela)
f=0.16
1-g1=0.08
h1/h2=0.927
J1057-5226
(B1055-52)
f=0.6
1-g1=0.15
h1/h2=0.933
J1709-4429
(B1706-44)
f=0.25
1-g1=0.05
h1/h2=0.947
J1952+3252
(B1951+32)
f=0.22
1-g1=0.08
h1/h2=0.927
J2021+4026
f=0.5
1-g1=0.06
h1/h2=0.927
E2F (MeV/cm2/s)
E (MeV)

2. MSP

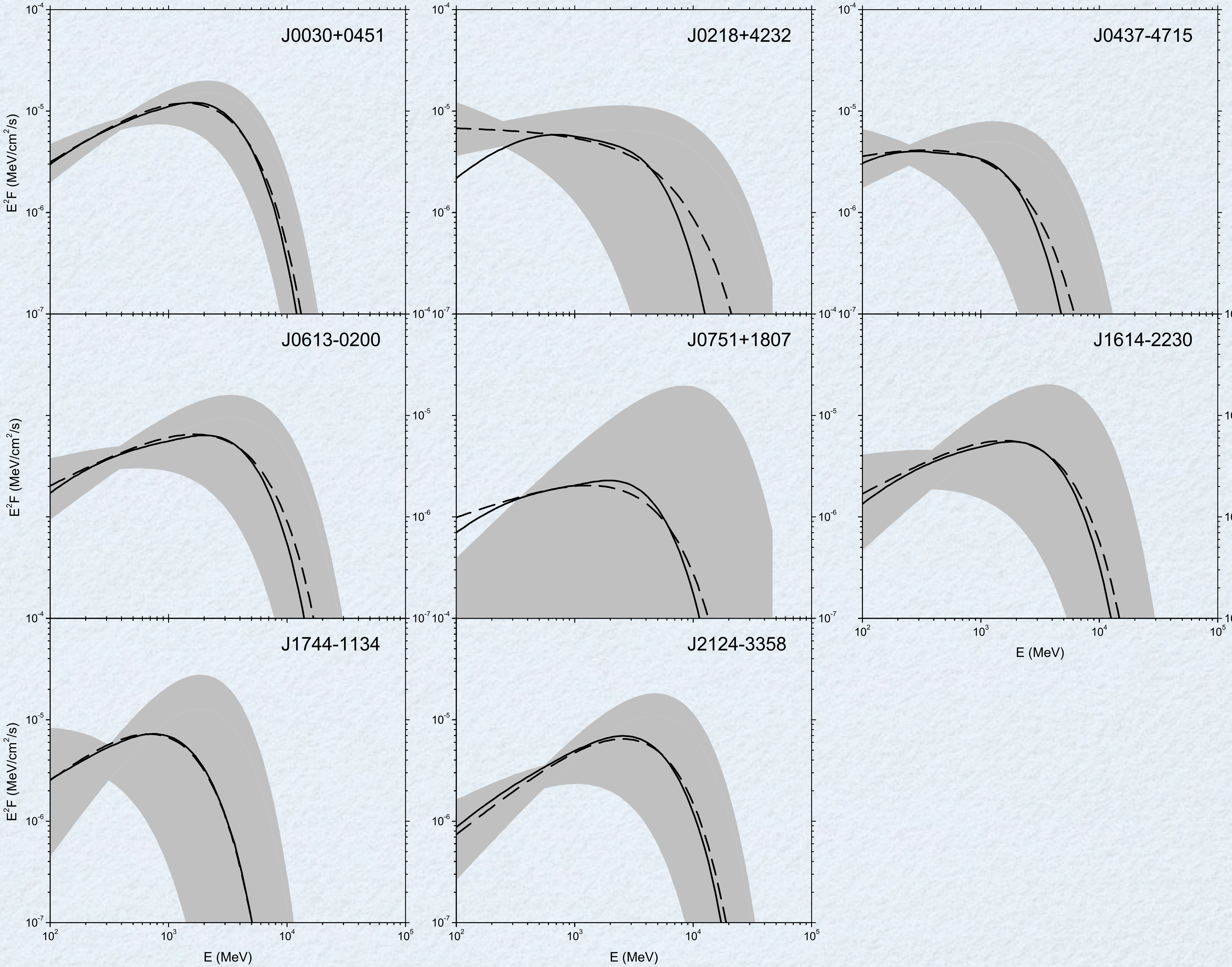
J0030+0451
J0218+4232
J0437-4715
J0613-0200
J0751+1807
J1614-2230
J1744-1134
J2124-3358
E²F (MeV/cm²/s)
E (MeV)

3. 3-D MODEL

The 3-D model is an extension of the two-layer model to a 3-D magnetic field structure.

3. 3-D MODEL

The 3-D model is an extension of the two-layer model to a 3-D magnetic field structure.

Why 3D?

3. 3-D MODEL

The 3-D model is an extension of the two-layer model to a 3-D magnetic field structure.

Why 3D?

The two-layer model can only be used to study the phase-averaged spectrum, it dose not consider the inclination angle and viewing angle of the pulsar, and it cannot provide the light curve and the phase-resolved spectra, which can tell us the most detailed information from the pulsar magnetosphere.

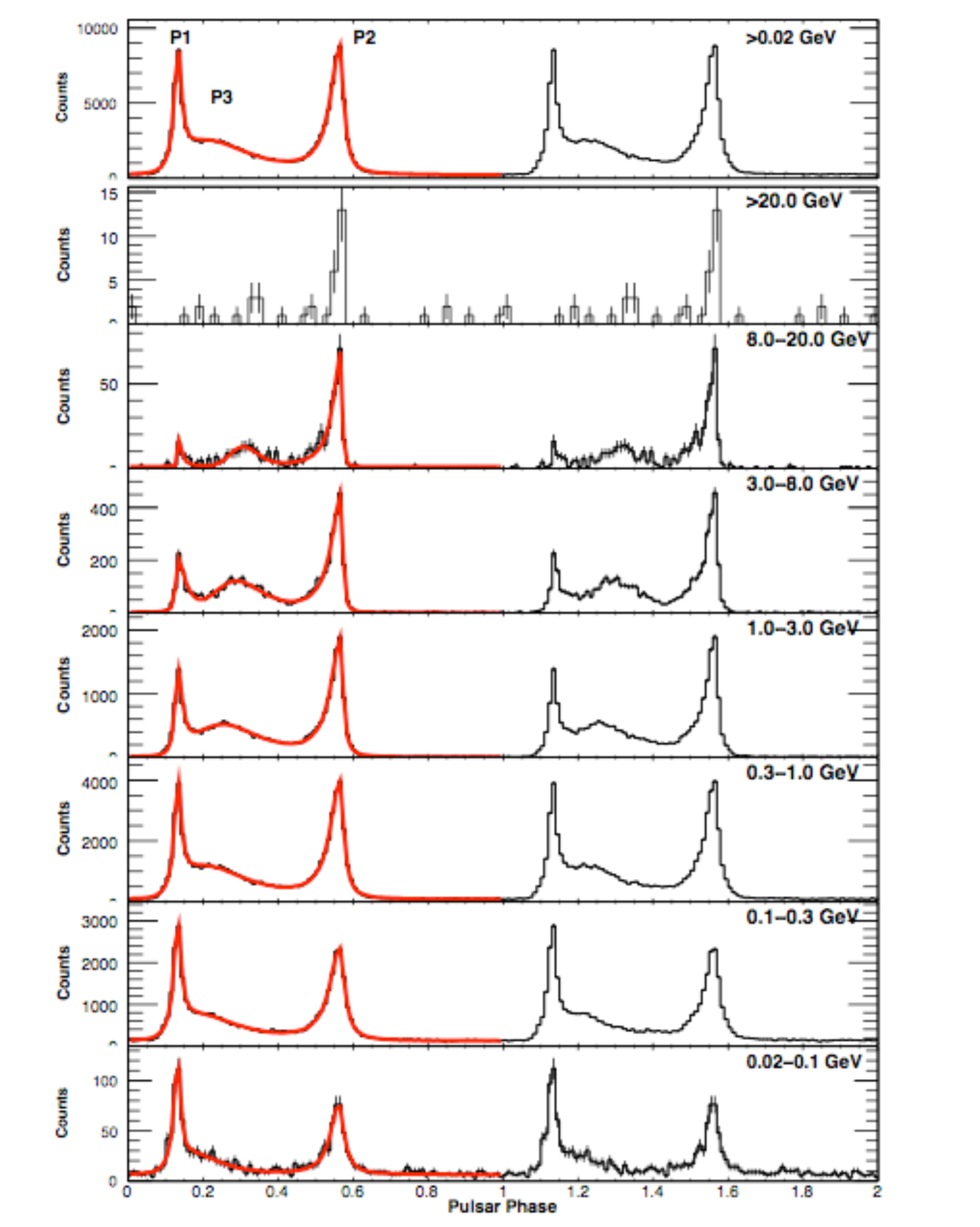

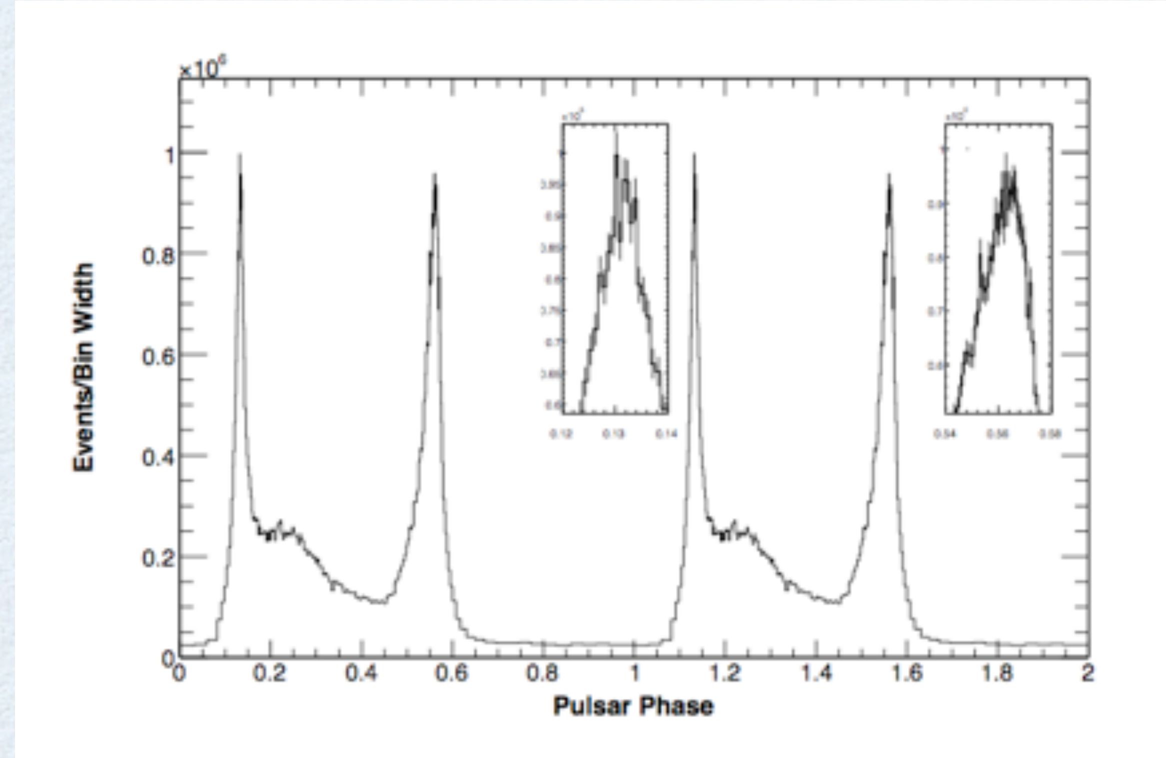

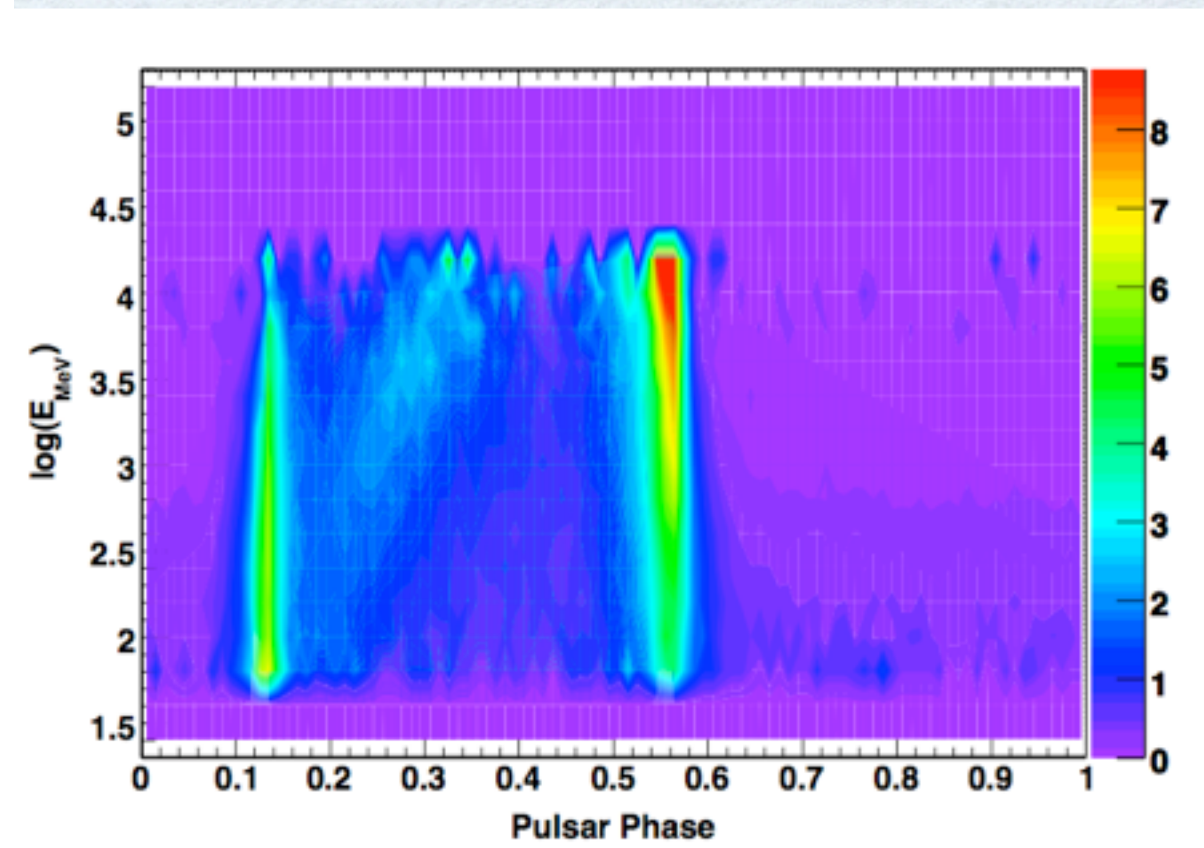

Abdo et al. (2009)

Table 1:: Parameters

Name	P (ms)	B_{12}	d^{obs} (kpc)	$F_{100}^{obs}(10^{-8}$ph cm^{-2}s$^{-1})$	f_{fit}	$1-g_1$	h_1/h_2	$\Delta\Omega d^2$ (kpc^2)	η_{gap}	L_γ^{fit} (10^{33}erg/s)	$\Delta\Omega_{fit}$	$d(\Delta\Omega=1)$
			Observed Parameters		Fitting Parameters					Deduced Parameters		
J0007+7303	316	10.6	1.4 ± 0.3	30.7 ± 1.3	0.65	0.06	0.967	4.508	0.538	124.1	$2.3^{+1.42}_{-0.74}$	2.12
J0248+6021*	217	3.44	2-9	3.7 ± 1.8	0.37	0.10	0.953	6.875	0.561	10.63	0.08-1.72	2.62
J0357+32	444	1.9	···	10.4 ± 1.2	0.80	0.12	0.927	0.72	0.577	2.56	···	0.85
J0631+1036*	288	5.44	0.75-3.62	2.8 ± 1.2	0.55	0.10	0.953	18	0.561	28.78	1.37-32	4.24
J0633+0632	297	4.84	···	8.4 ± 1.4	0.53	0.10	0.947	4.81	0.562	17.72	···	2.19
J0633+1746	237	1.59	$0.250^{+0.120}_{-0.062}$	305.3 ± 3.5	0.76	0.15	0.933	0.125	0.590	14.49	$2^{+1.54}_{-1.09}$	0.35
J0659+1414*	385	4.34	$0.288^{+0.033}_{-0.027}$	10 ± 1.4	0.23	0.05	0.920	0.12442	0.545	0.4624	$1.5^{+0.32}_{-0.29}$	0.35
J0742-2822*	167	1.67	$2.07^{+1.38}_{-1.07}$	3.18 ± 1.2	0.30	0.08	0.920	4.2849	0.559	3.861	$1^{+3.28}_{-0.64}$	2.07
J0835-4510*	89.3	3.40	$0.287^{+0.019}_{-0.017}$	1061 ± 7.0	0.16	0.08	0.927	0.08237	0.557	28.18	$1^{+0.13}_{-0.12}$	0.29
J1028-5819*	91.4	1.21	2.33 ± 0.70	19.6 ± 3.1	0.27	0.09	0.947	1.9544	0.557	16.38	$0.36^{+0.38}_{-0.15}$	1.40
J1048-5832*	124	3.48	2.71 ± 0.81	19.7 ± 3.0	0.20	0.10	0.947	1.98291	0.562	16.08	$0.27^{+0.28}_{-0.11}$	1.41
J1057-5226*	197	1.08	0.72 ± 0.2	30.45 ± 1.7	0.60	0.15	0.933	0.72576	0.590	6.48	$1.4^{+1.28}_{-0.54}$	0.85
J1418-6058	111	4.37	2-5	27.7 ± 8.3	0.16	0.10	0.940	2.2	0.564	20.27	0.09-0.55	1.48
J1420-6048*	68.2	2.38	5.6 ± 1.7	24.2 ± 7.9	0.11	0.06	0.947	1.2544	0.543	13.31	$0.04^{+0.04}_{-0.02}$	1.12
J1459-60	103	1.6	···	17.8 ± 3.4	0.22	0.05	0.927	1.45	0.543	9.786	···	1.20
J1509-5850*	88.9	0.90	2.6 ± 0.8	8.7 ± 1.4	0.41	0.09	0.960	7.098	0.554	35.49	$1.05^{+1.14}_{-0.44}$	2.66
J1709-4429*	102	3.04	1.4-3.6	149.8 ± 4.1	0.25	0.05	0.947	0.63	0.538	53.28	0.05-0.32	0.79
J1718-3825*	74.7	0.99	3.82 ± 1.15	9.1 ± 5.8	0.18	0.11	0.947	2.48071	0.567	7.29	$0.17^{+0.18}_{-0.07}$	1.58
J1732-31	197	2.24	···	25.3 ± 3.0	0.50	0.11	0.933	1.62	0.570	17	···	1.27
J1741-2054	414	2.31	0.38 ± 0.11	20.3 ± 2.0	0.70	0.10	0.960	0.361	0.559	3.087	$2.5^{+2.45}_{-1.00}$	0.60
J1747-2958*	98.8	2.46	2-5	18.2 ± 4.2	0.15	0.10	0.953	1.2	0.561	8.471	0.05-0.30	1.10
J1809-2332	147	2.24	1.7 ± 1.0	49.5 ± 3.0	0.35	0.07	0.947	0.7225	0.548	18.44	$0.25^{+1.22}_{-0.15}$	0.85
J1813-1246	48.1	0.92	···	28.1 ± 3.5	0.13	0.05	0.927	1.25	0.543	13.75	···	1.12
J1826-1256	110	3.64	···	41.8 ± 4.1	0.19	0.07	0.947	1.28	0.548	24.56	···	1.13

(Wang, Takata, & Cheng, 2010)

Table 1:: Parameters

			Observed Parameters			Fitting Parameters				Deduced Parameters		
Name	P (ms)	B_{12}	d^{obs} (kpc)	$F_{100}^{obs}(10^{-8}$ph cm^{-2}s$^{-1})$	f_{fit}	$1-g_1$	h_1/h_2	$\Delta\Omega d^2$ (kpc^2)	η_{gap}	L_γ^{fit} (10^{33}erg/s)	$\Delta\Omega_{fit}$	$d(\Delta\Omega=1)$
J0835-4510*	89.3	3.40	$0.287^{+0.019}_{-0.017}$	1061 ± 7.0	0.16	0.08	0.927	0.08237	0.557	28.18	$1^{+0.13}_{-0.12}$	0.29

(Wang, Takata, & Cheng, 2010)

Table 1:: Parameters

	Observed Parameters				Fitting Parameters					Deduced Parameters		
Name	P (ms)	B_{12}	d^{obs} (kpc)	$F_{100}^{obs}(10^{-8}\mathrm{ph\ cm^{-2}s^{-1}})$	f_{fit}	$1-g_1$	h_1/h_2	$\Delta\Omega d^2$ (kpc^2)	η_{gap}	L_γ^{fit} (10^{33}erg/s)	$\Delta\Omega_{fit}$	$d(\Delta\Omega=1)$
J0835-4510*	89.3	3.40	$0.287^{+0.019}_{-0.017}$	1061 ± 7.0	0.16	0.08	0.927	0.08237	0.557	28.18	$1^{+0.13}_{-0.12}$	0.29

(Wang, Takata, & Cheng, 2010)

Table 1:: Parameters

	Observed Parameters				Fitting Parameters					Deduced Parameters		
Name	P (ms)	B_{12}	d^{obs} (kpc)	$F^{obs}_{100}(10^{-8}\mathrm{ph\ cm^{-2}s^{-1}})$	f_{fit}	$1-g_1$	h_1/h_2	$\Delta\Omega d^2$ (kpc^2)	η_{gap}	L_γ^{fit} (10^{33}erg/s)	$\Delta\Omega_{fit}$	$d(\Delta\Omega=1)$
J0835-4510*	89.3	3.40	$0.287^{+0.019}_{-0.017}$	1061 ± 7.0	0.16	0.08	0.927	0.08237	0.557	28.18	$1^{+0.13}_{-0.12}$	0.29

$$1 - g_1 = 0.08$$

$$d = 0.287kpc \qquad h_1/h_2 = 0.927$$

$$f_{fit} = 0.16$$

(Wang, Takata, & Cheng, 2010)

definition of “a”

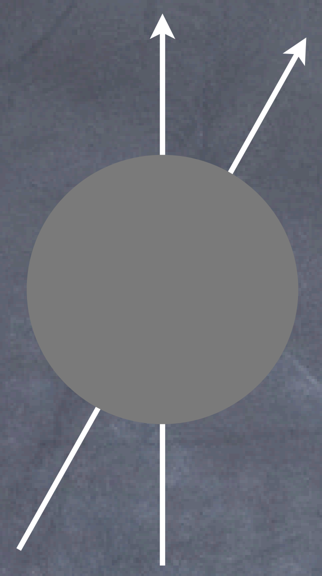

definition of “a”

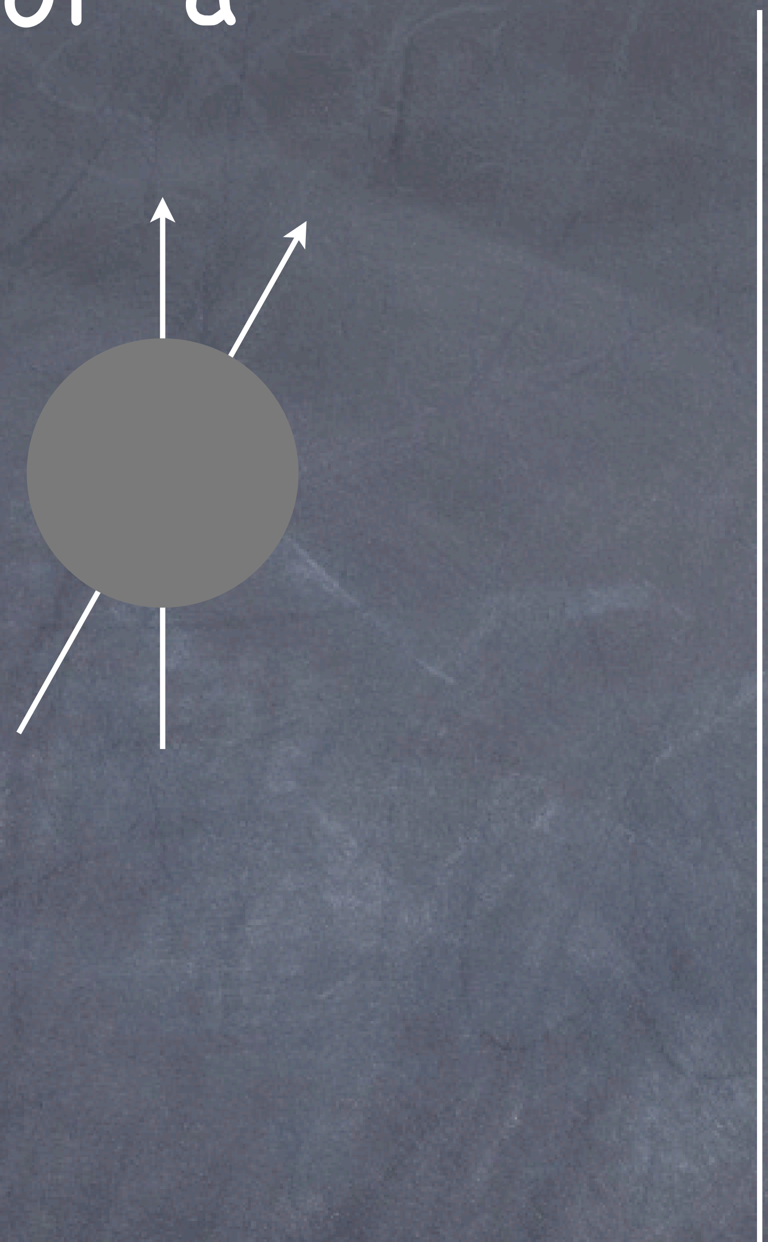

definition of "a"

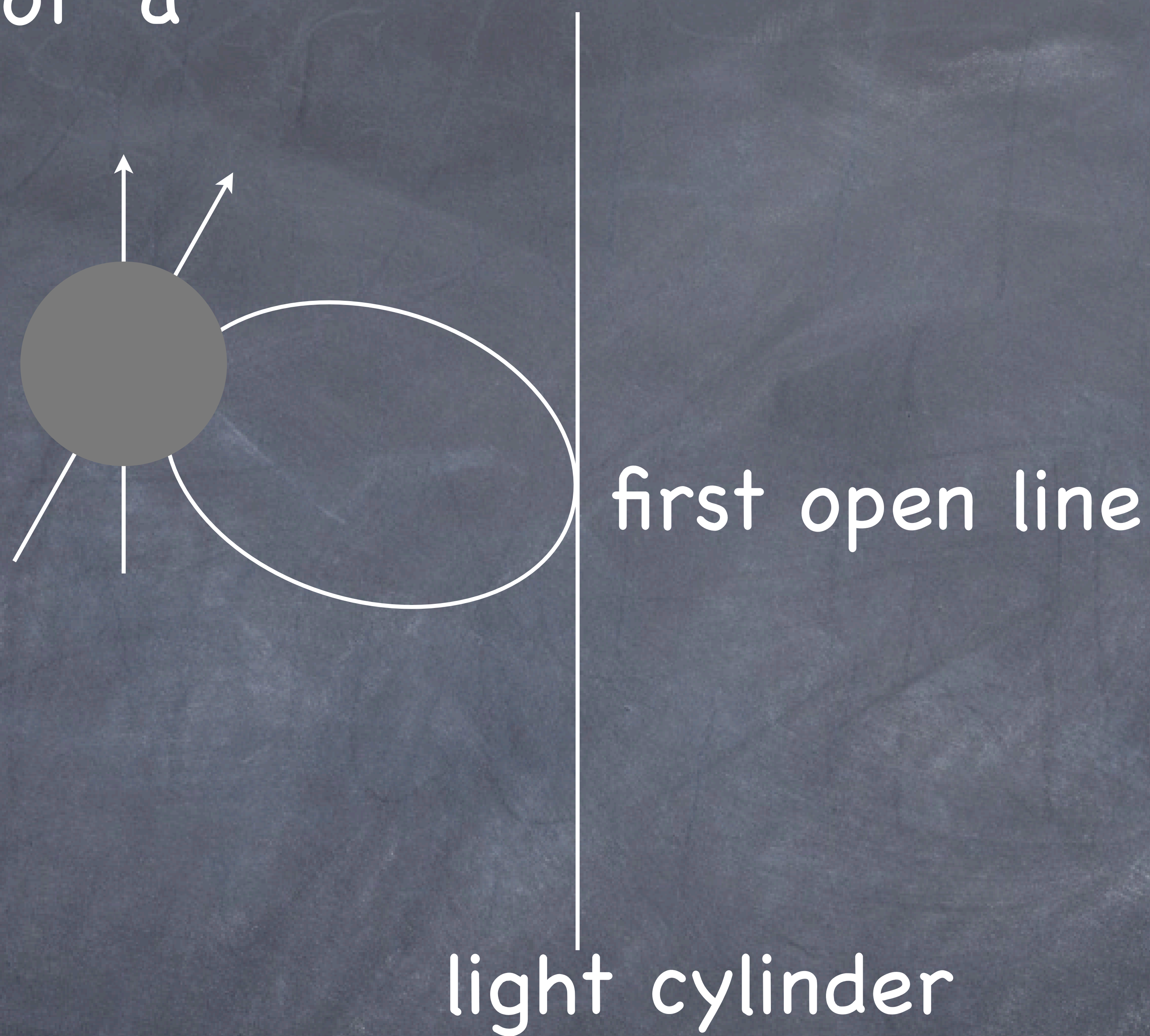

definition of "a"

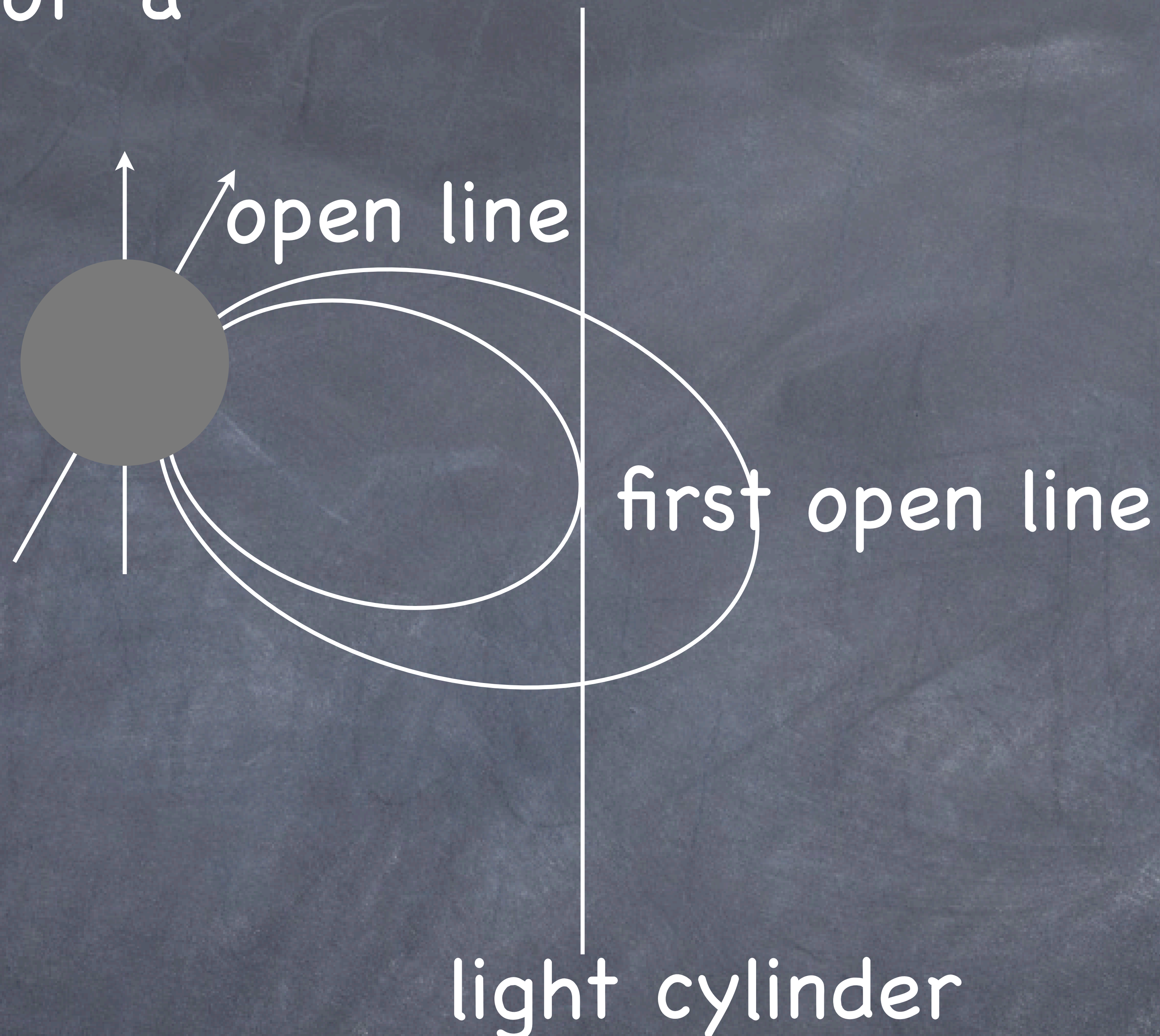

definition of “a”

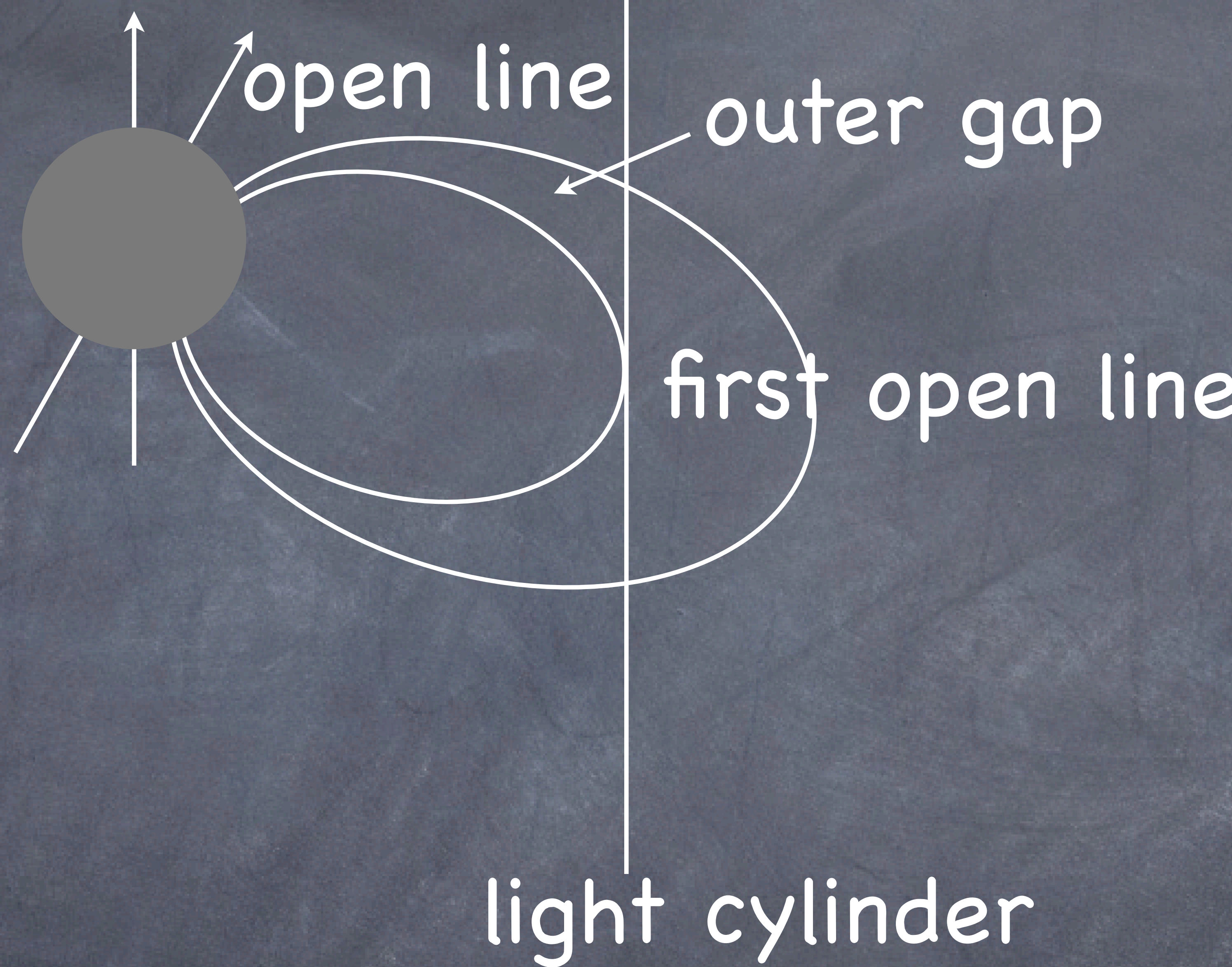

definition of "a"

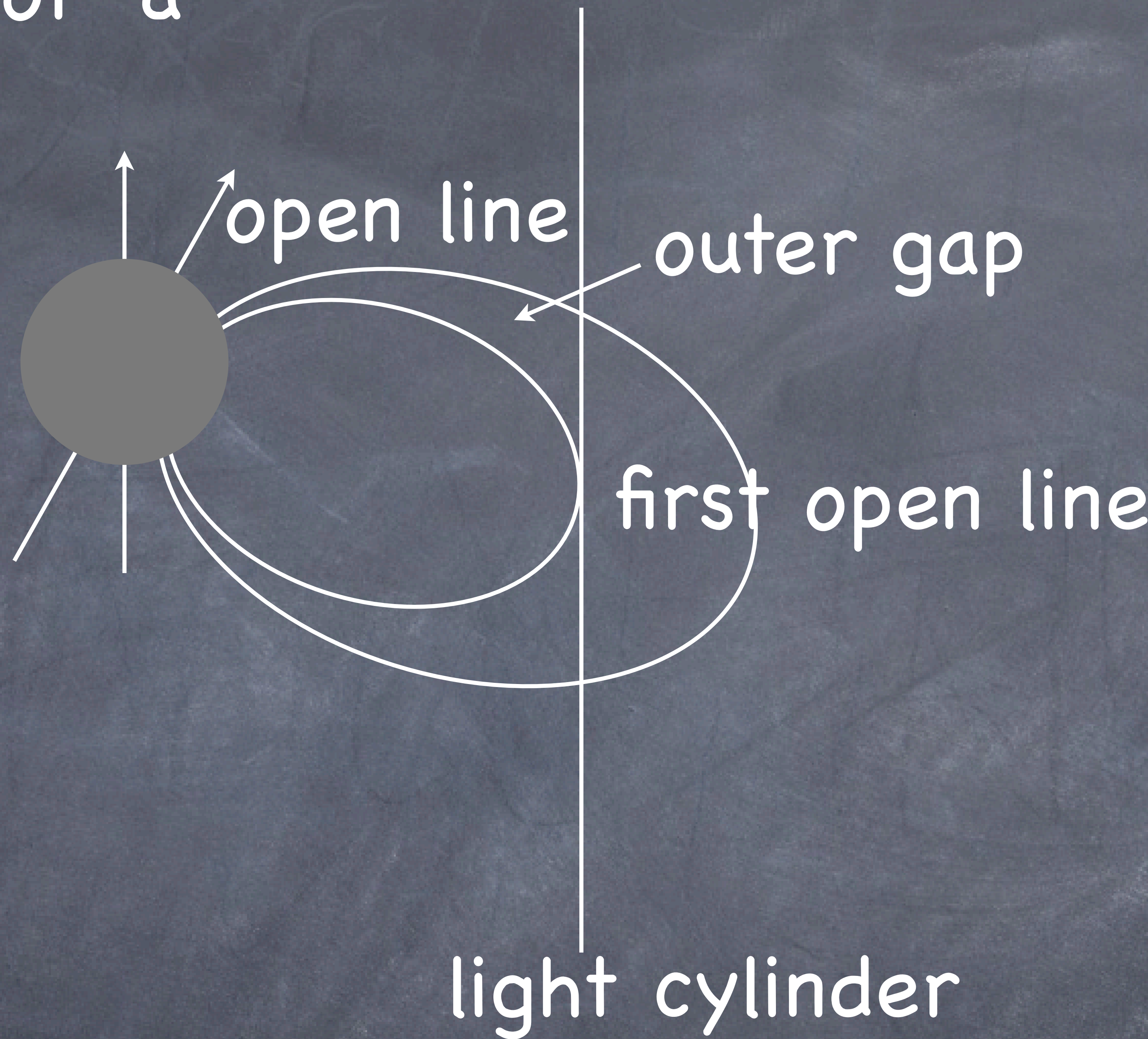

introduce a parameter "a" to represent the position of the field line

definition of "a"

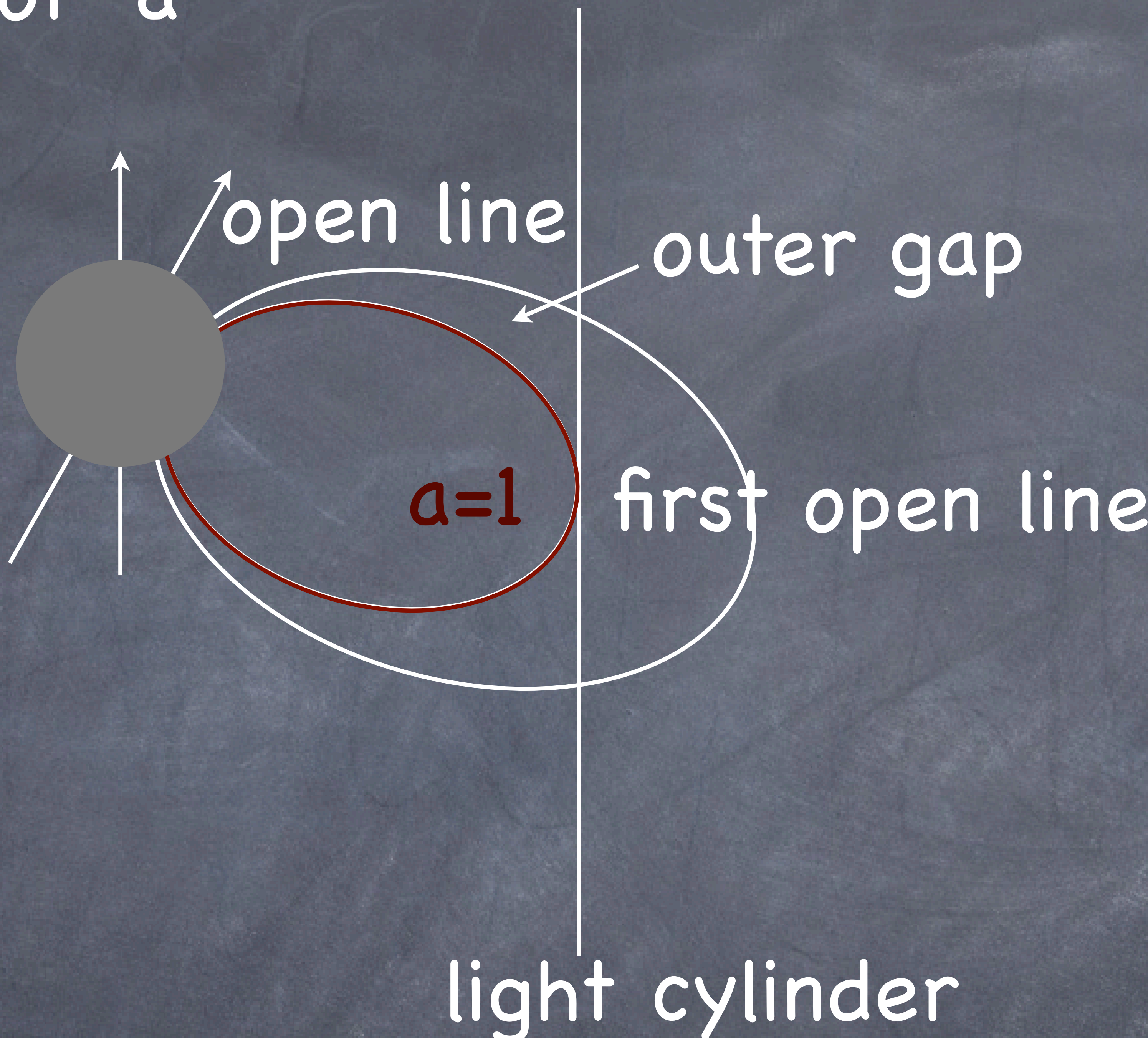

introduce a parameter "a" to represent the position of the field line

definition of “a”

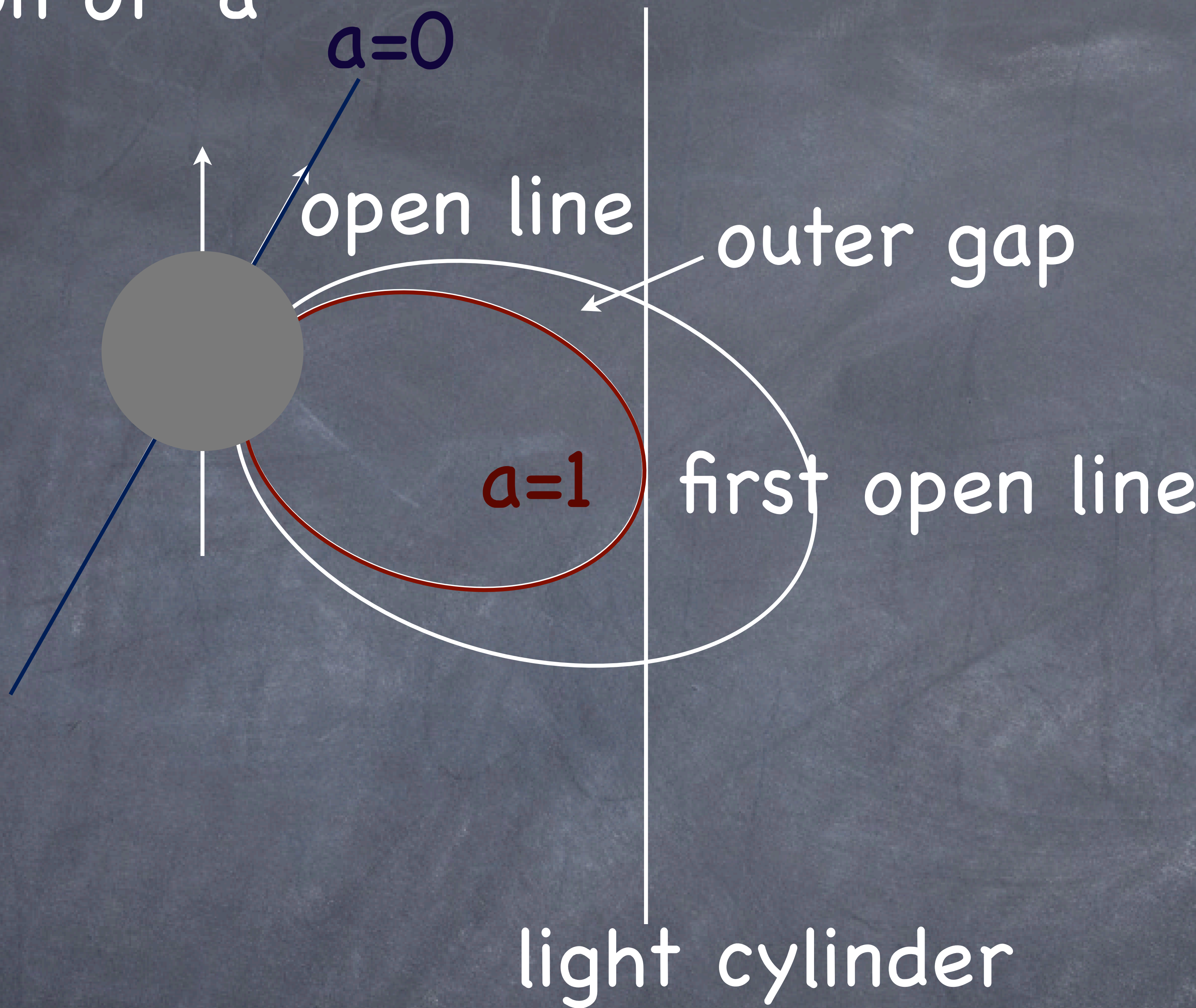

introduce a parameter “a” to represent the position of the field line

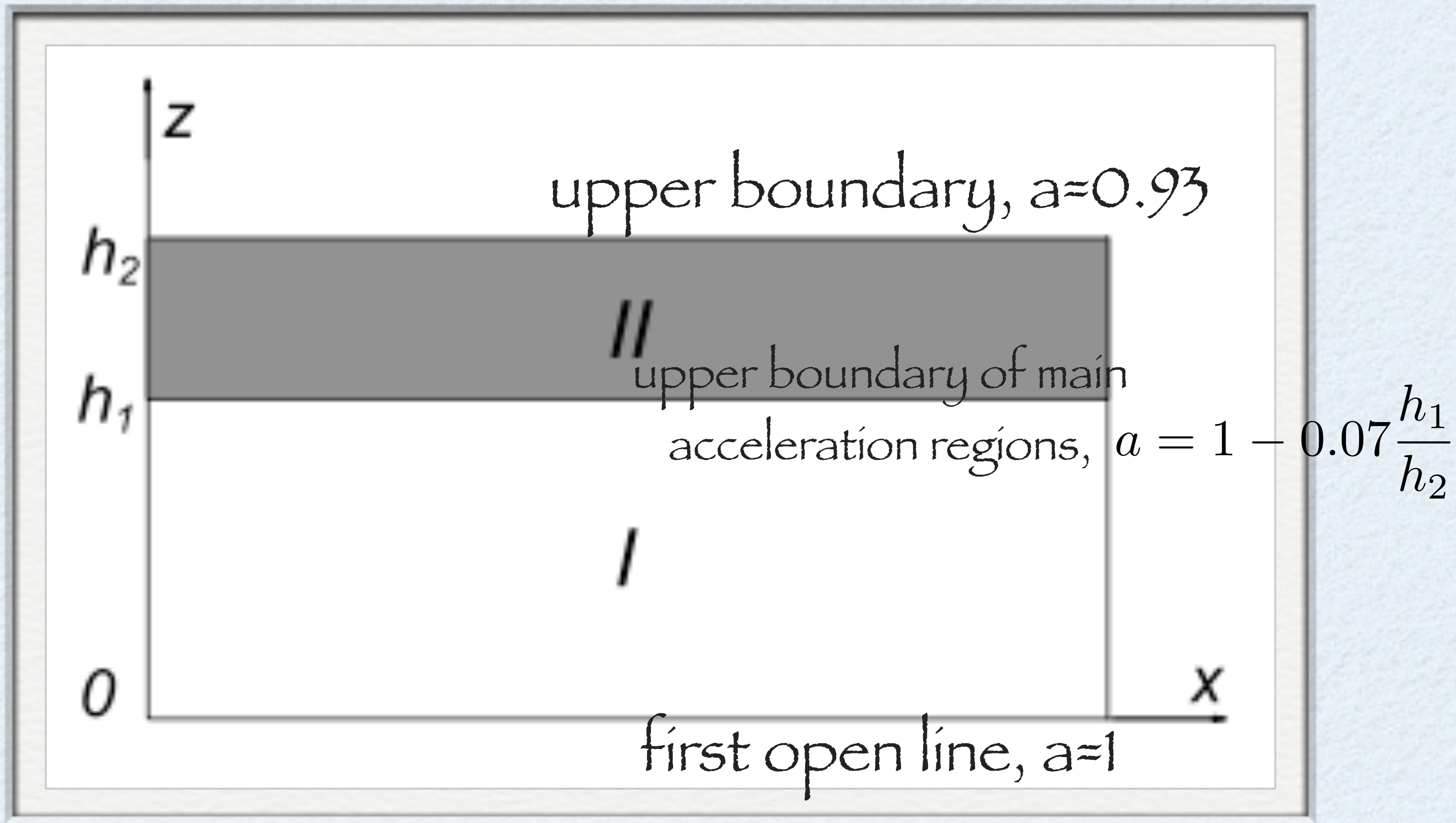

$$f_{fit} = 0.16$$

$$\downarrow$$

$$a = 0.93 - 1$$

$$\downarrow$$

$$\begin{cases} \text{main acceleration region,} & \text{if} \quad 1 - 0.07\frac{h_1}{h_2} \le a \le 1 \\ \text{screening region,} & \text{if} \quad 0.93 < a \le 1 - 0.07\frac{h_1}{h_2} \end{cases},$$

Divide the gap into many layers, then calculate the radiation from each layer, and add them together.

Find the inclination angle and viewing angle by making the light curve determined by the field line structure

Find the inclination angle and viewing angle by making the light curve determined by the field line structure

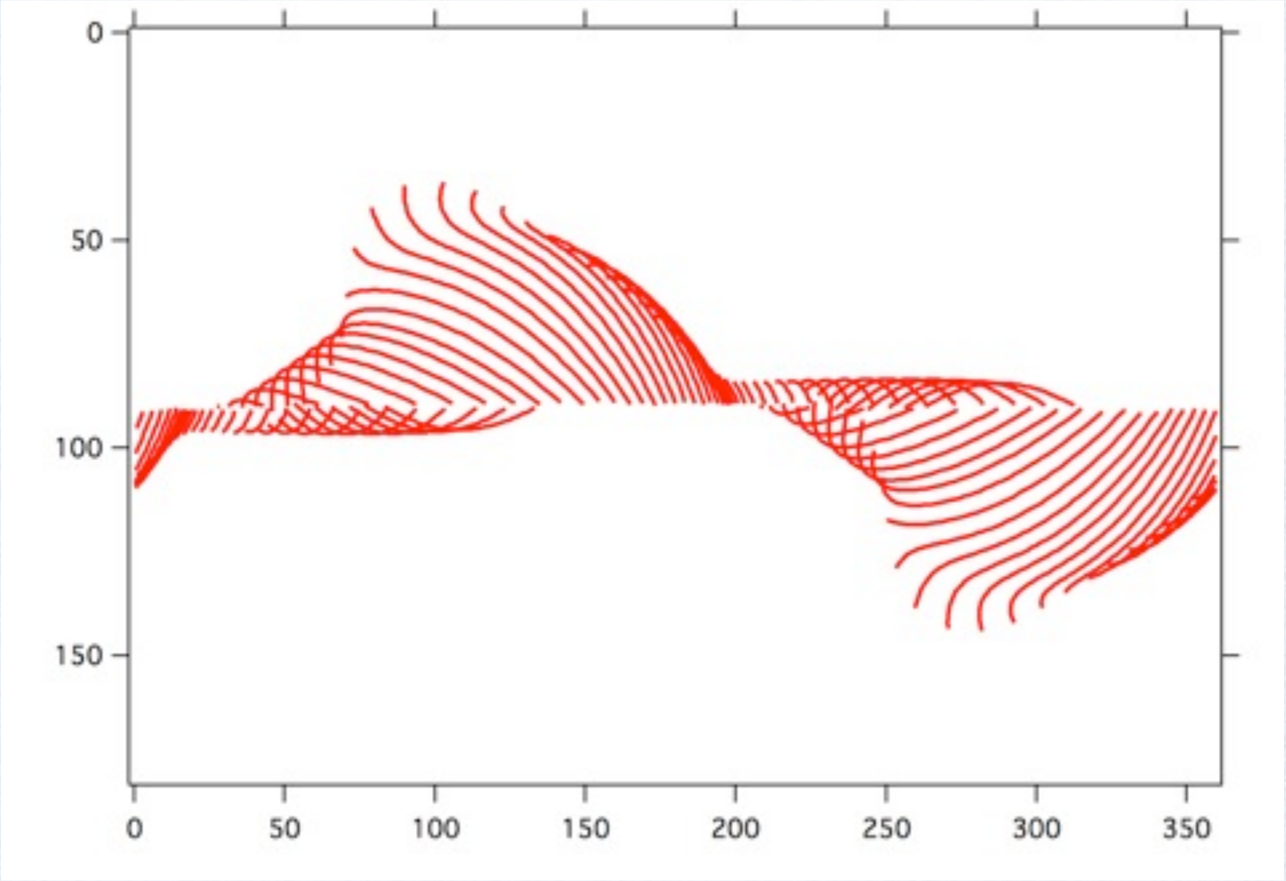

Find the inclination angle and viewing angle by making the light curve determined by the field line structure

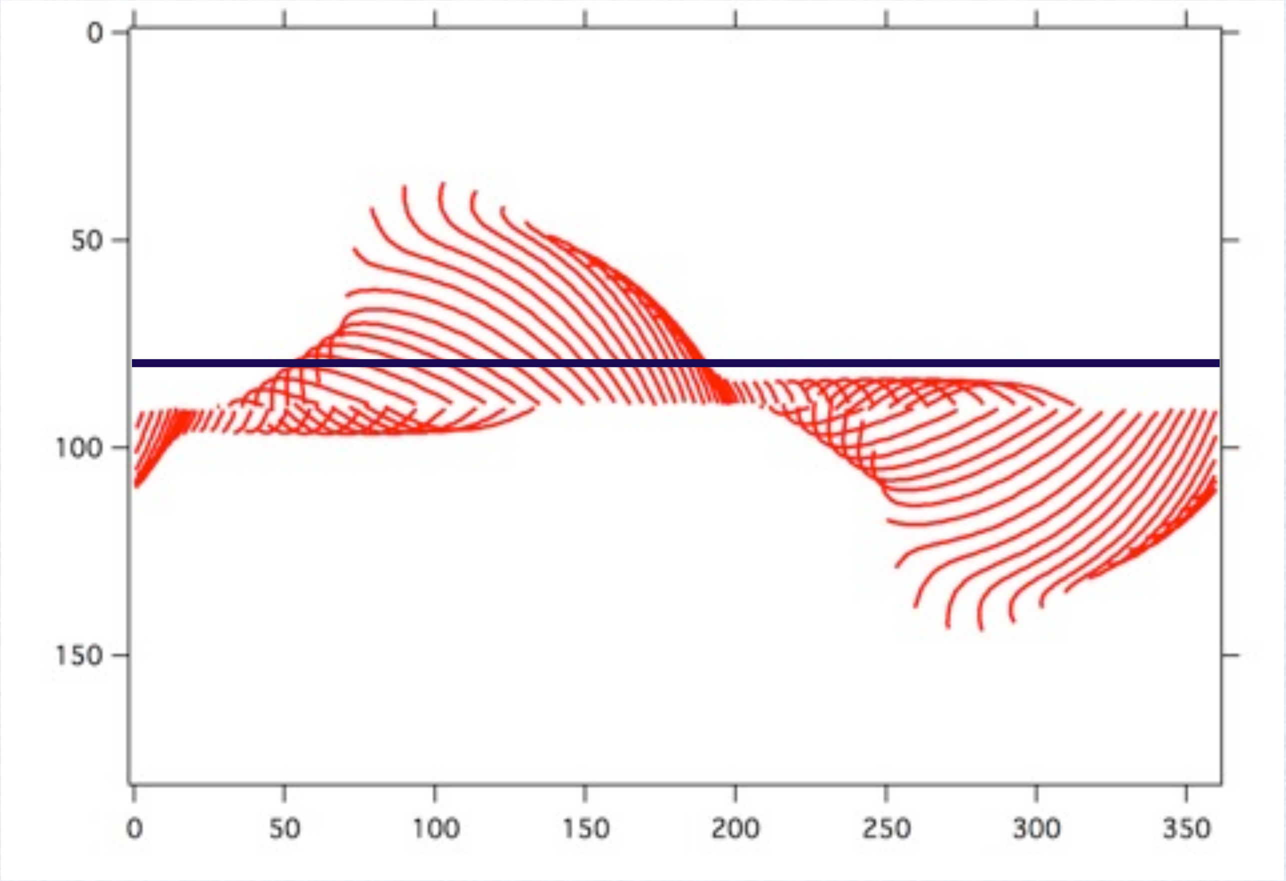

Find the inclination angle and viewing angle by making the light curve determined by the field line structure

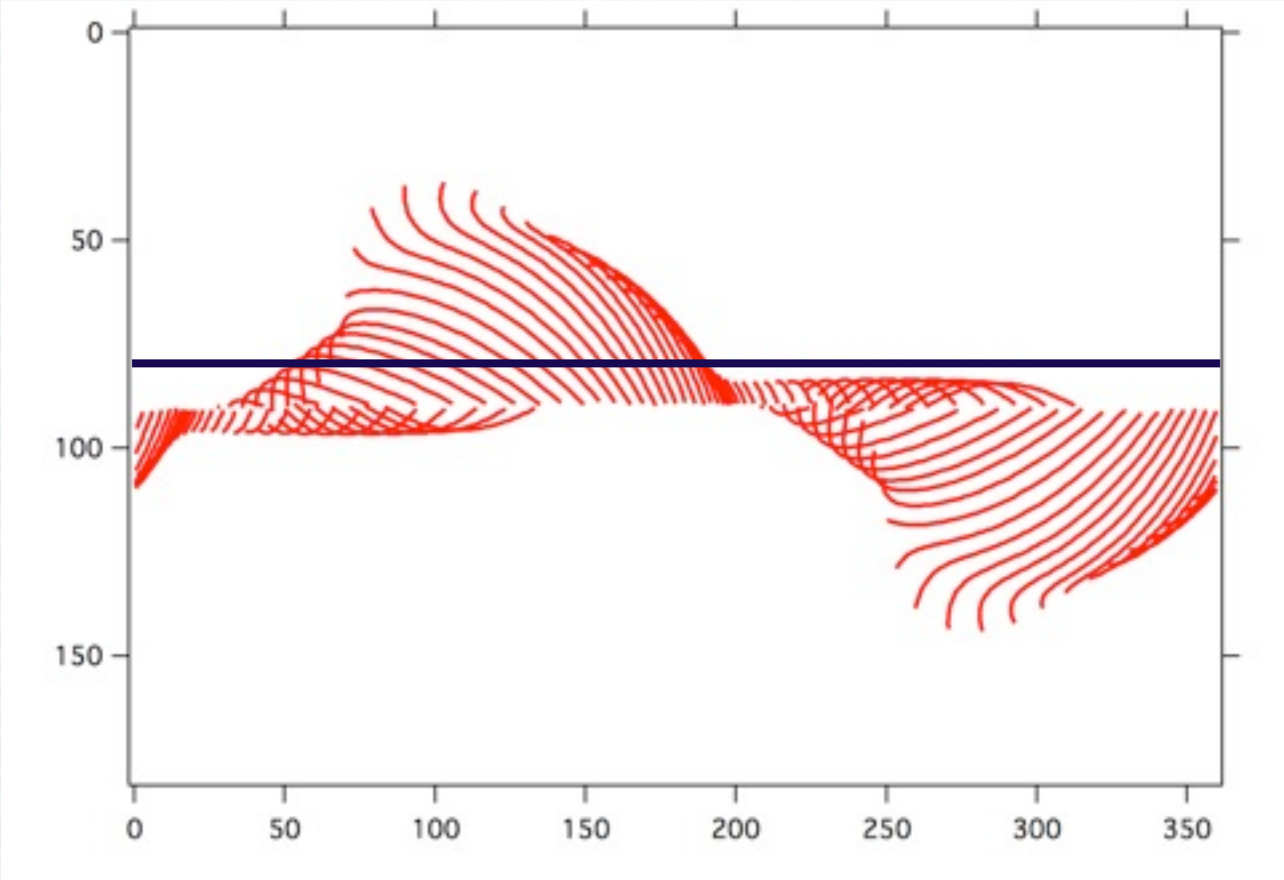

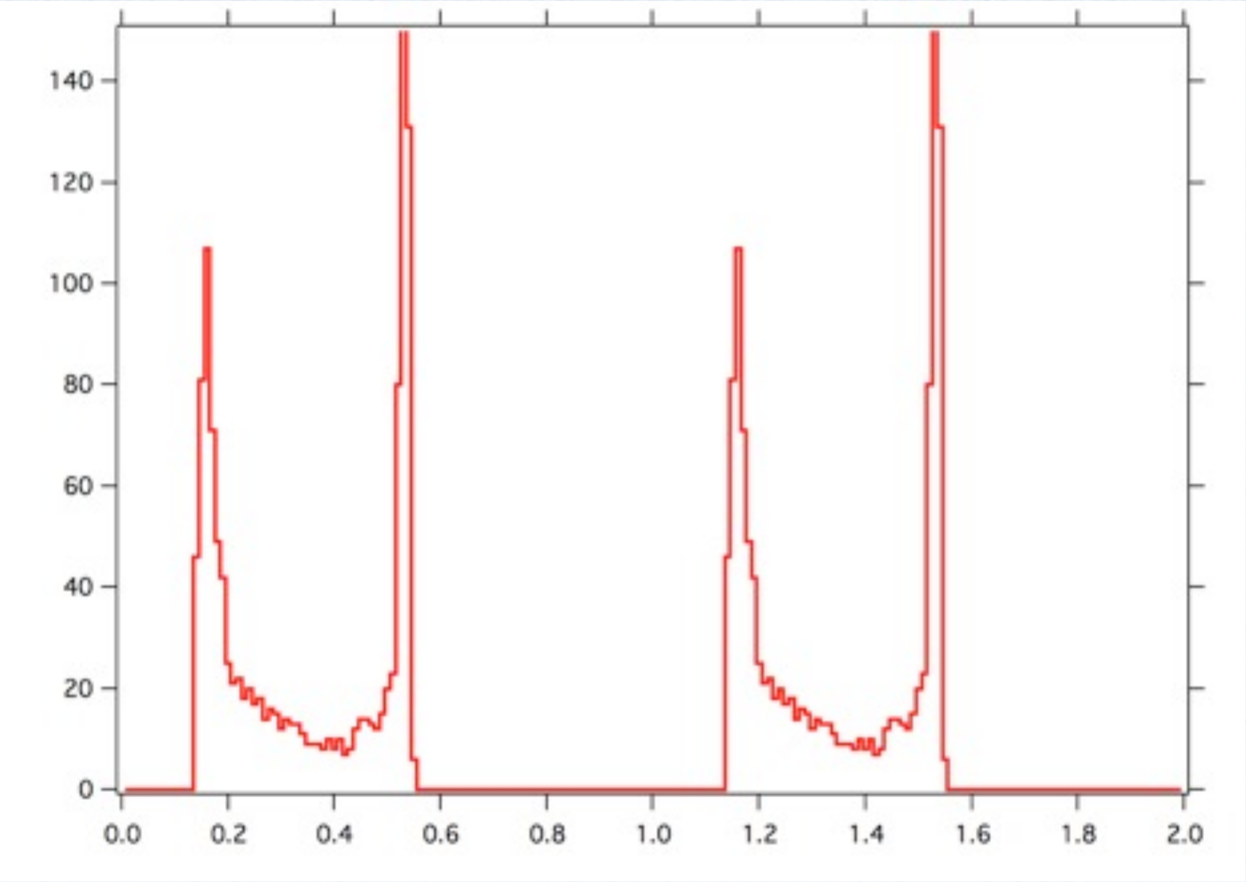

Find the inclination angle and viewing angle by making the light curve determined by the field line structure

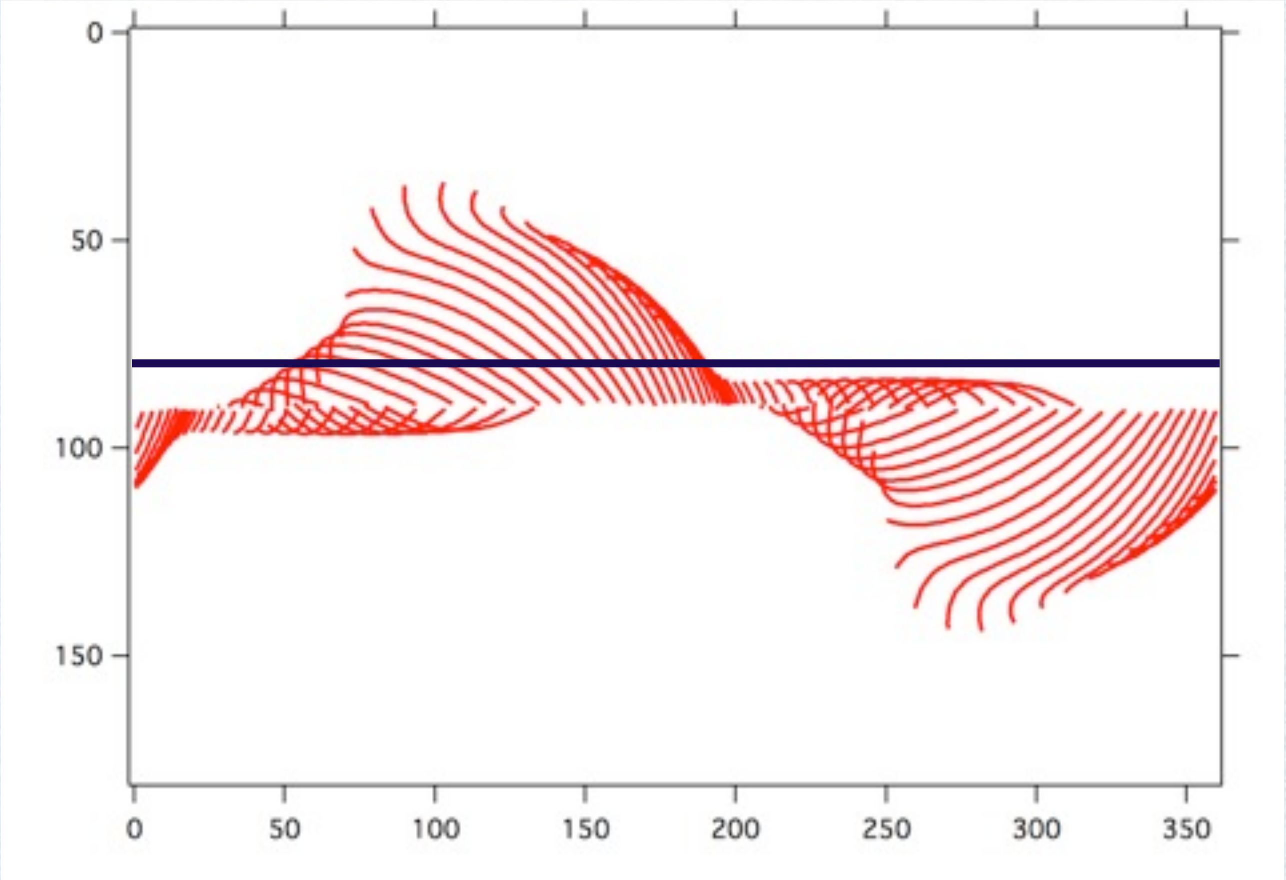

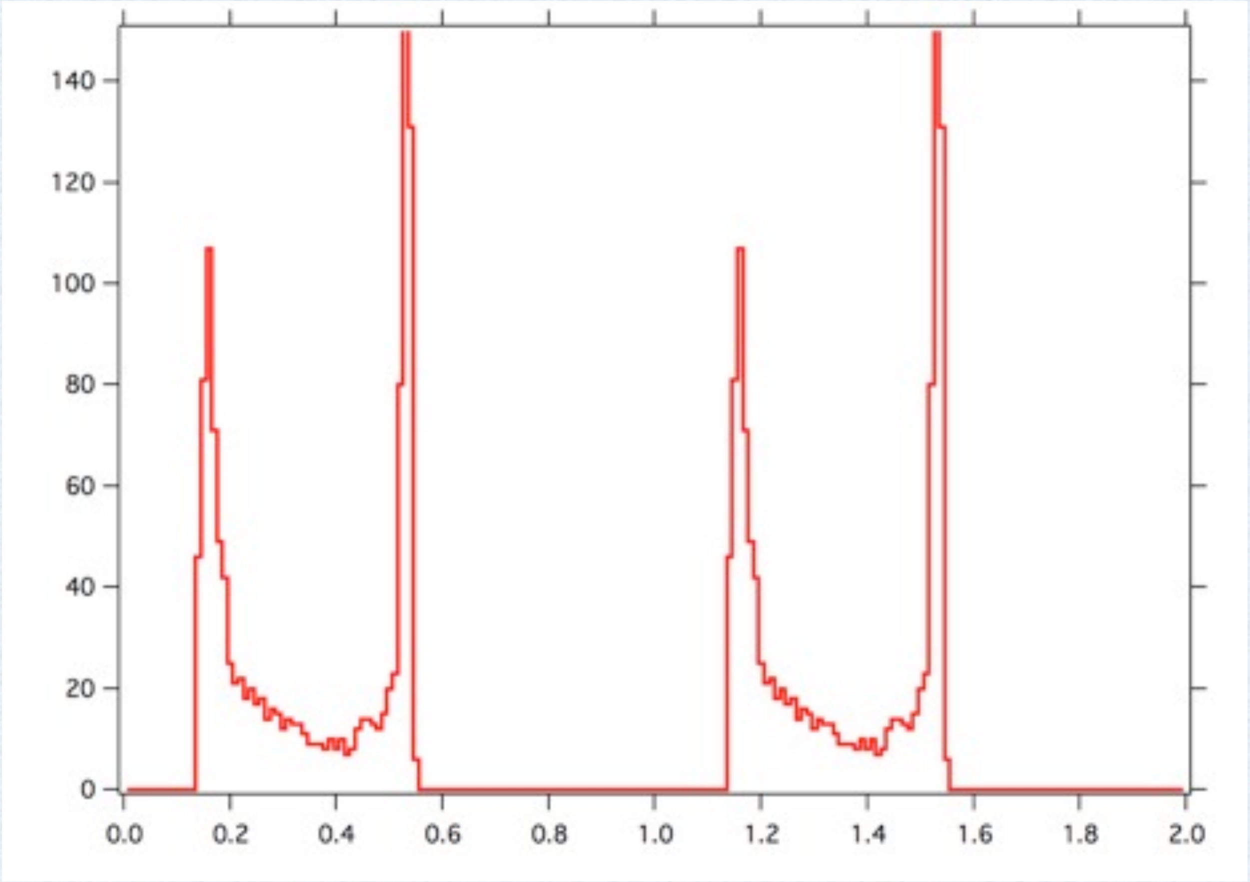

$$\alpha = 56deg$$

$$\beta = 80deg$$

Using the method in Tang et al (2008) to calculate the phase averaged spectrum……

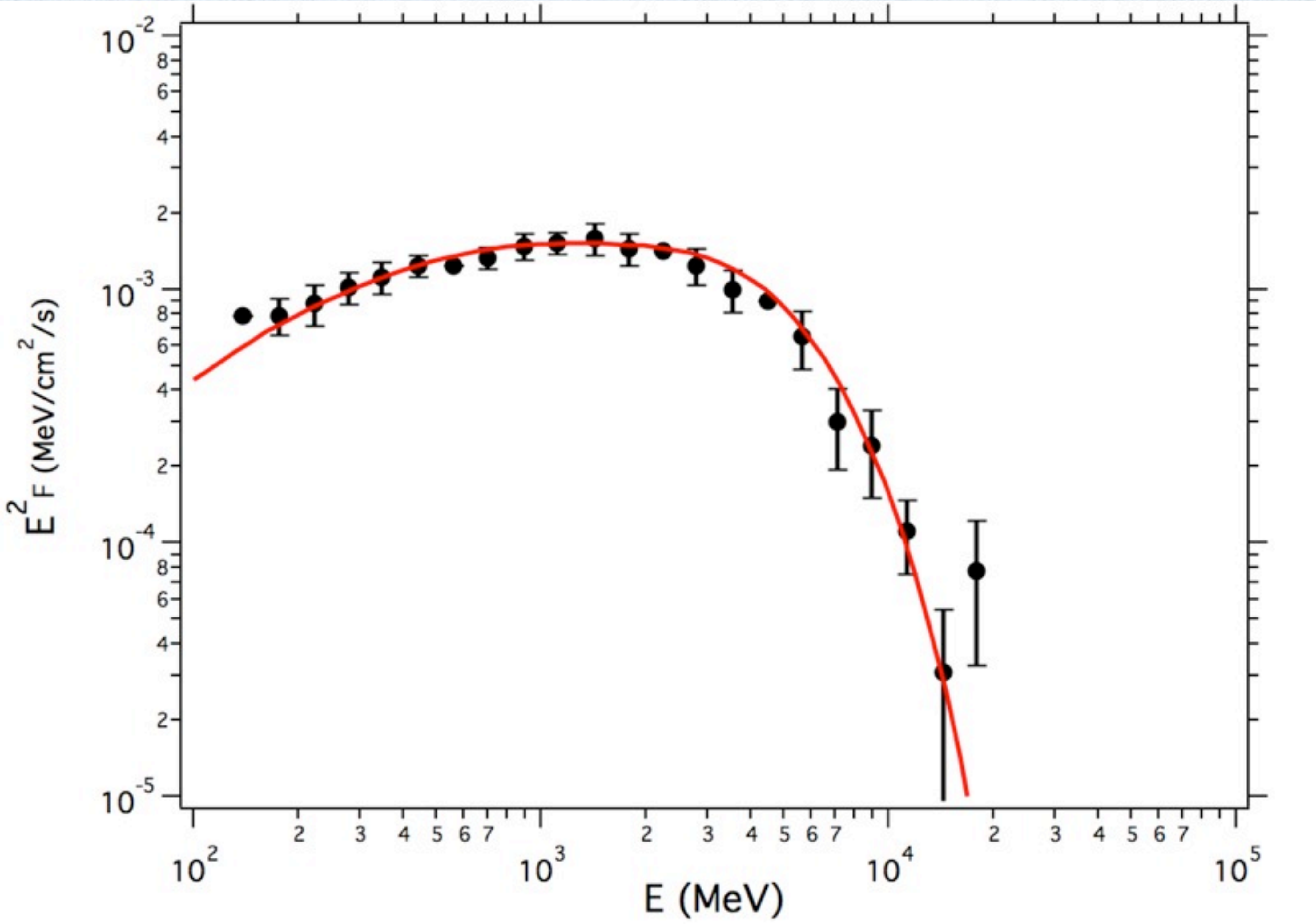

The circles are the observed data from the Fermi LAT, which are taken from Abdo et al. (2009)

$1 - g_1 = 0.08 \quad h_1/h_2 = 0.927$ the same with those of two-layer model

What about the energy dependent light curve!?

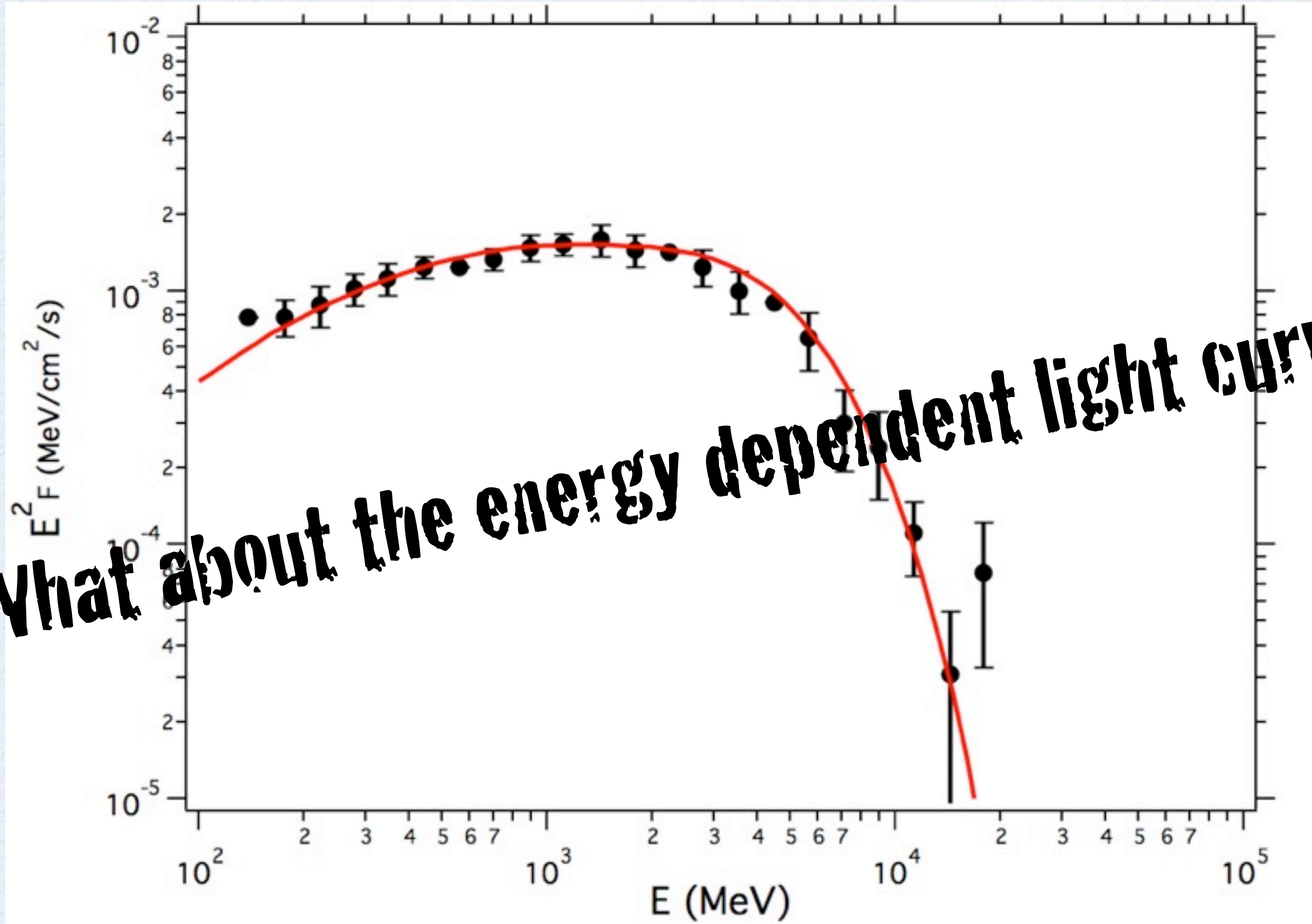

The circles are the observed data from the Fermi LAT, which are taken from Abdo et al. (2009)

$1 - g_1 = 0.08 \quad h_1/h_2 = 0.927$ the same with those of two-layer model

We use the method introduced in Tang et al (2008) to calculate the phase resolved spectra, then integrate them......

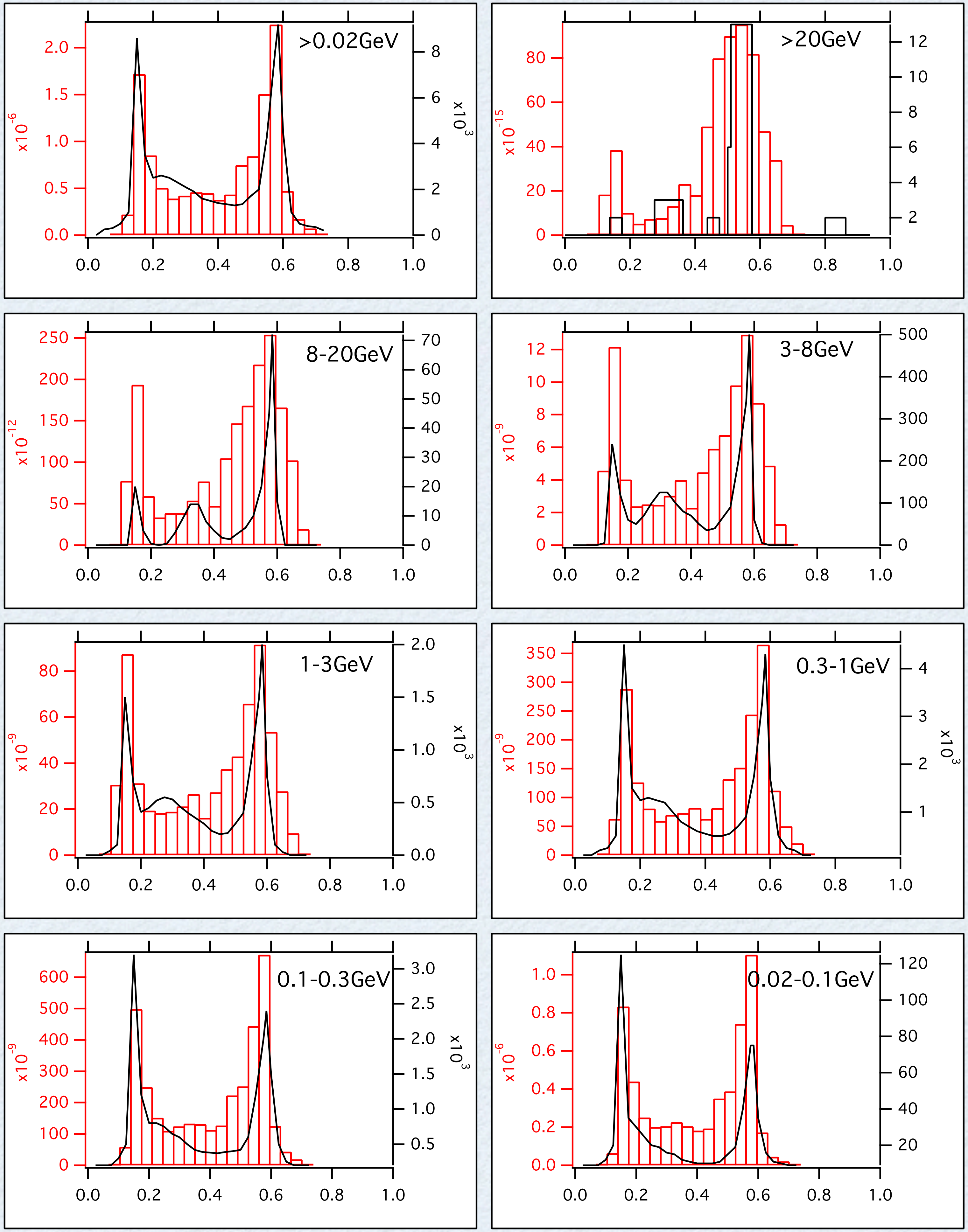

The black lines are the observed energy dependent light curves of Vela from the Fermi LAT, which are taken from Abdo et al. (2009)

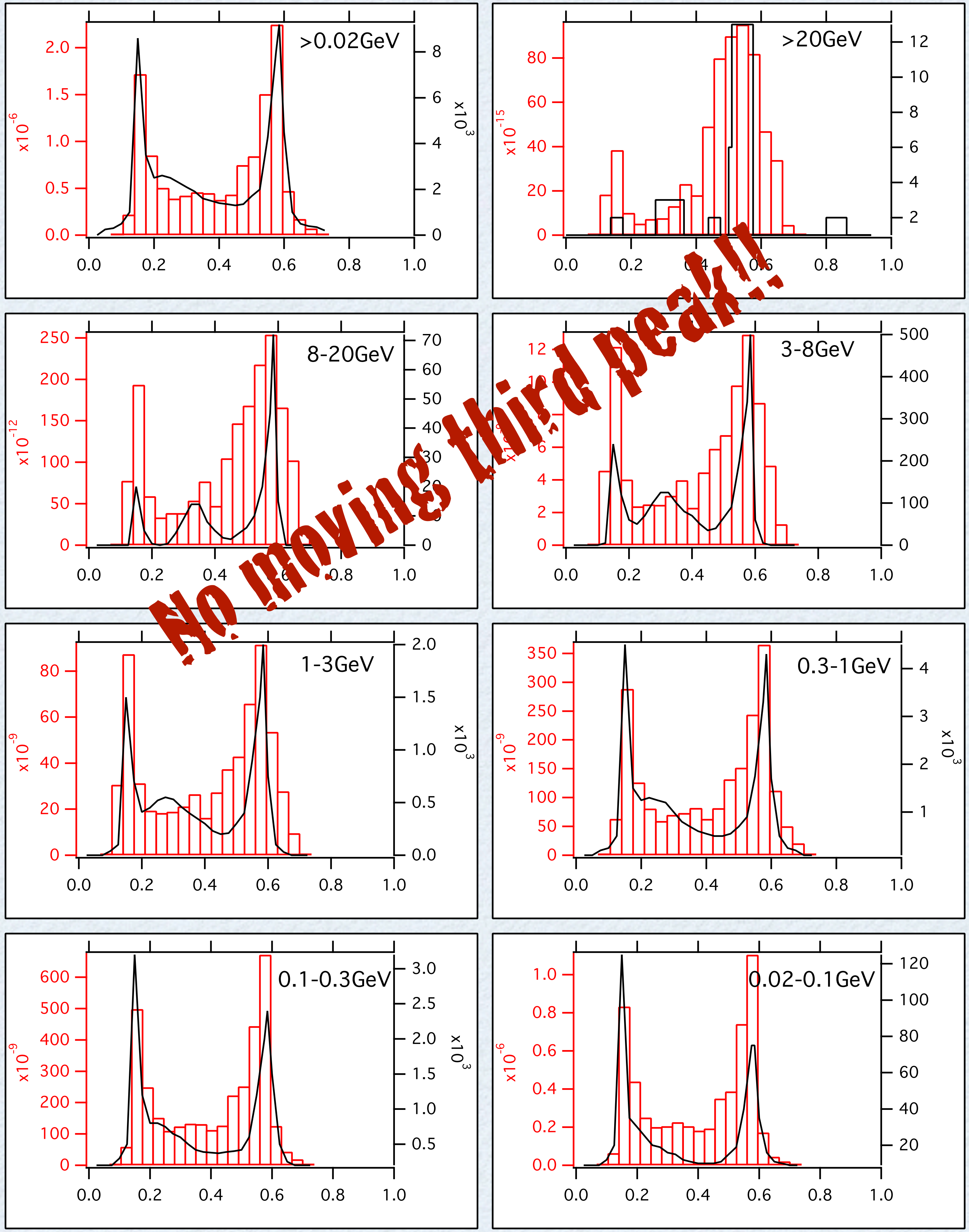

The black lines are the observed energy dependent light curves of Vela from the Fermi LAT, which are taken from Abdo et al. (2009)

Distribution of $1 - g_1$, h_1/h_2 and f are needed

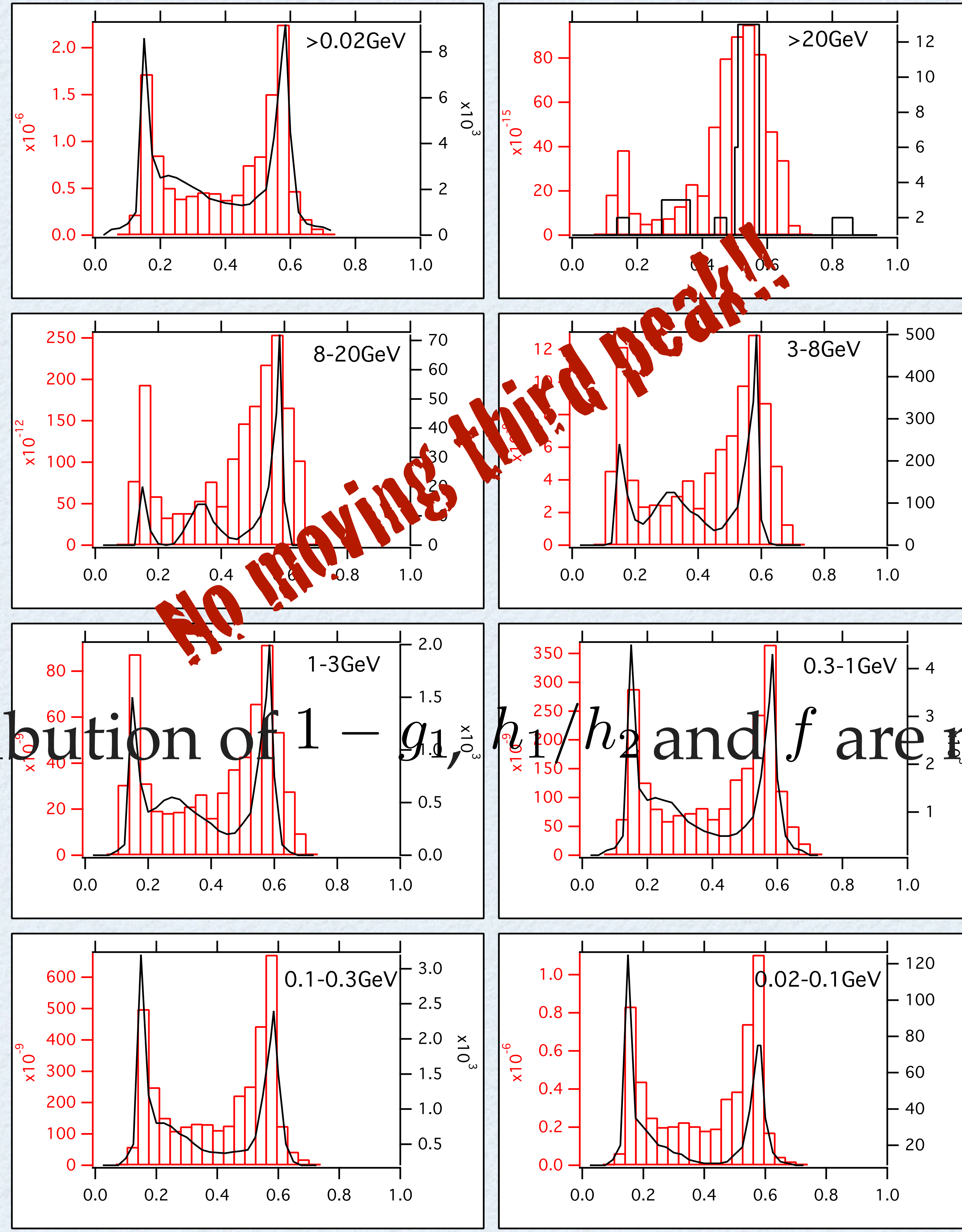

The black lines are the observed energy dependent light curves of Vela from the Fermi LAT, which are taken from Abdo et al. (2009)

Distribution of f

$$f \equiv \frac{h_m}{r_p} = \frac{f(R_{lc})}{R_{lc}}$$

h_m is constant (Takata, Wang & Cheng, 2010)

$$f(\phi_p) = \frac{C}{r_p(\phi_p)}$$

ϕ_p is azimuthal angle around magnetic axis

C is a constant

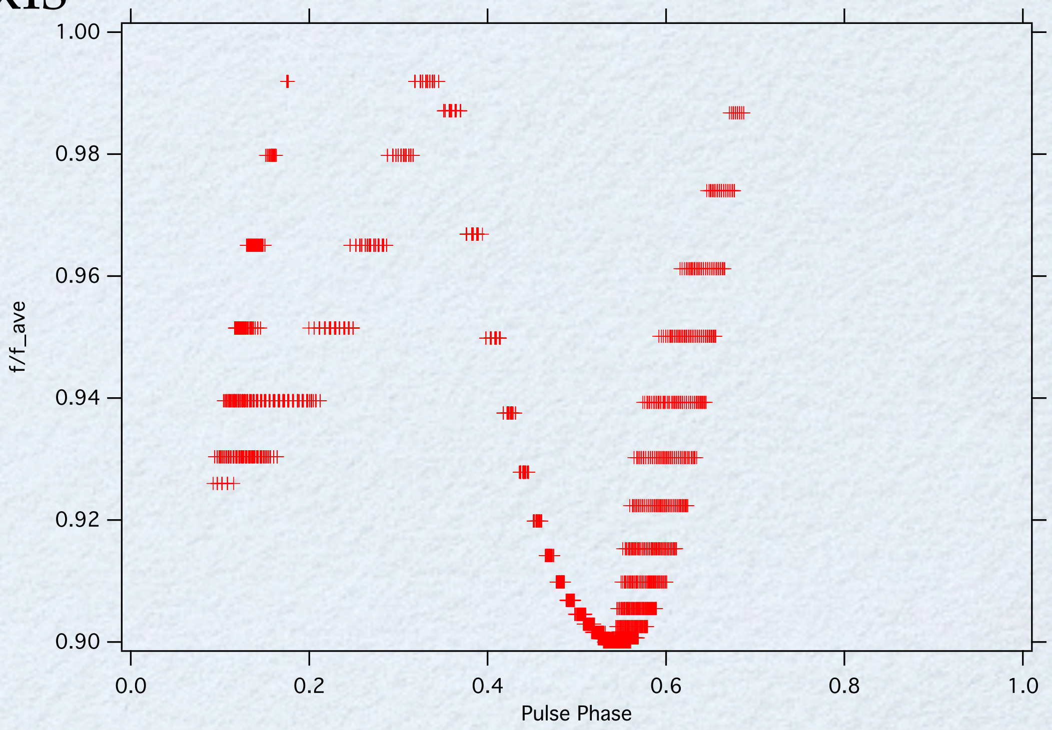

Distribution of the thickness of the screening region

Distribution of the thickness of the screening region

Most of the pairs screen out the acceleration electric field are come from the stellar surface.

(Takata, Wang & Cheng, 2010)

Distribution of the thickness of the screening region

Most of the pairs screen out the acceleration electric field are come from the stellar surface.

(Takata, Wang & Cheng, 2010)

More pairs available in the screening region, the thinner it is.

Distribution of the thickness of the screening region

Most of the pairs screen out the acceleration electric field are come from the stellar surface.

(Takata, Wang & Cheng, 2010)

More pairs available in the screening region, the thinner it is.

The closer the null charge surface to the stellar surface, the more pairs available.

Distribution of the thickness of the screening region

Most of the pairs screen out the acceleration electric field are come from the stellar surface.

(Takata, Wang & Cheng, 2010)

More pairs available in the screening region, the thinner it is.

The closer the null charge surface to the stellar surface, the more pairs available.

The closer the NCS is to the stellar surface, the thinner the screening region is.

Distribution of the thickness of the screening region

Most of the pairs screen out the acceleration electric field are come from the stellar surface.

(Takata, Wang & Cheng, 2010)

More pairs available in the screening region, the thinner it is.

The closer the null charge surface to the stellar surface, the more pairs available.

The closer the NCS is to the stellar surface, the thinner the screening region is.

$$\frac{h_1}{h_2}(\phi_p) = C_1 + \frac{C_2}{r_{null}(\phi_p)}$$

$$\frac{h_1}{h_2}(\phi_p) < 1$$

Distribution of the thickness of the screening region

Most of the pairs screen out the acceleration electric field are come from the stellar surface.

(Takata, Wang & Cheng, 2010)

More pairs available in the screening region, the thinner it is.

The closer the null charge surface to the stellar surface, the more pairs available.

The closer the NCS is to the stellar surface, the thinner the screening region is.

$$\frac{h_1}{h_2}(\phi_p) = C_1 + \frac{C_2}{r_{null}(\phi_p)}$$

$$\frac{h_1}{h_2}(\phi_p) < 1$$

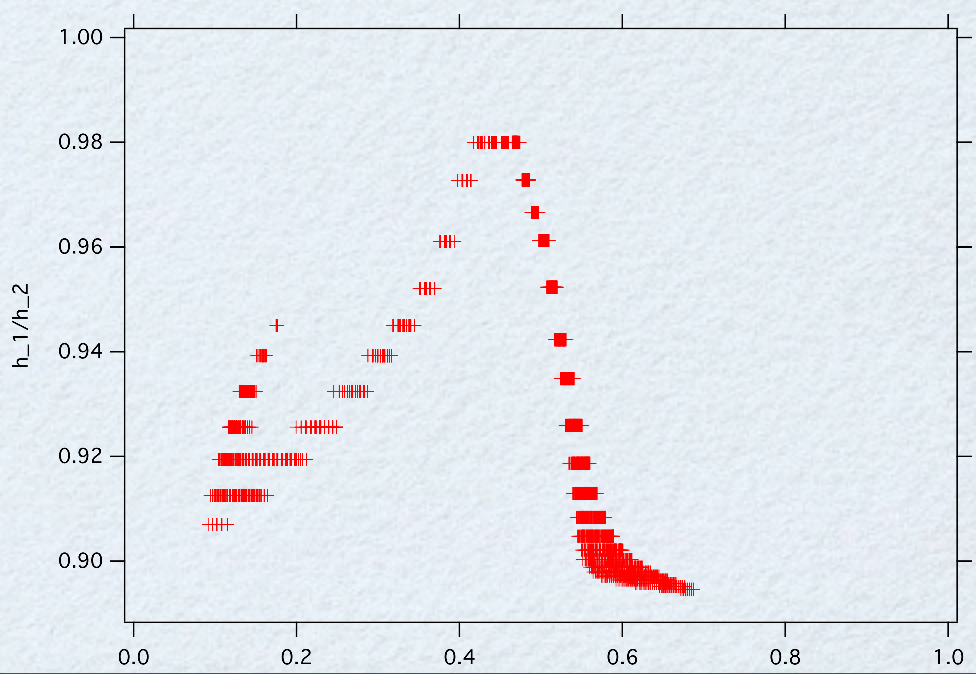

Distribution of the currents in the screening region and main acceleration region

Distribution of the currents in the screening region and main acceleration region

If the gap is thicker, there are more particles in it.

Distribution of the currents in the screening region and main acceleration region

If the gap is thicker, there are more particles in it.

$$N = h_2 \bar{\rho} \propto f$$

Distribution of the currents in the screening region and main acceleration region

If the gap is thicker, there are more particles in it.

$$N = h_2 \bar{\rho} \propto f$$

Because of the $\vec{E} \times \vec{B}$ drift

Distribution of the currents in the screening region and main acceleration region

If the gap is thicker, there are more particles in it.

$$N = h_2 \bar{\rho} \propto f$$

Because of the $\vec{E} \times \vec{B}$ drift

$$h_2(\phi_p)\bar{\rho}(\phi_p) \propto f(\phi_p + \Delta\phi_p)$$

Distribution of the currents in the screening region and main acceleration region

If the gap is thicker, there are more particles in it.

$$N = h_2 \bar{\rho} \propto f$$

Because of the $\vec{E} \times \vec{B}$ drift

$$h_2(\phi_p)\bar{\rho}(\phi_p) \propto f(\phi_p + \Delta\phi_p)$$

$$h_2(\phi_p) \sim f(\phi_p) r(\phi_p)$$

Distribution of the currents in the screening region and main acceleration region

If the gap is thicker, there are more particles in it.

$$N = h_2\bar{\rho} \propto f$$

Because of the $\vec{E} \times \vec{B}$ drift

$$h_2(\phi_p)\bar{\rho}(\phi_p) \propto f(\phi_p + \Delta\phi_p)$$

$$h_2(\phi_p) \sim f(\phi_p)r(\phi_p)$$

$$\bar{\rho}(\phi_p) \propto \frac{f(\phi_p + \Delta\phi_p)}{f(\phi_p)r(\phi_p)}$$

Distribution of the currents in the screening region and main acceleration region

If the gap is thicker, there are more particles in it.

$$N = h_2 \bar{\rho} \propto f$$

Because of the $\vec{E} \times \vec{B}$ **drift**

$$h_2(\phi_p)\bar{\rho}(\phi_p) \propto f(\phi_p + \Delta\phi_p)$$

$$h_2(\phi_p) \sim f(\phi_p) r(\phi_p)$$

$$\bar{\rho}(\phi_p) \propto \frac{f(\phi_p + \Delta\phi_p)}{f(\phi_p) r(\phi_p)}$$

$$\bar{\rho}(\phi_p) = C_1 + C_2 \frac{f(\phi_p + \Delta\phi_p)}{f(\phi_p) r(\phi_p)}$$

Distribution of the currents in the screening region and main acceleration region

If the gap is thicker, there are more particles in it.

$$N = h_2 \bar{\rho} \propto f$$

Because of the $\vec{E} \times \vec{B}$ drift

$$h_2(\phi_p)\bar{\rho}(\phi_p) \propto f(\phi_p + \Delta\phi_p)$$

$$h_2(\phi_p) \sim f(\phi_p) r(\phi_p)$$

$$\bar{\rho}(\phi_p) \propto \frac{f(\phi_p + \Delta\phi_p)}{f(\phi_p) r(\phi_p)}$$

$$\bar{\rho}(\phi_p) = C_1 + C_2 \frac{f(\phi_p + \Delta\phi_p)}{f(\phi_p) r(\phi_p)}$$

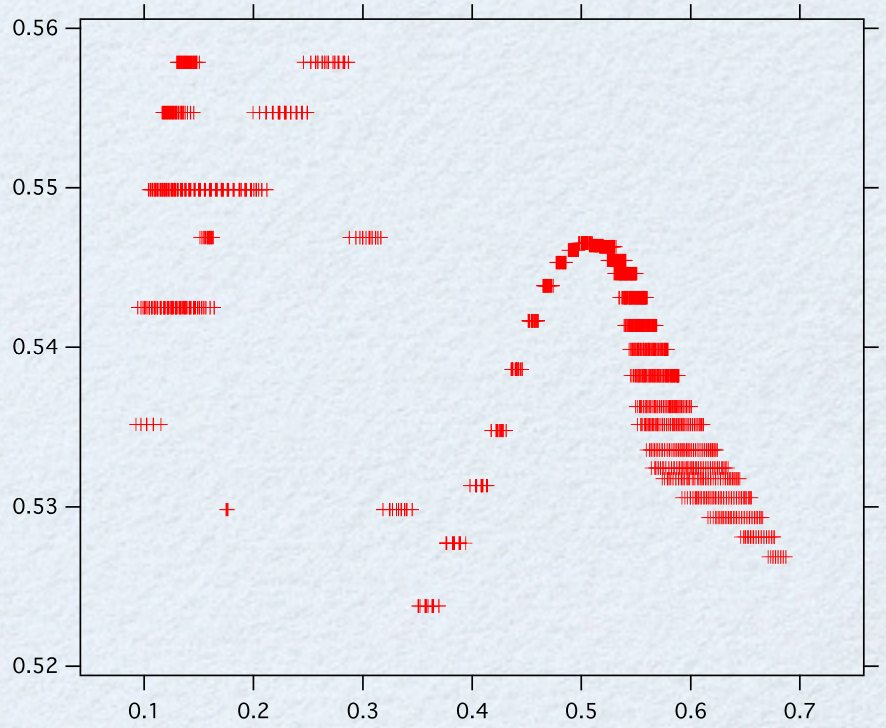

$$h_2\bar{\rho}(\phi_p) = h_1\rho_1 + (h_2 - h_1)\rho_2$$

$$(\frac{h_2}{h_1})^2 = 1 + g_1/g_2$$

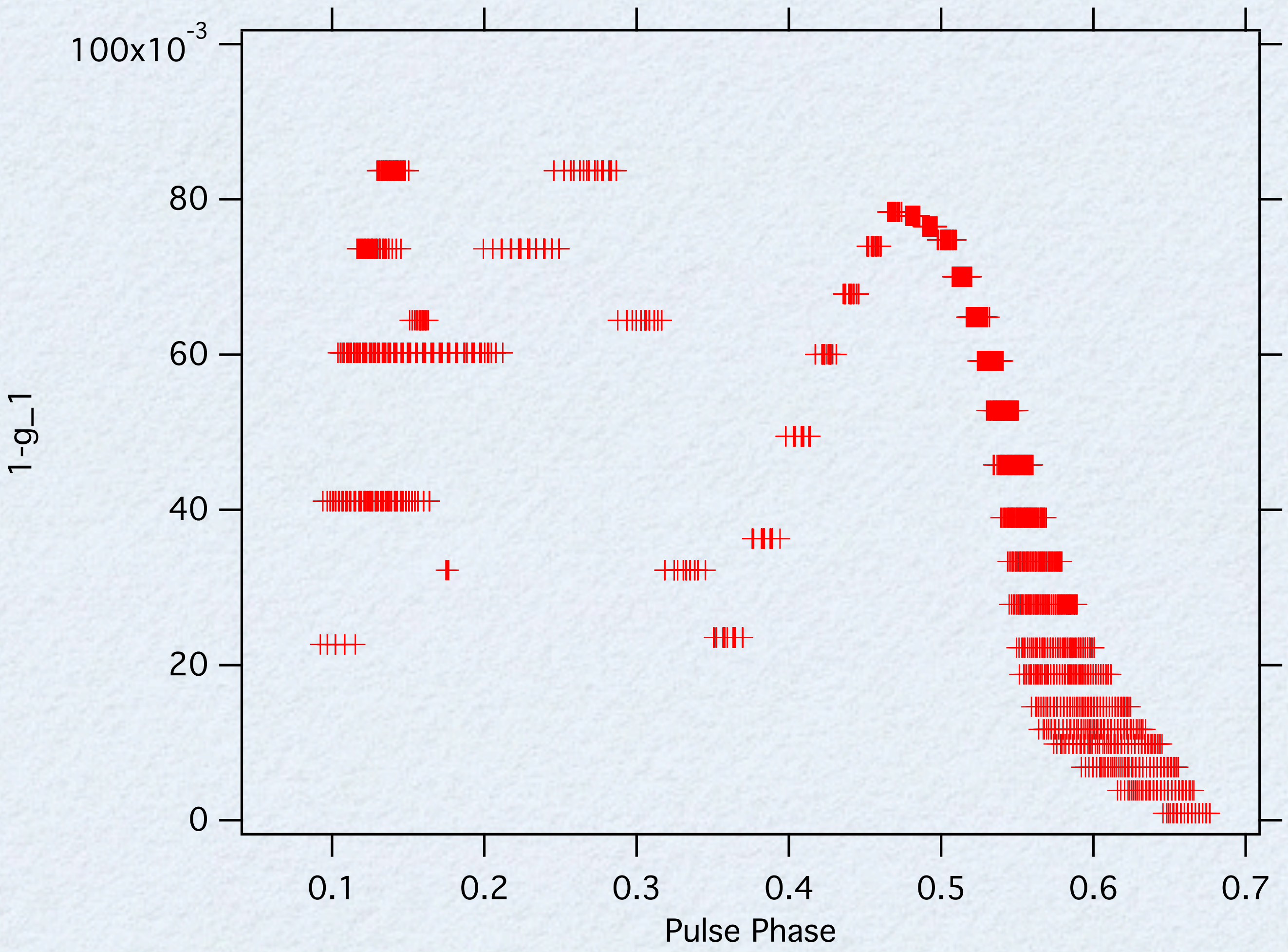

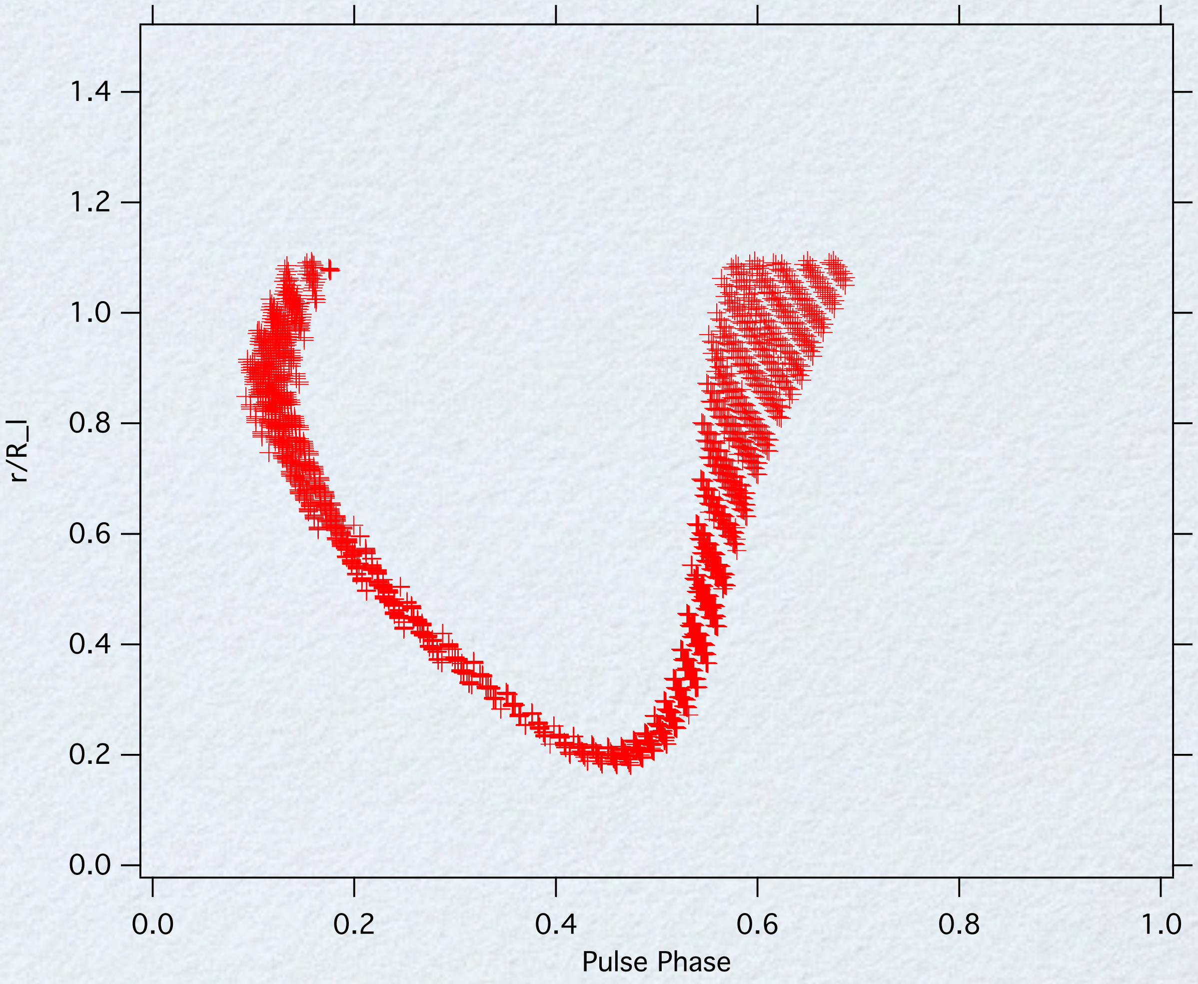

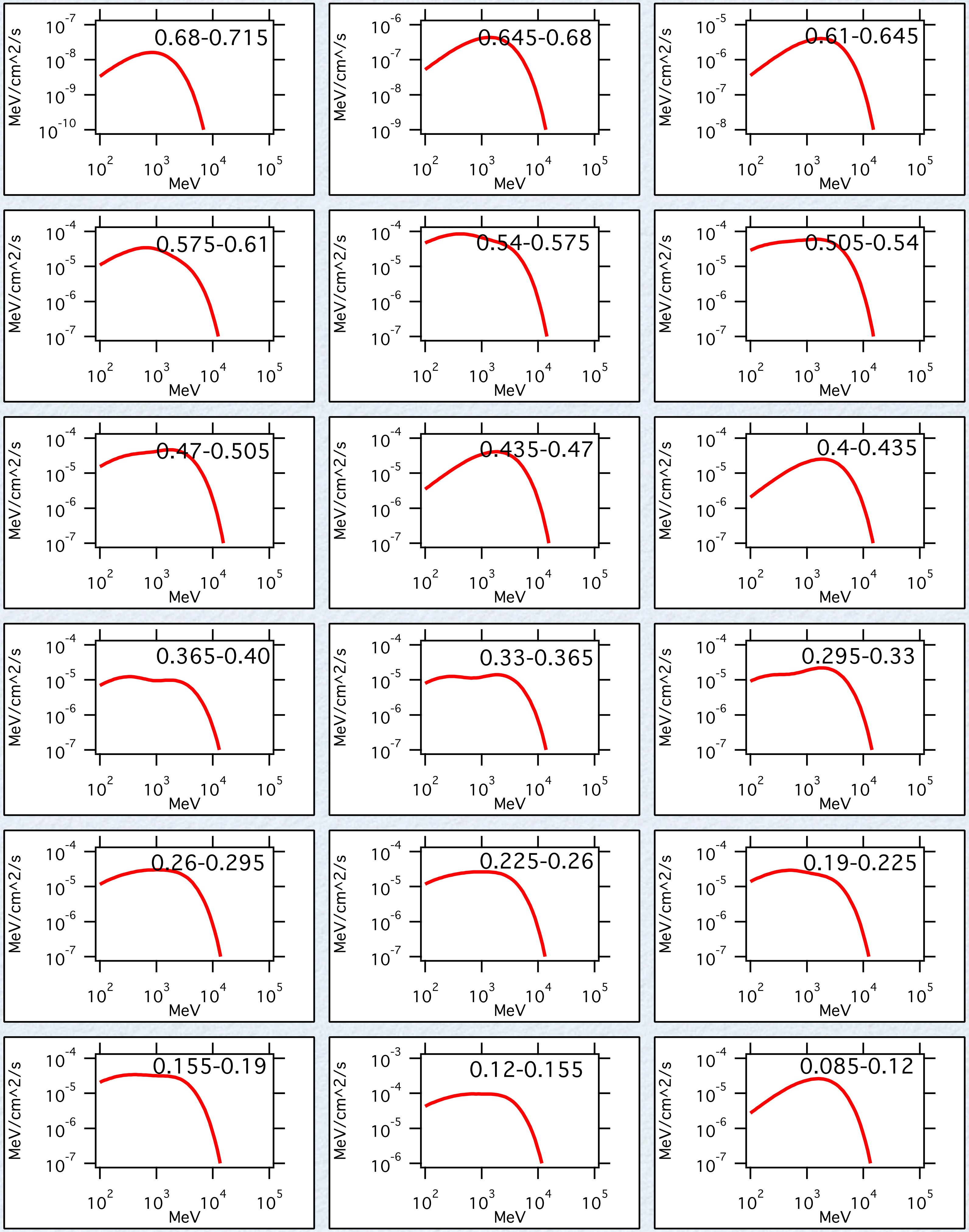

0.68-0.715
0.645-0.68
0.61-0.645
0.575-0.61
0.54-0.575
0.505-0.54
0.47-0.505
0.435-0.47
0.4-0.435
0.365-0.40
0.33-0.365
0.295-0.33
0.26-0.295
0.225-0.26
0.19-0.225
0.155-0.19
0.12-0.155
0.085-0.12
MeV/cm^2/s
MeV

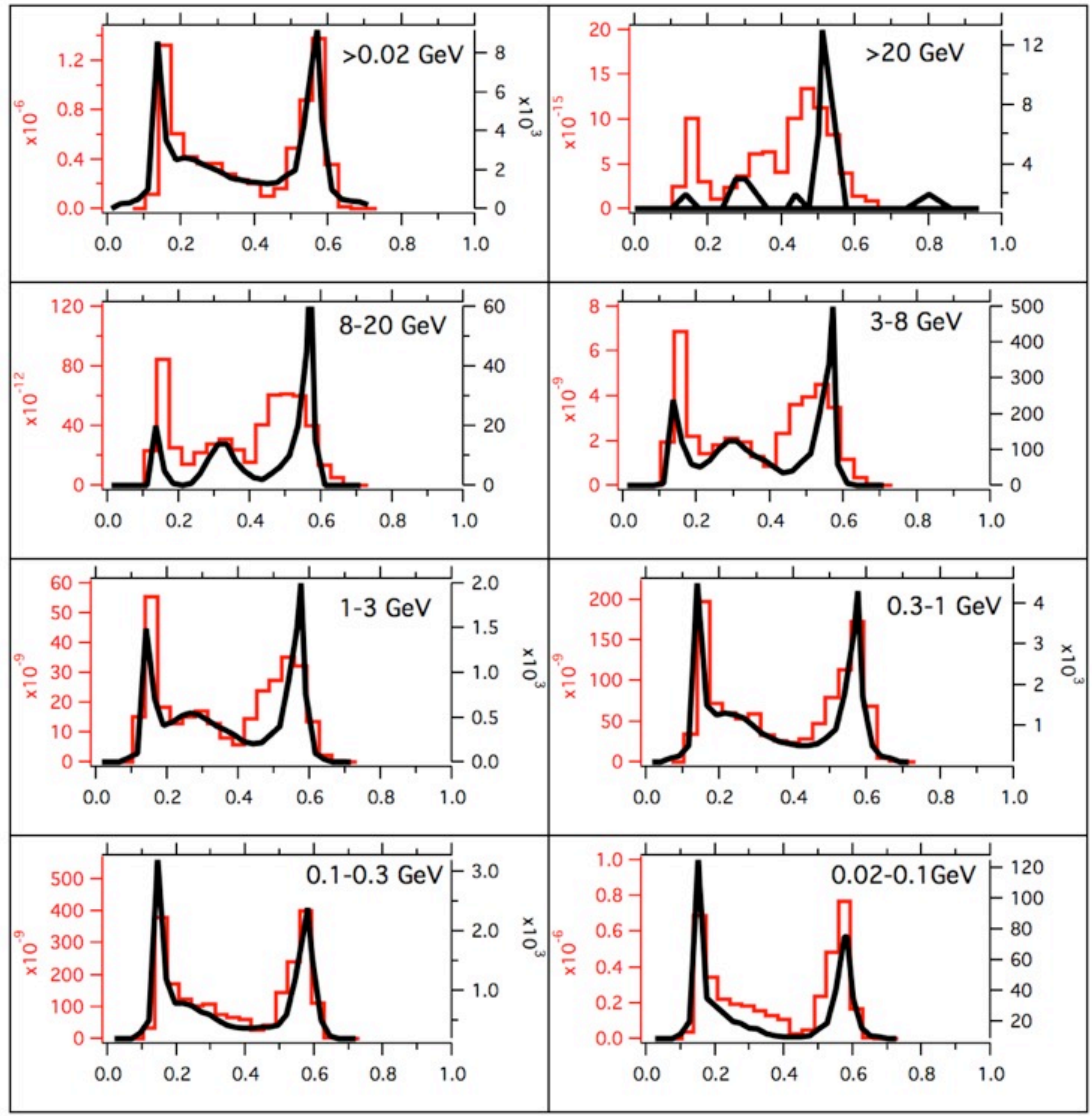

The black lines are the observed energy dependent light curves of Vela from the Fermi LAT, which are taken from Abdo et al. (2009)

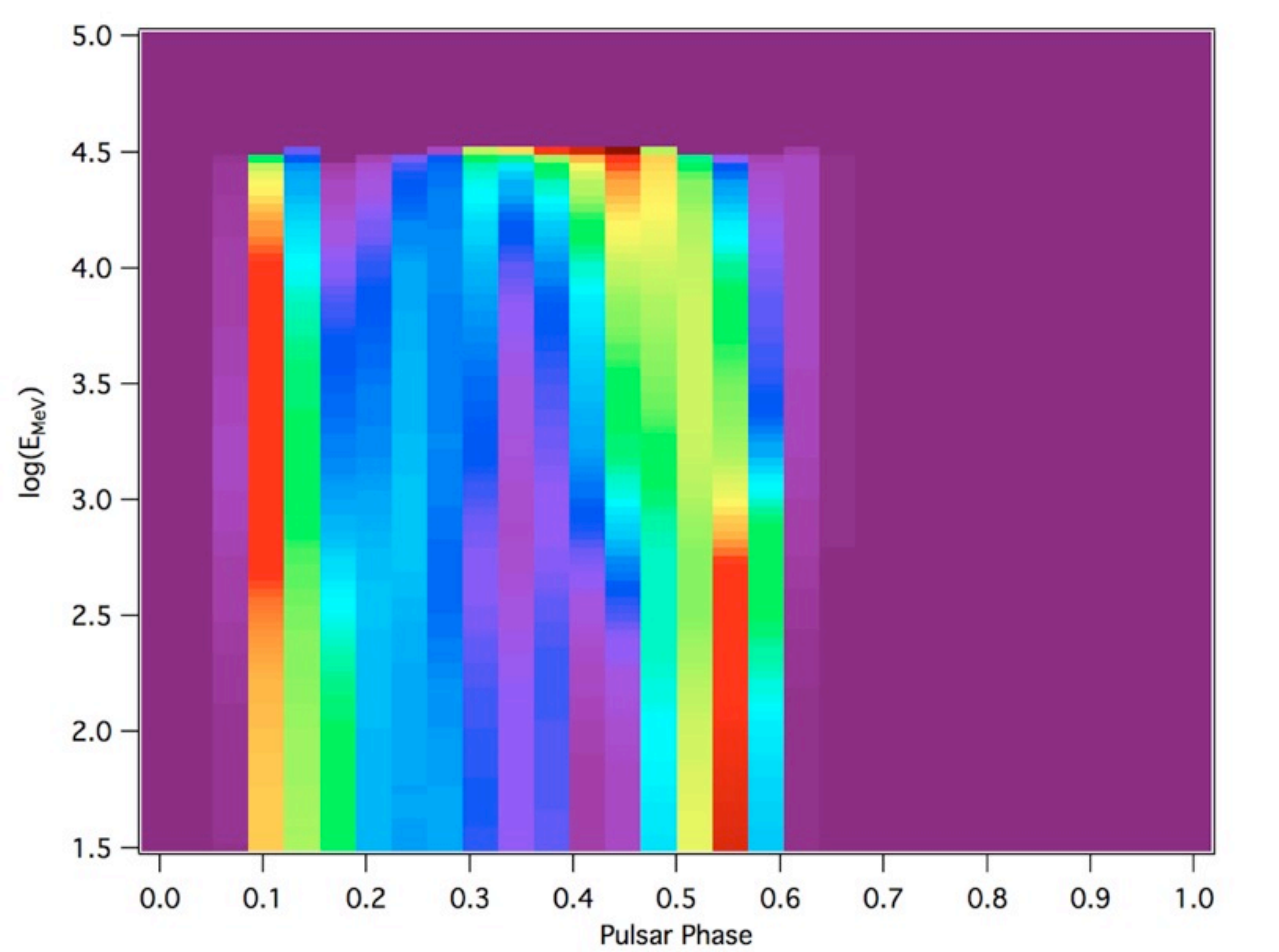

5.0
4.5
4.0
3.5
3.0
2.5
2.0
1.5
log(E_MeV)
0.0
0.1
0.2
0.3
0.4
0.5
0.6
0.7
0.8
0.9
1.0
Pulsar Phase

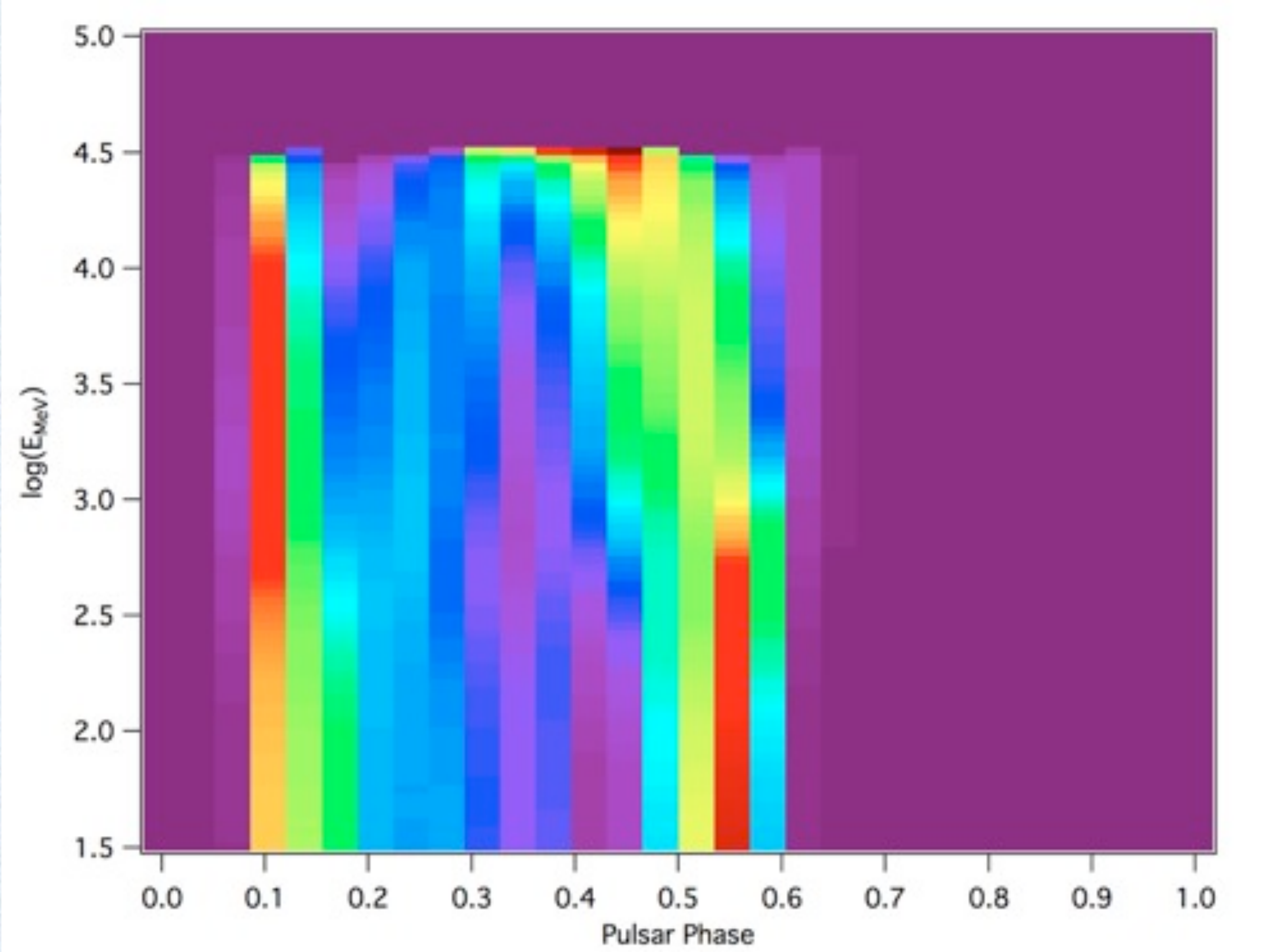

5.0
4.5
4.0
3.5
3.0
2.5
2.0
1.5
log(E_MeV)
0.0
0.1
0.2
0.3
0.4
0.5
0.6
0.7
0.8
0.9
1.0
Pulsar Phase

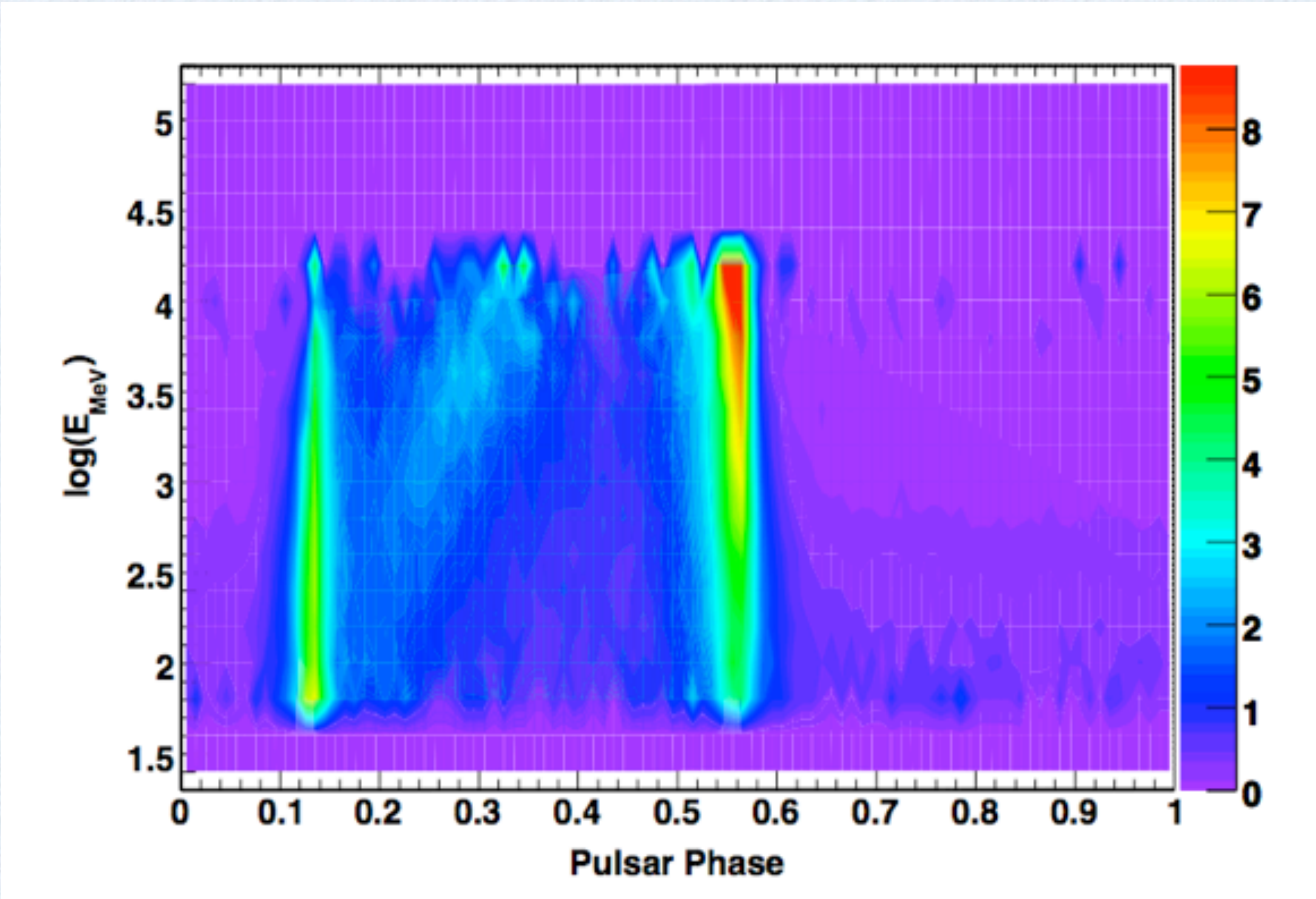

Abdo et al. (2009)

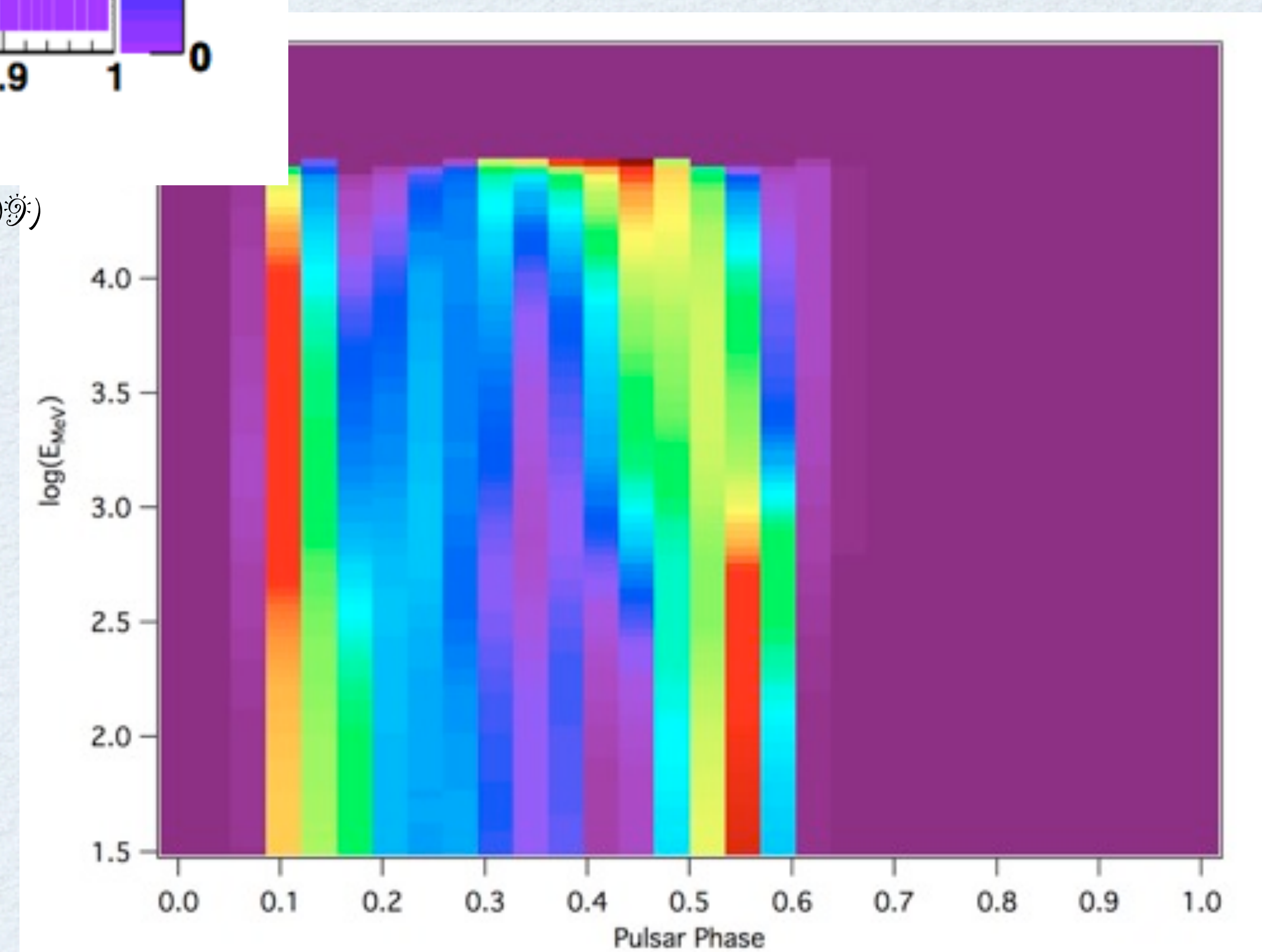

Why the P3 moves?

Why the P3 moves?

The reason will become clear after the effects of the distributions on the light curves are shown.

The effect of the distribution of current on the energy dependent light curves

The effect of the distribution of current on the energy dependent light curves

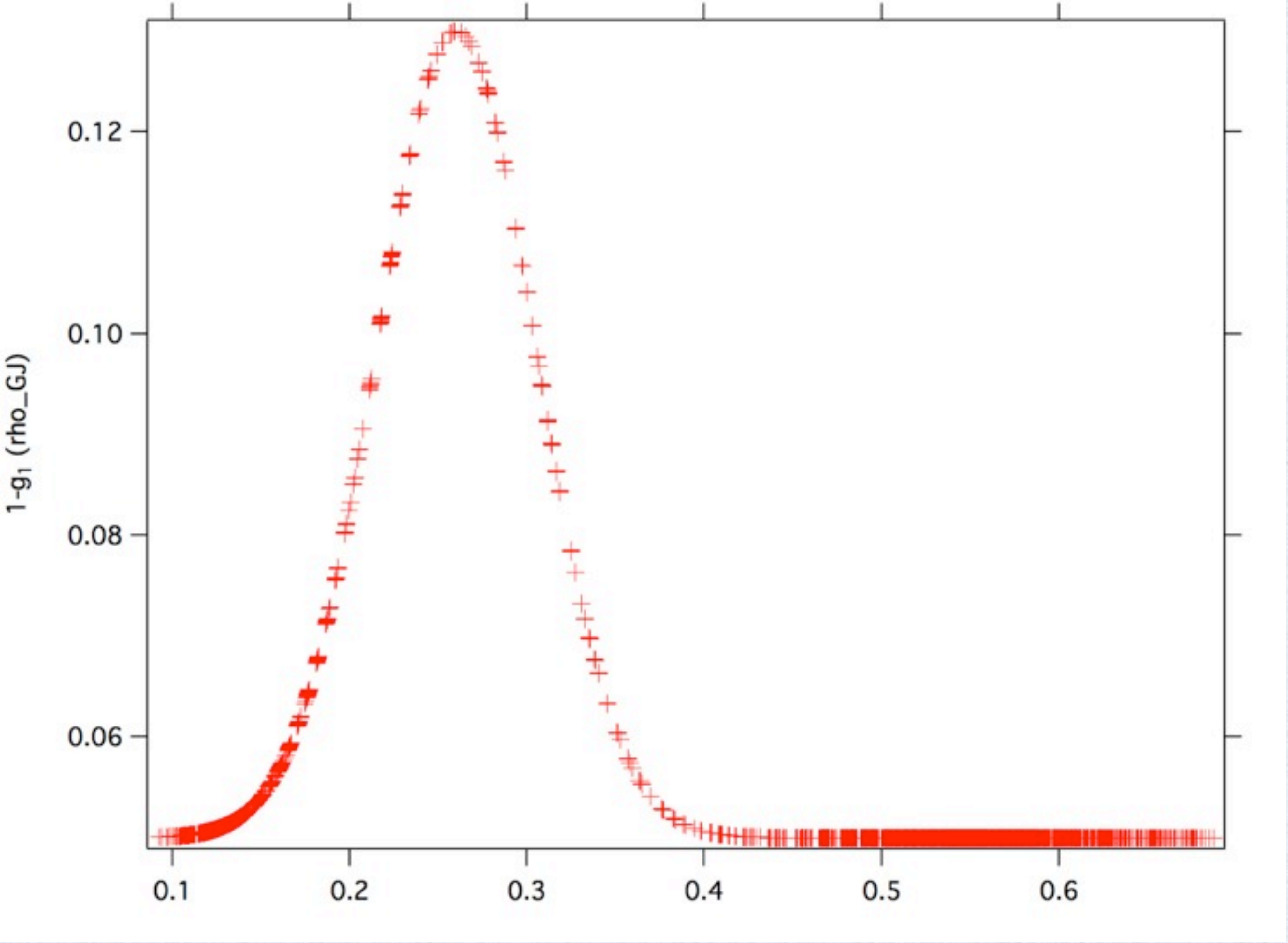

The effect of the distribution of current on the energy dependent light curves

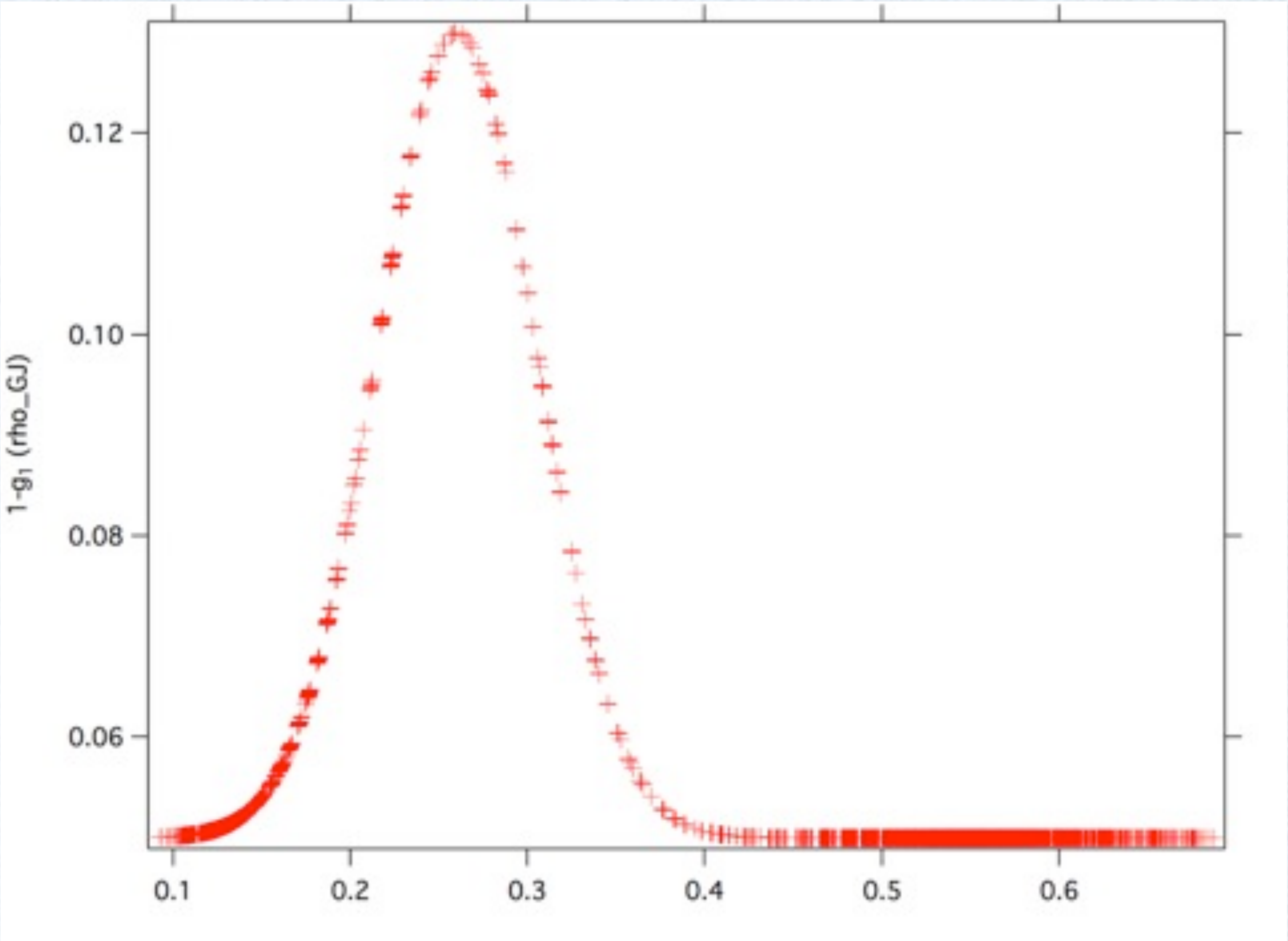

The effect of the distribution of current on the energy dependent light curves

$$h_1/h_2 = 0.927$$

$$f = 0.16$$

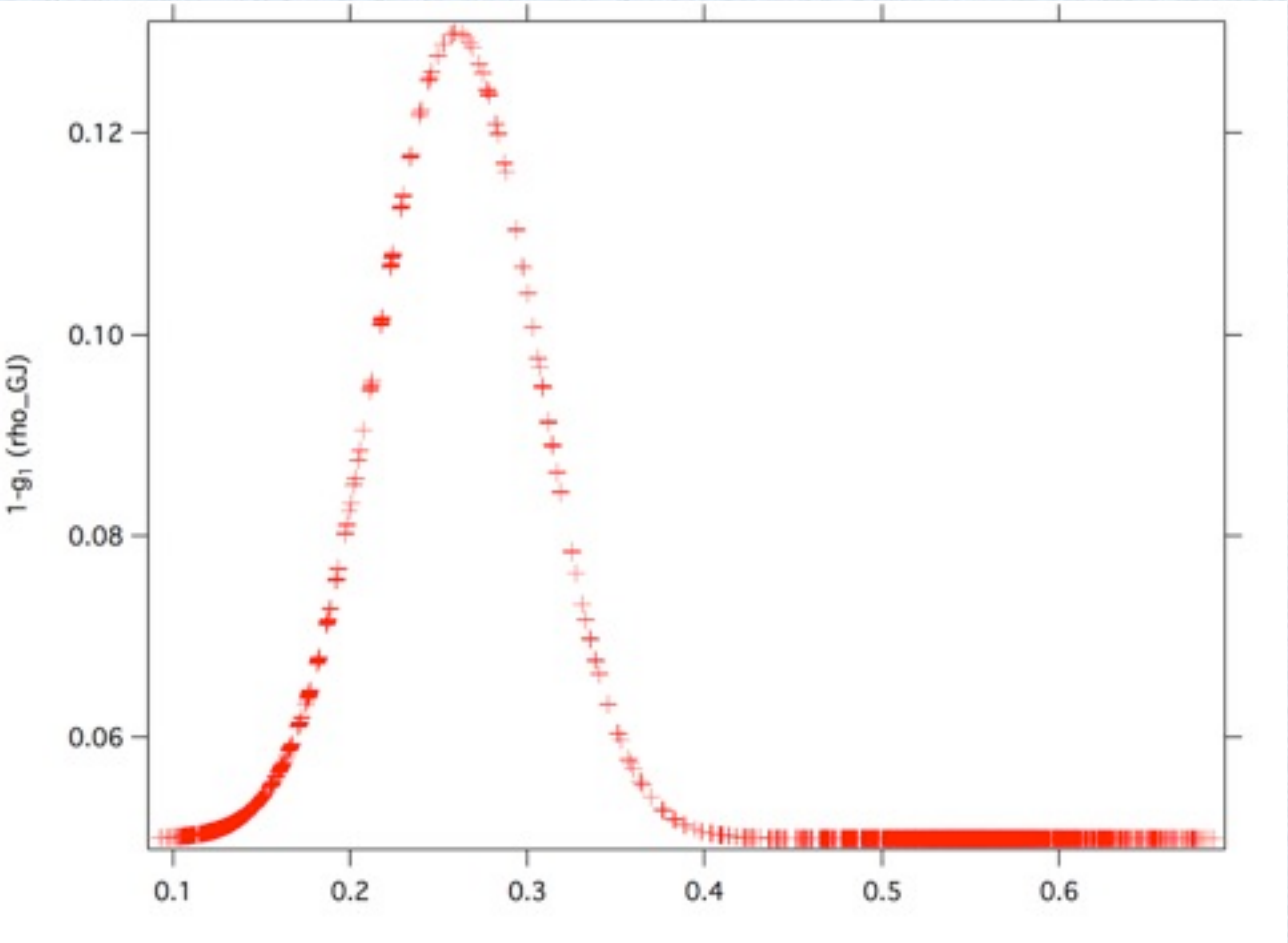

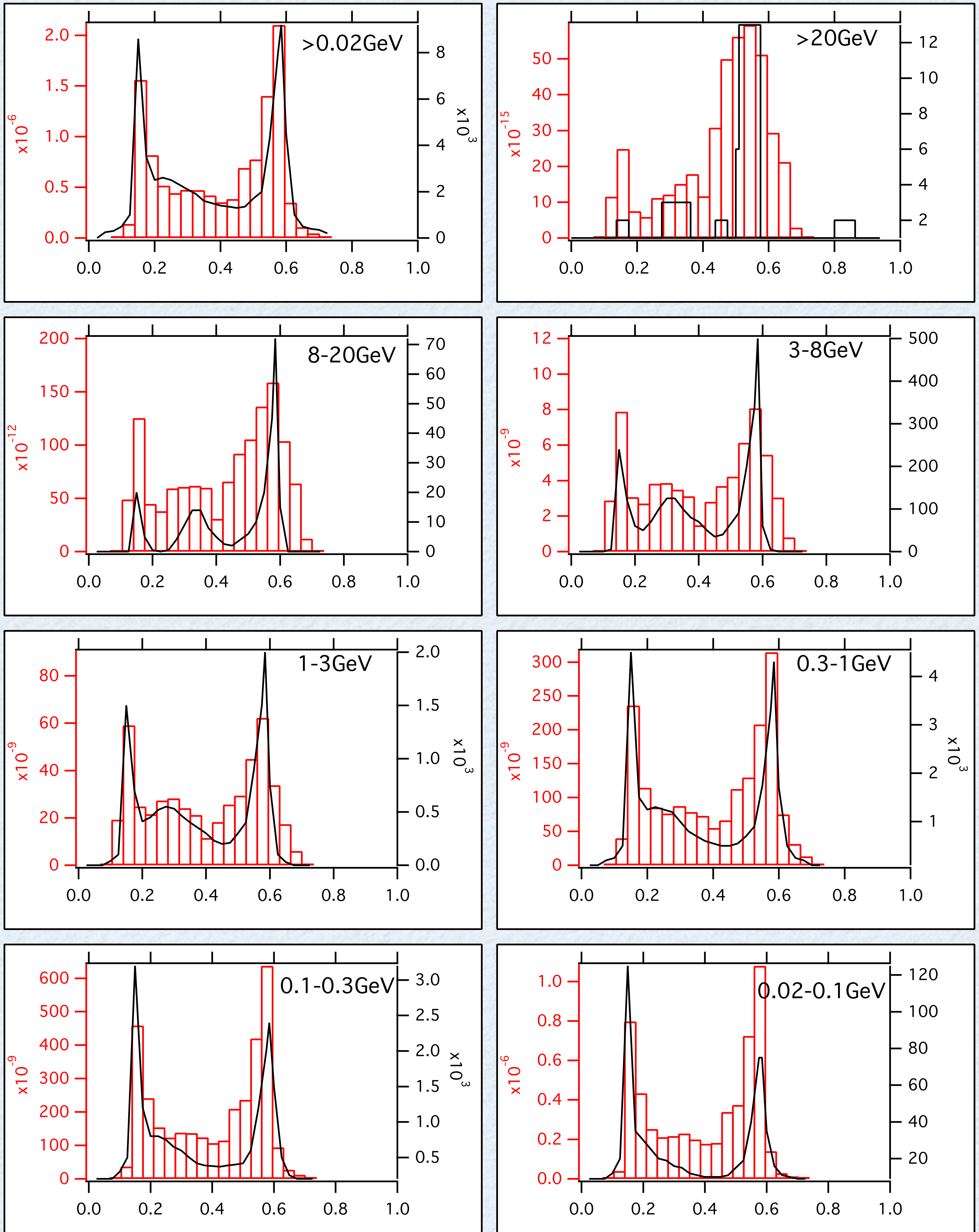

The black lines are the observed energy dependent light curves of Vela from the Fermi LAT, which are taken from Abdo et al. (2009)

The effect of the distribution of the "f" on the energy dependent light curves

The effect of the distribution of the “f” on the energy dependent light curves

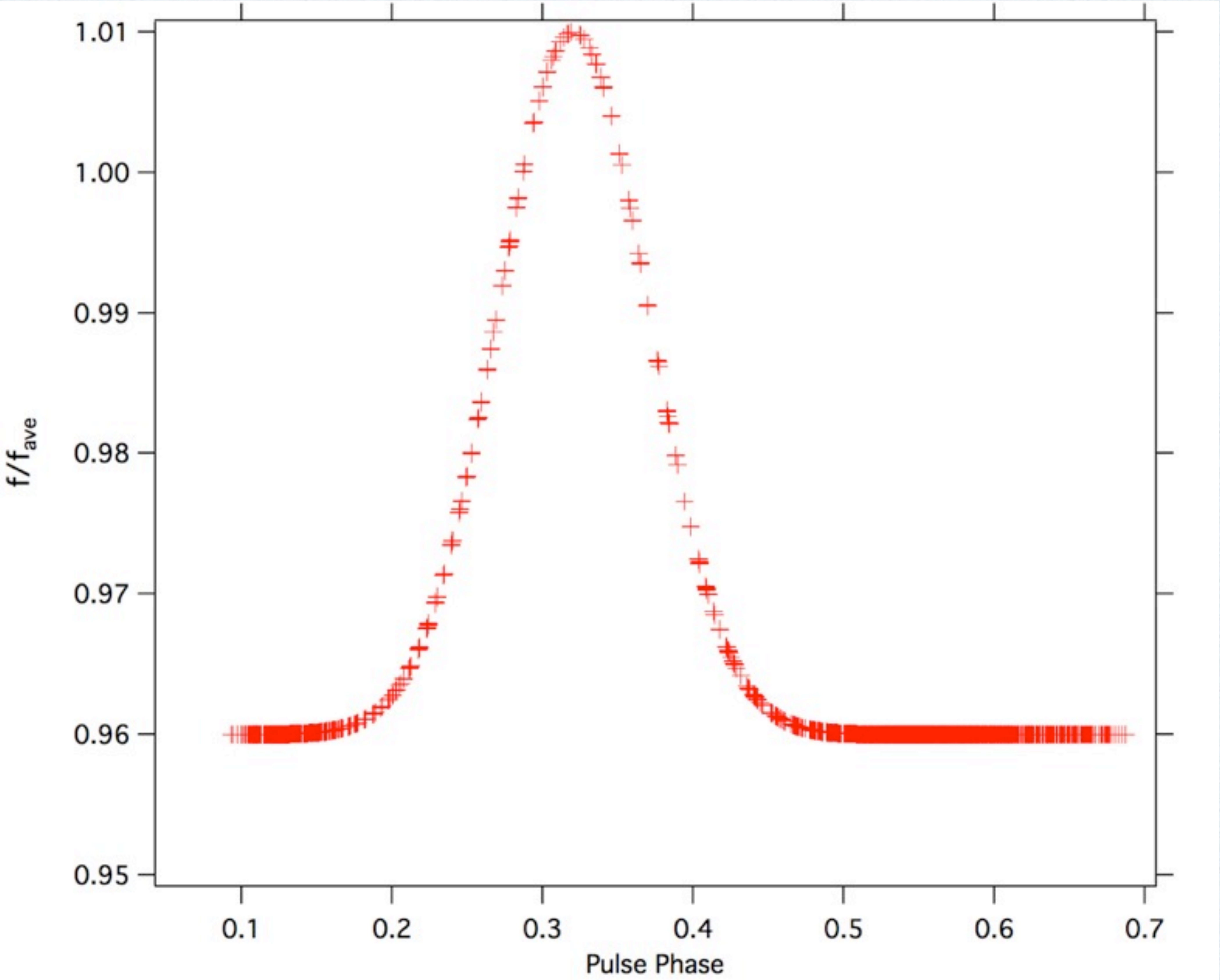

The effect of the distribution of the "f" on the energy dependent light curves

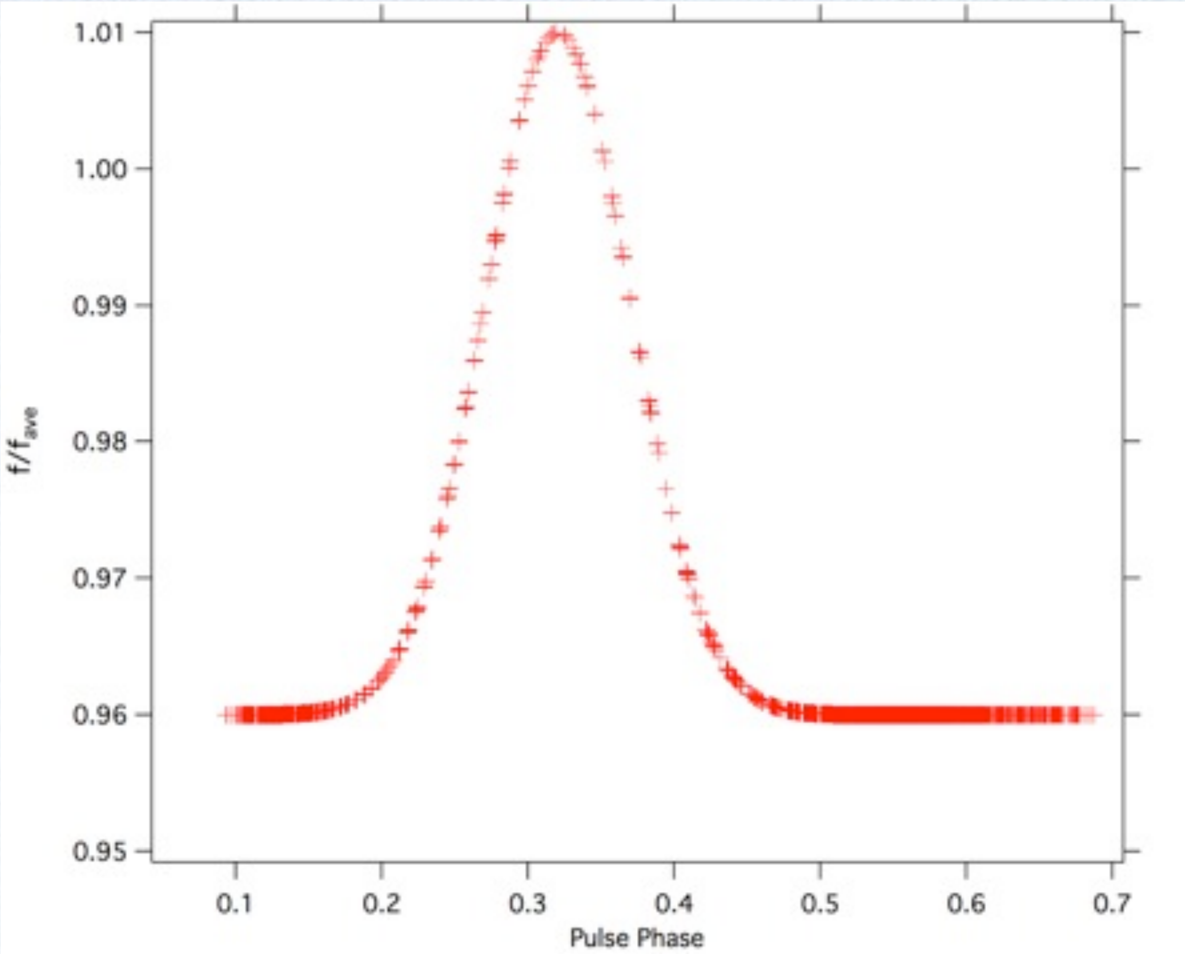

The effect of the distribution of the "f" on the energy dependent light curves

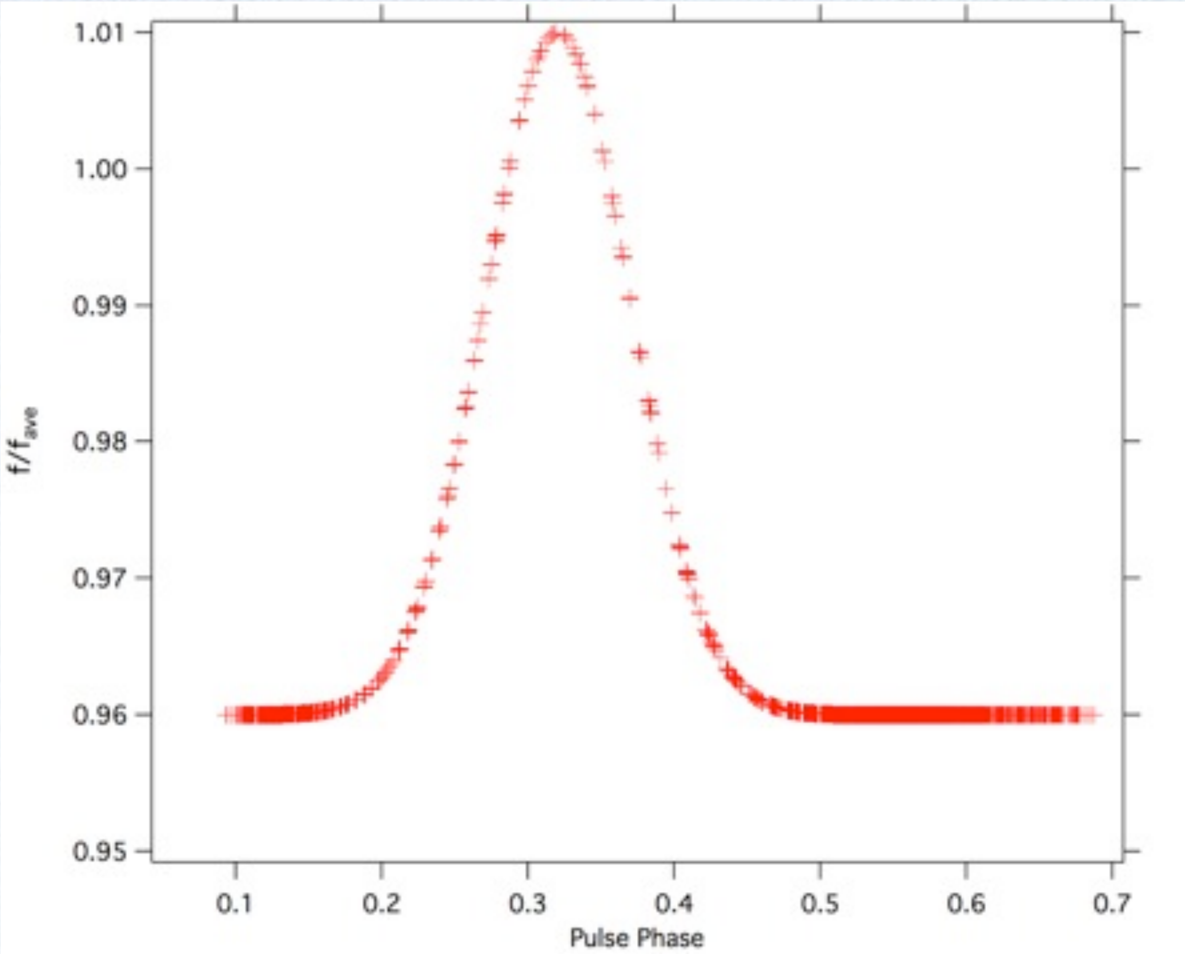

$$1 - g_1 = 0.08$$

$$h_1/h_2 = 0.927$$

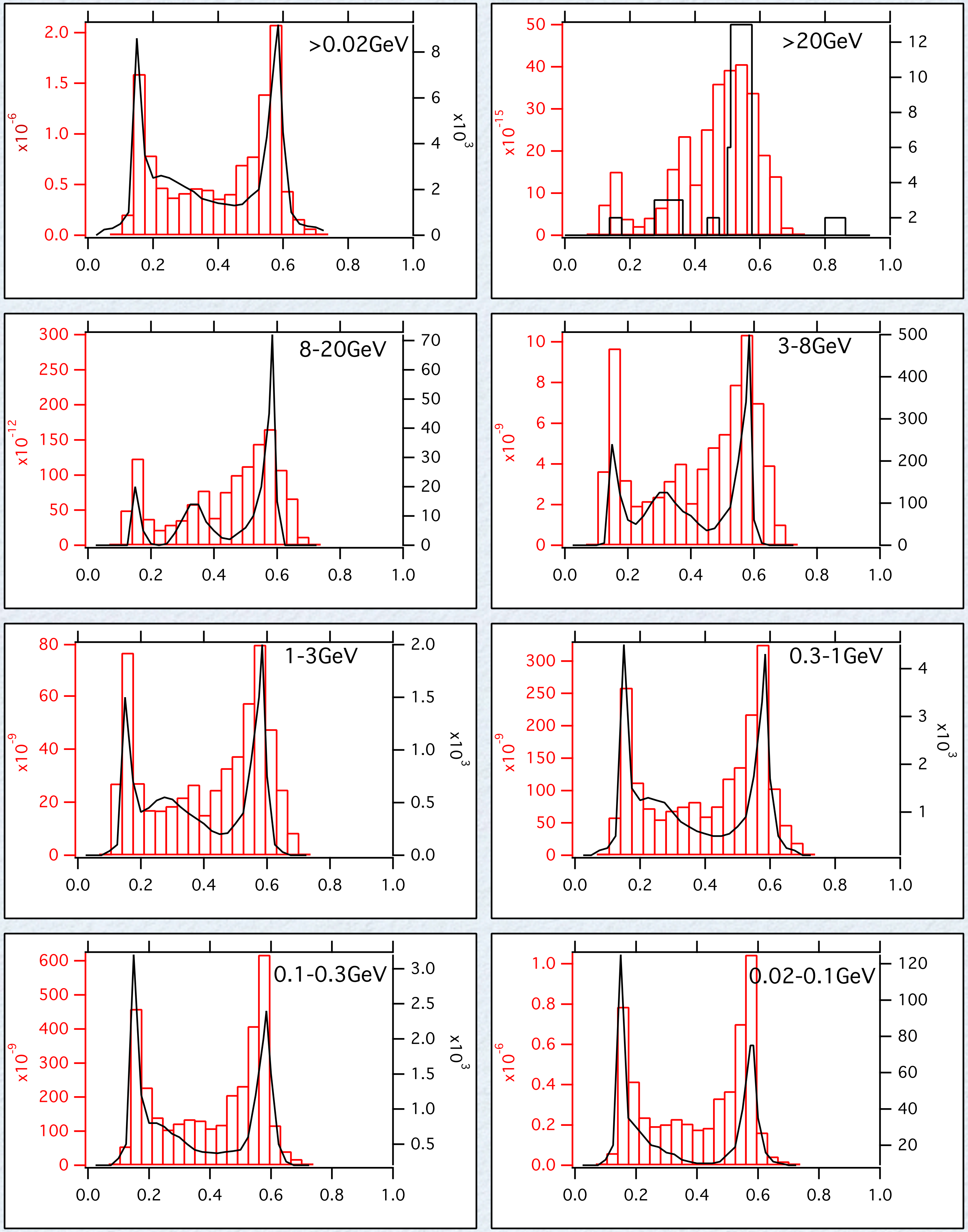

The black lines are the observed energy dependent light curves of Vela from the Fermi LAT, which are taken from Abdo et al. (2009)

The effect of the distribution of the thickness of the main acceleration region on the energy dependent light curves

The effect of the distribution of the thickness of the main acceleration region on the energy dependent light curves

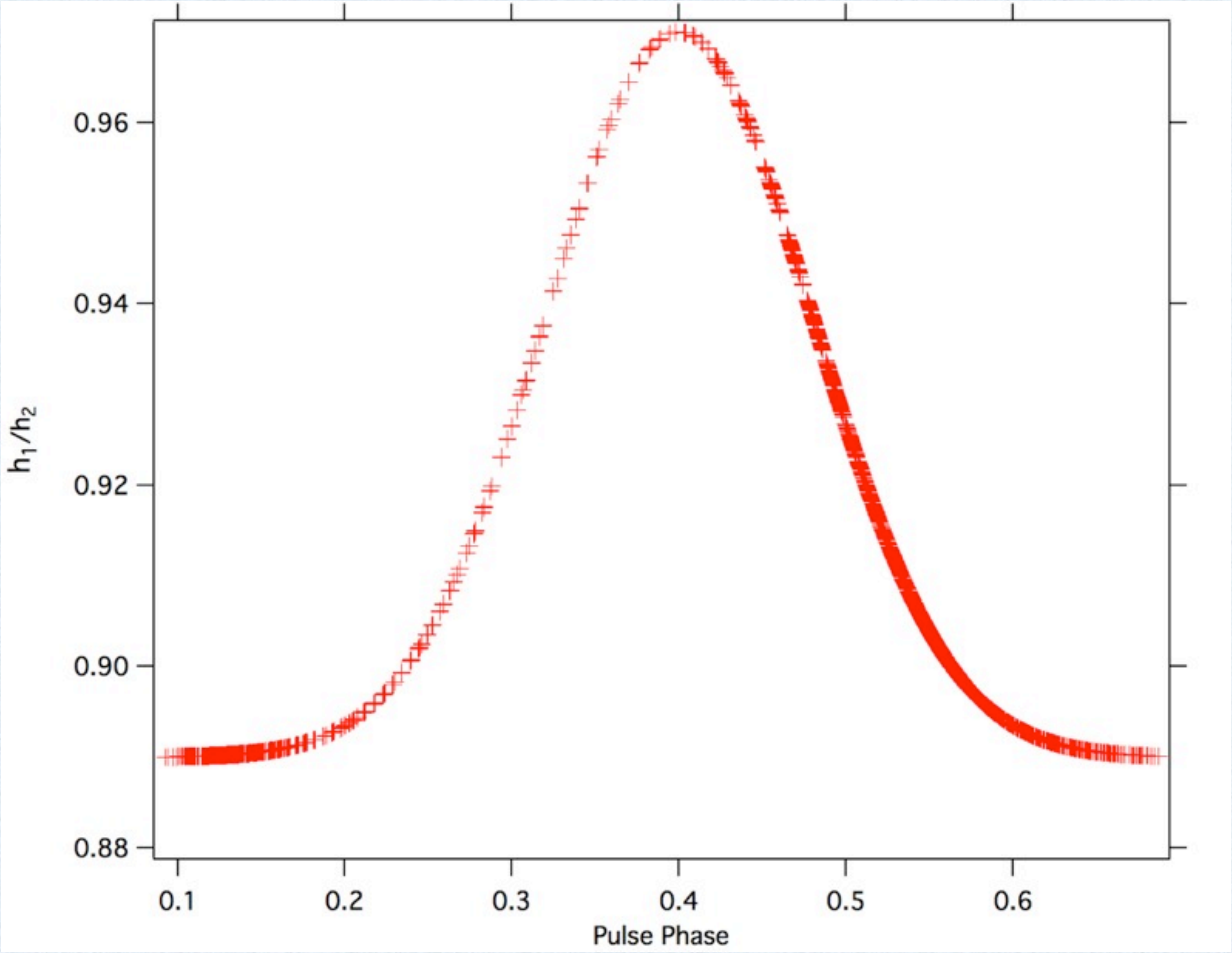

The effect of the distribution of the thickness of the main acceleration region on the energy dependent light curves

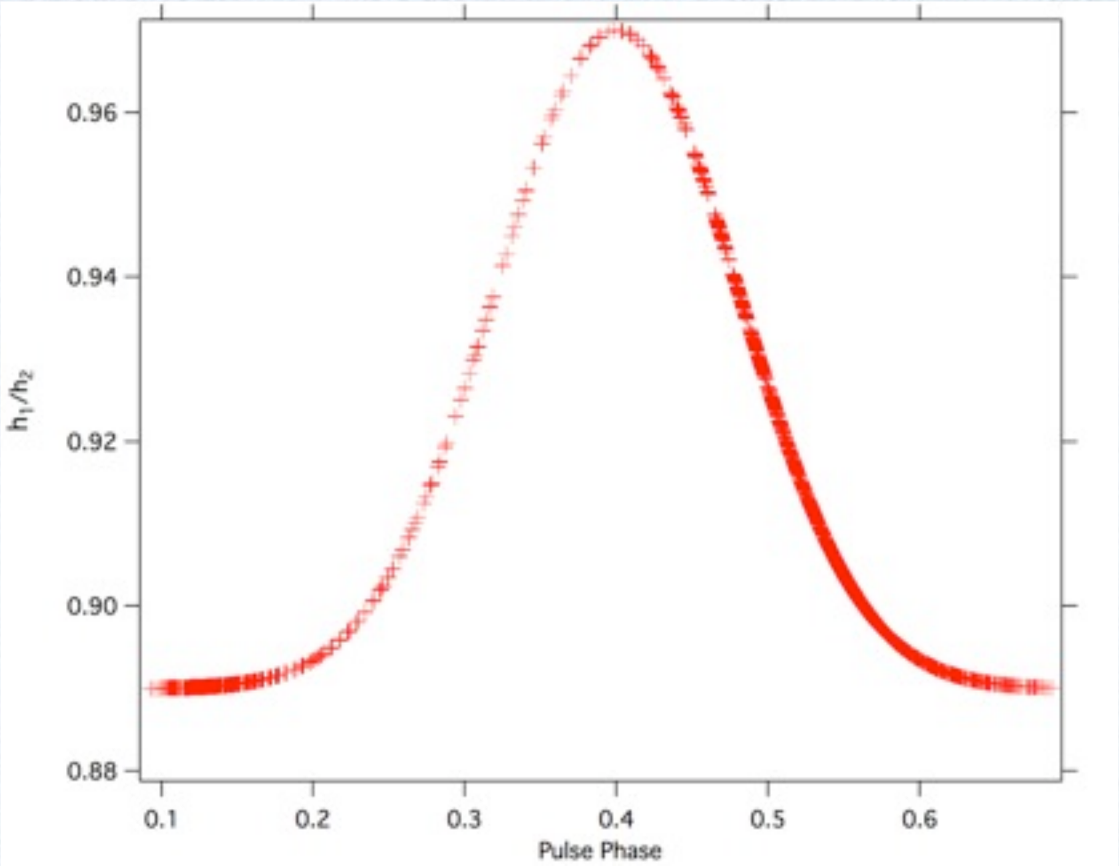

The effect of the distribution of the thickness of the main acceleration region on the energy dependent light curves

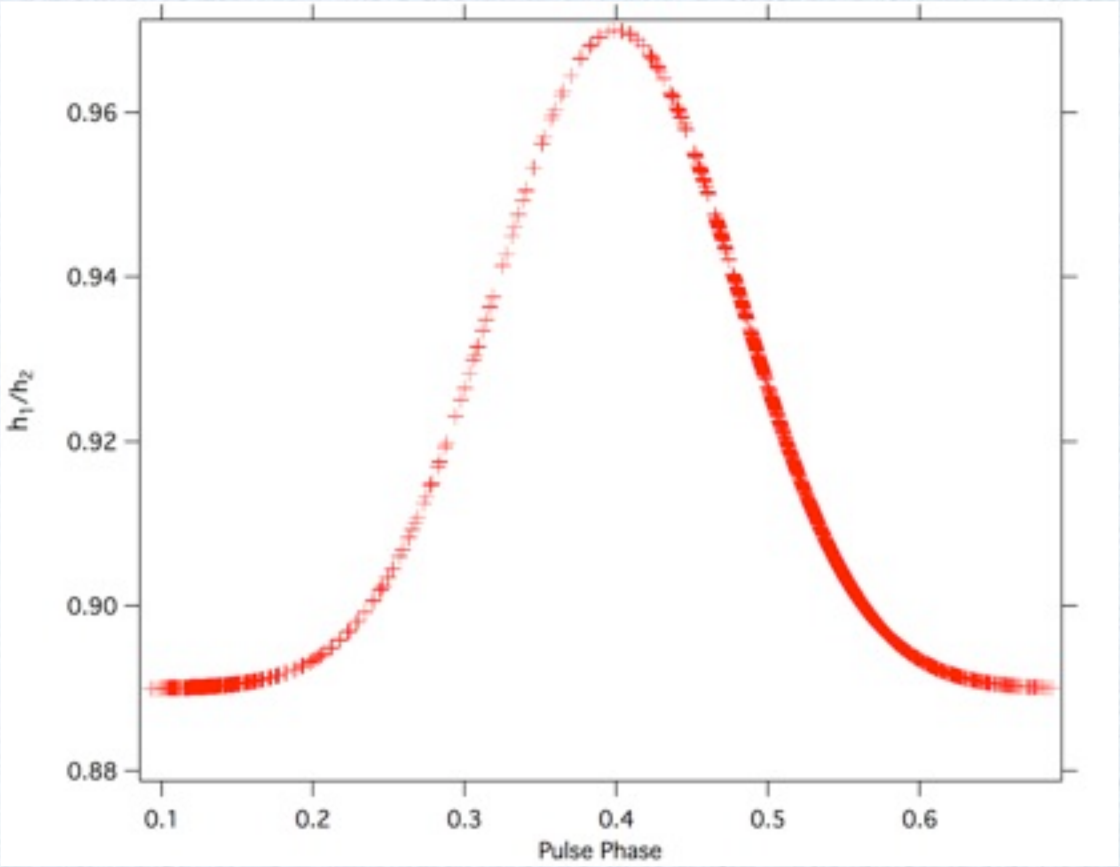

$$
\begin{aligned}
1 - g_1 &= 0.08 \\
f &= 0.16
\end{aligned}
$$

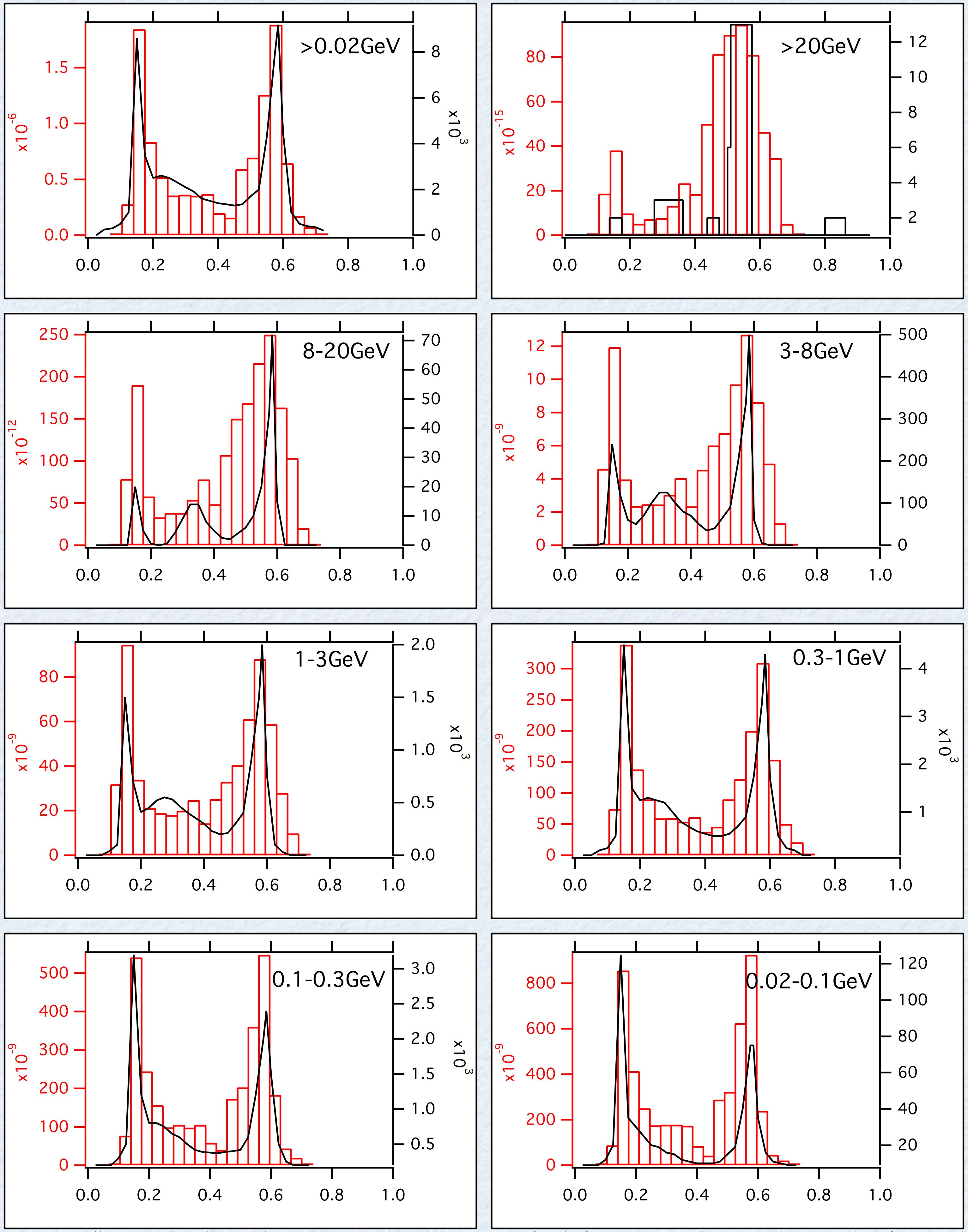

The black lines are the observed energy dependent light curves of Vela from the Fermi LAT, which are taken from Abdo et al. (2009)

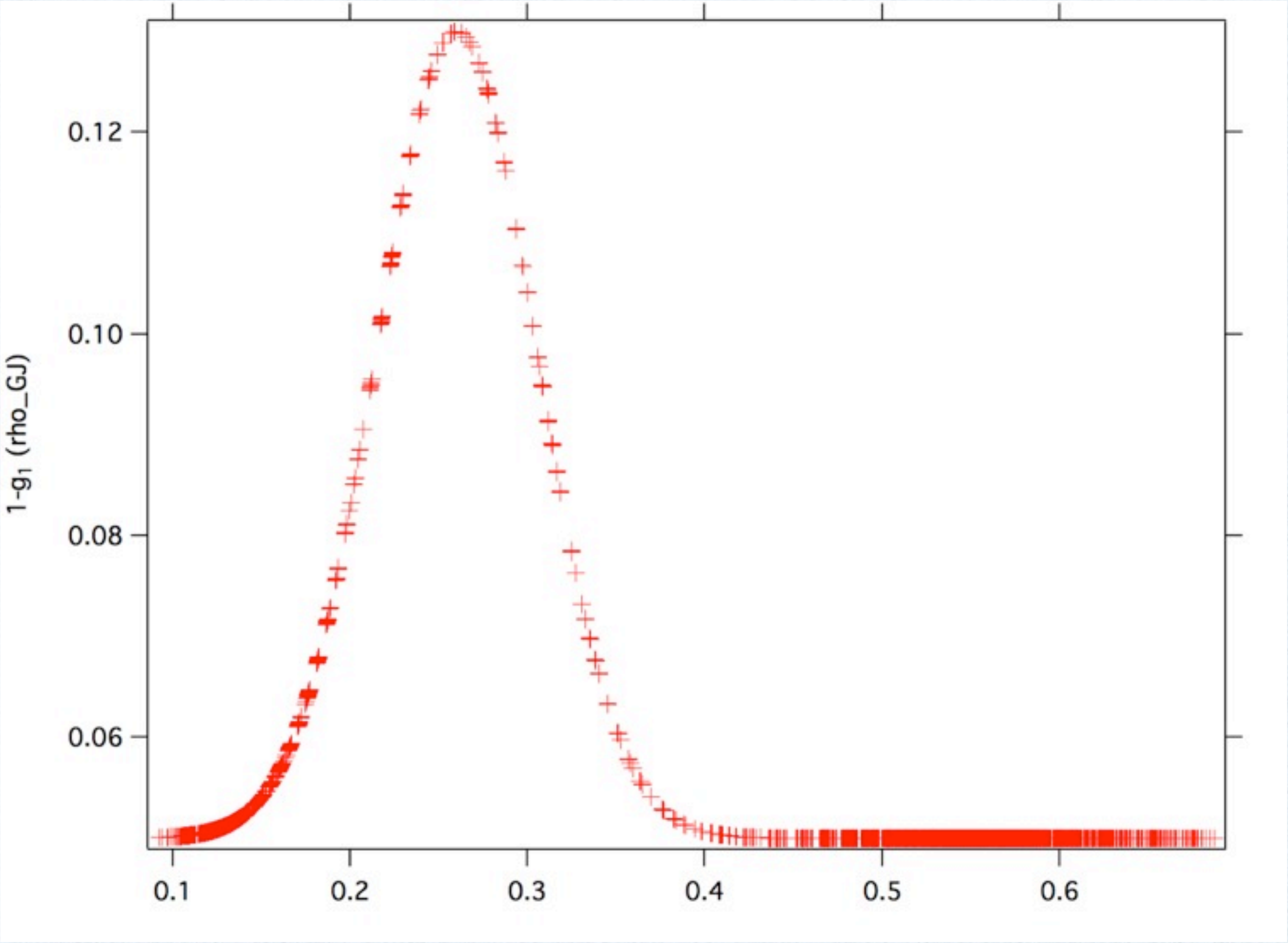
1-g1 (rho_GJ)
0.12
0.10
0.08
0.06
0.1
0.2
0.3
0.4
0.5
0.6

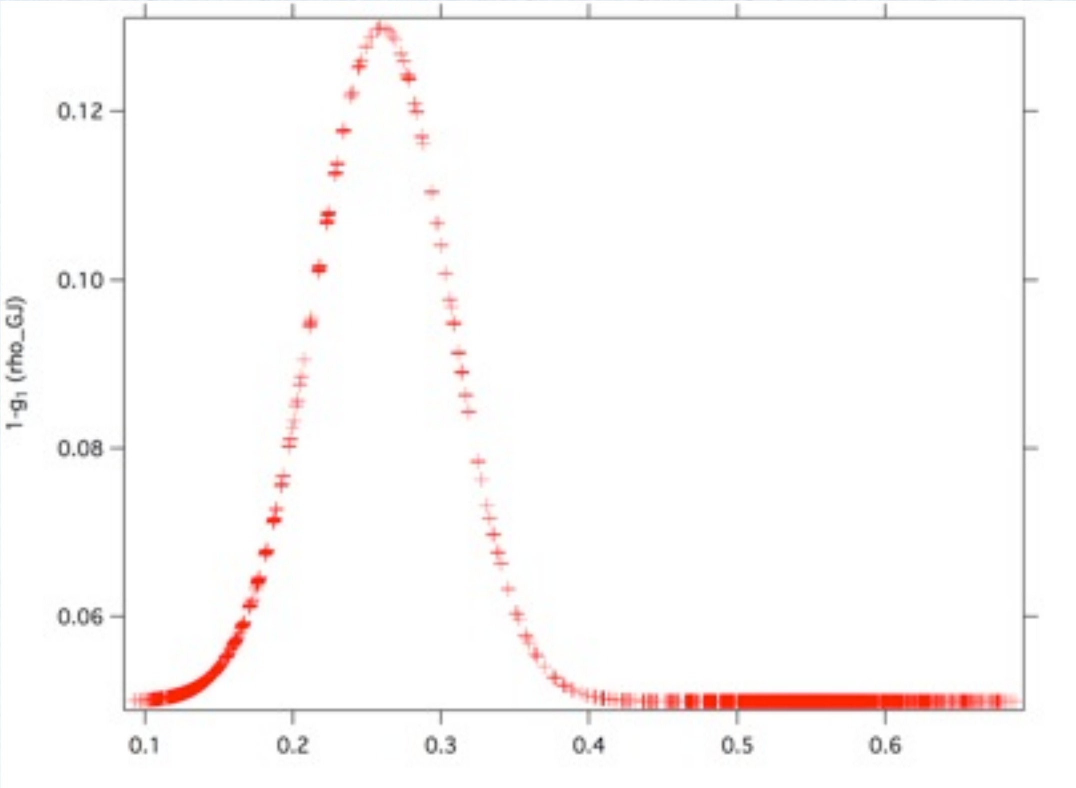

1-g1 (rho_GJ)
0.12
0.10
0.08
0.06
0.1
0.2
0.3
0.4
0.5
0.6

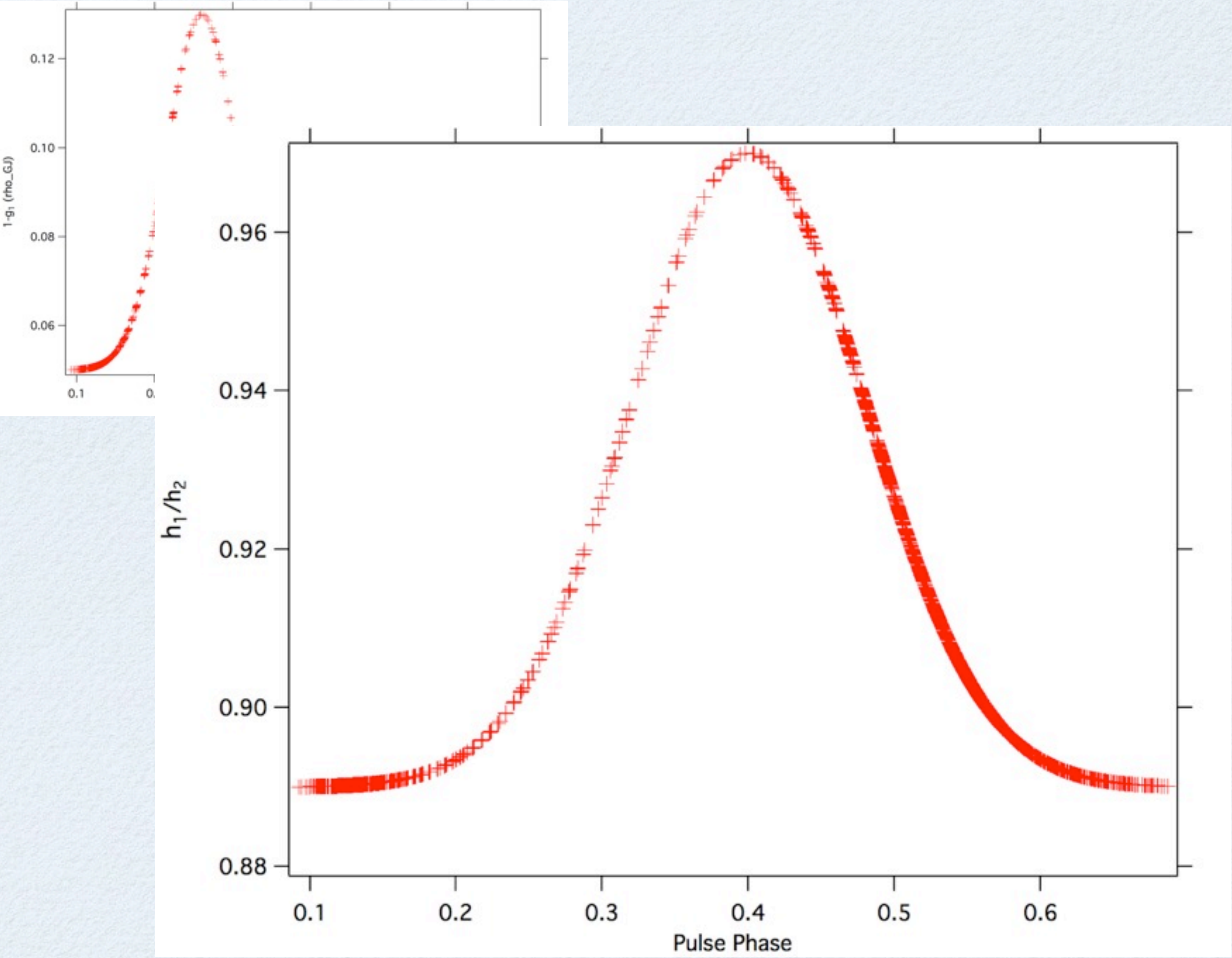

0.12
0.10
0.08
0.06
1-g1 (rho_GJ)
0.1
0.96
0.94
0.92
0.90
0.88
h1/h2
0.1
0.2
0.3
0.4
0.5
0.6
Pulse Phase

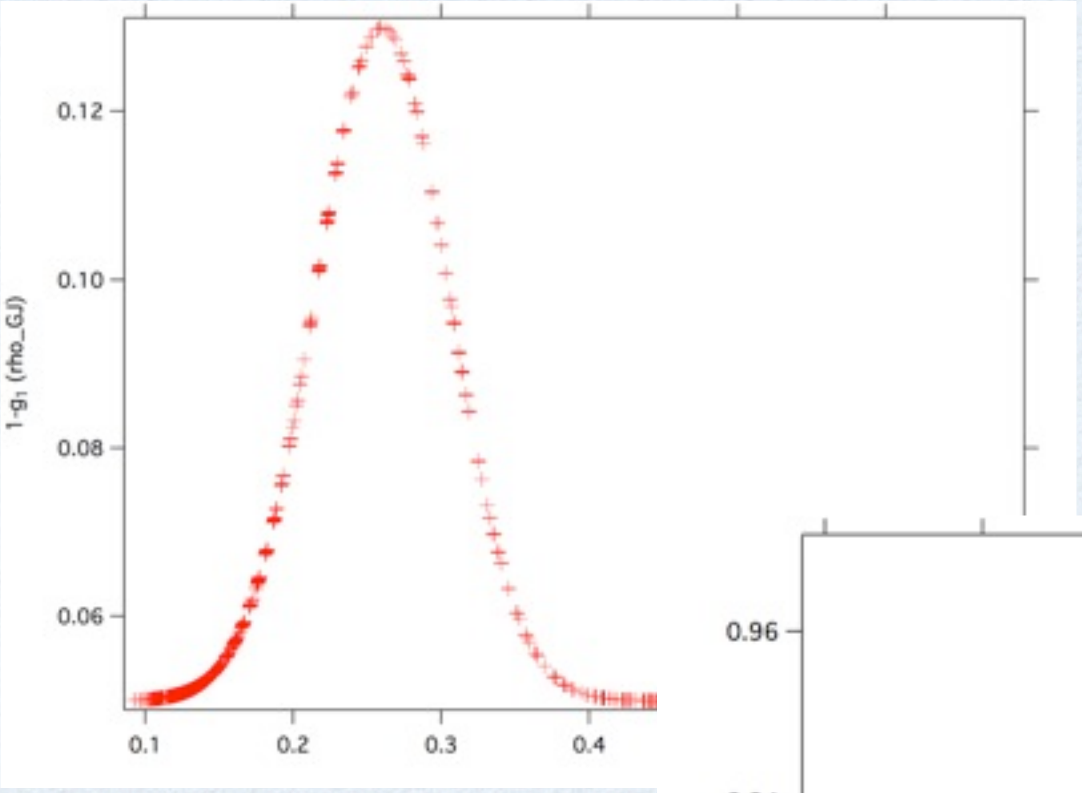

1-g1 (rho_GJ)
0.12
0.10
0.08
0.06
0.1
0.2
0.3
0.4

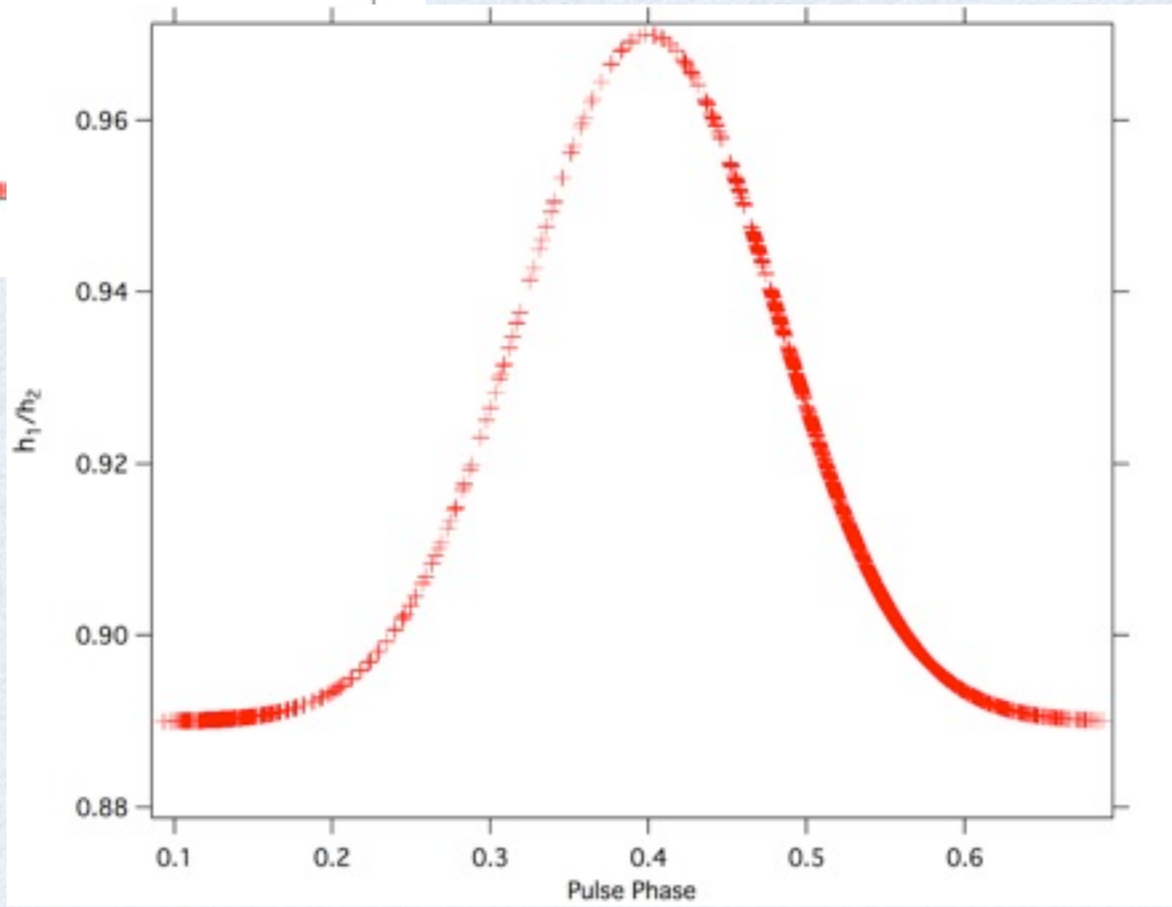

h1/h2
0.96
0.94
0.92
0.90
0.88
0.1
0.2
0.3
0.4
0.5
0.6
Pulse Phase

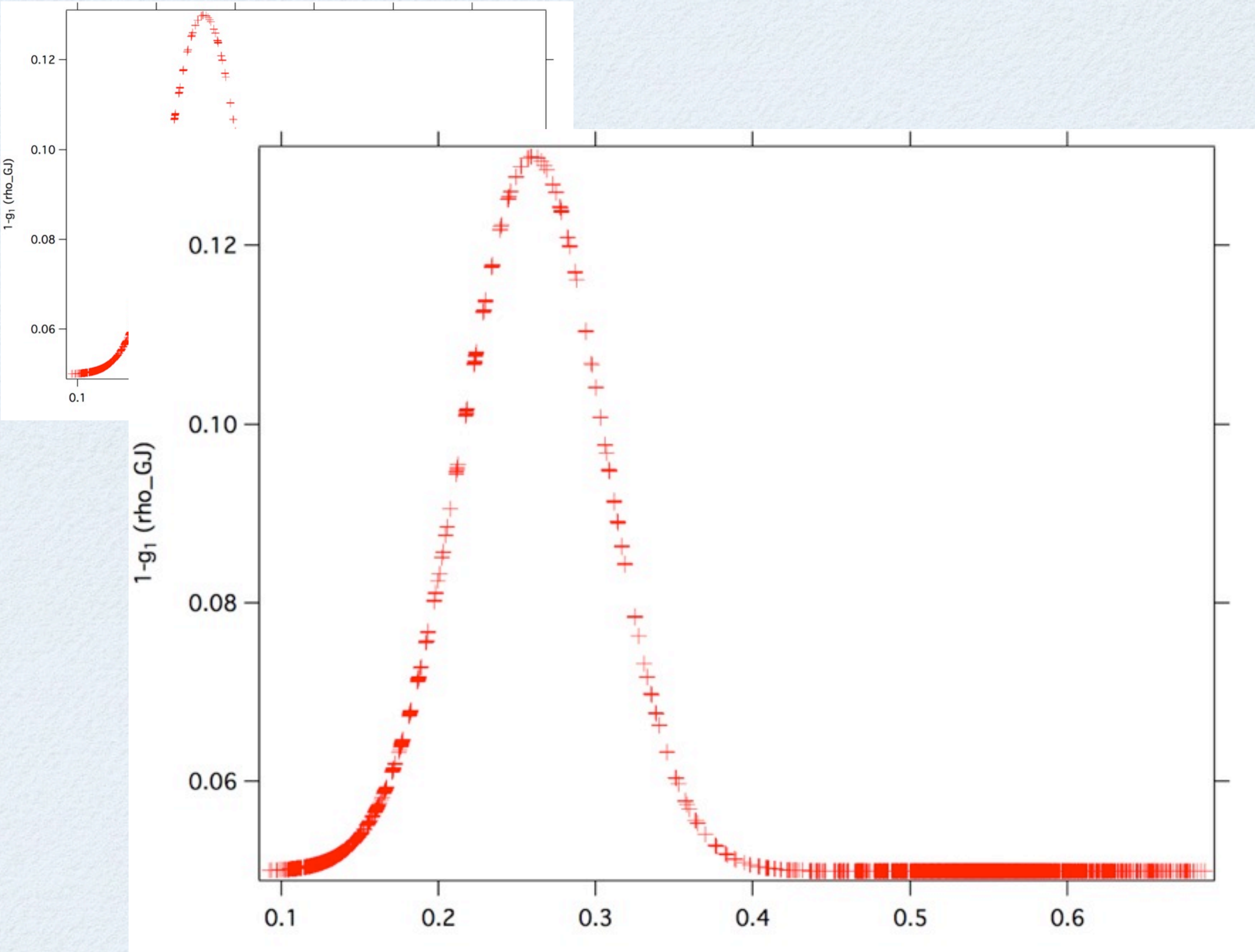

0.12
0.10
0.08
0.06
1-g₁ (rho_GJ)
0.1
0.2
0.3
0.4
0.5
0.6

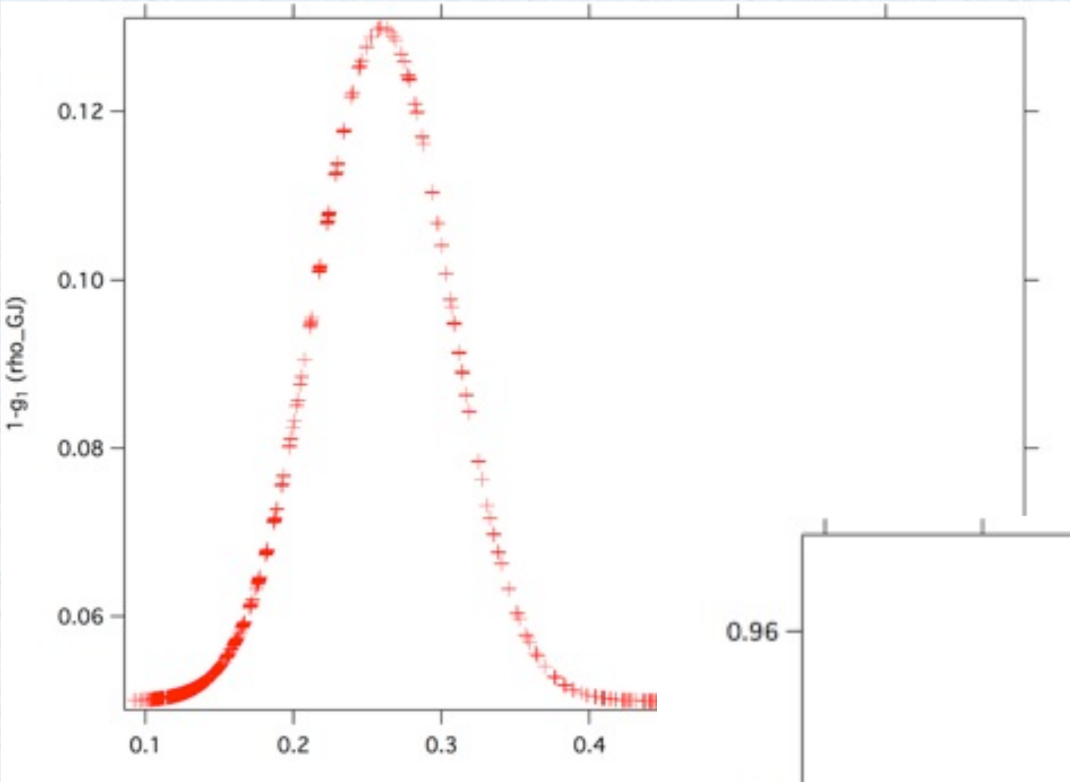
1-g1 (rho_GJ)
0.12
0.10
0.08
0.06
0.1
0.2
0.3
0.4

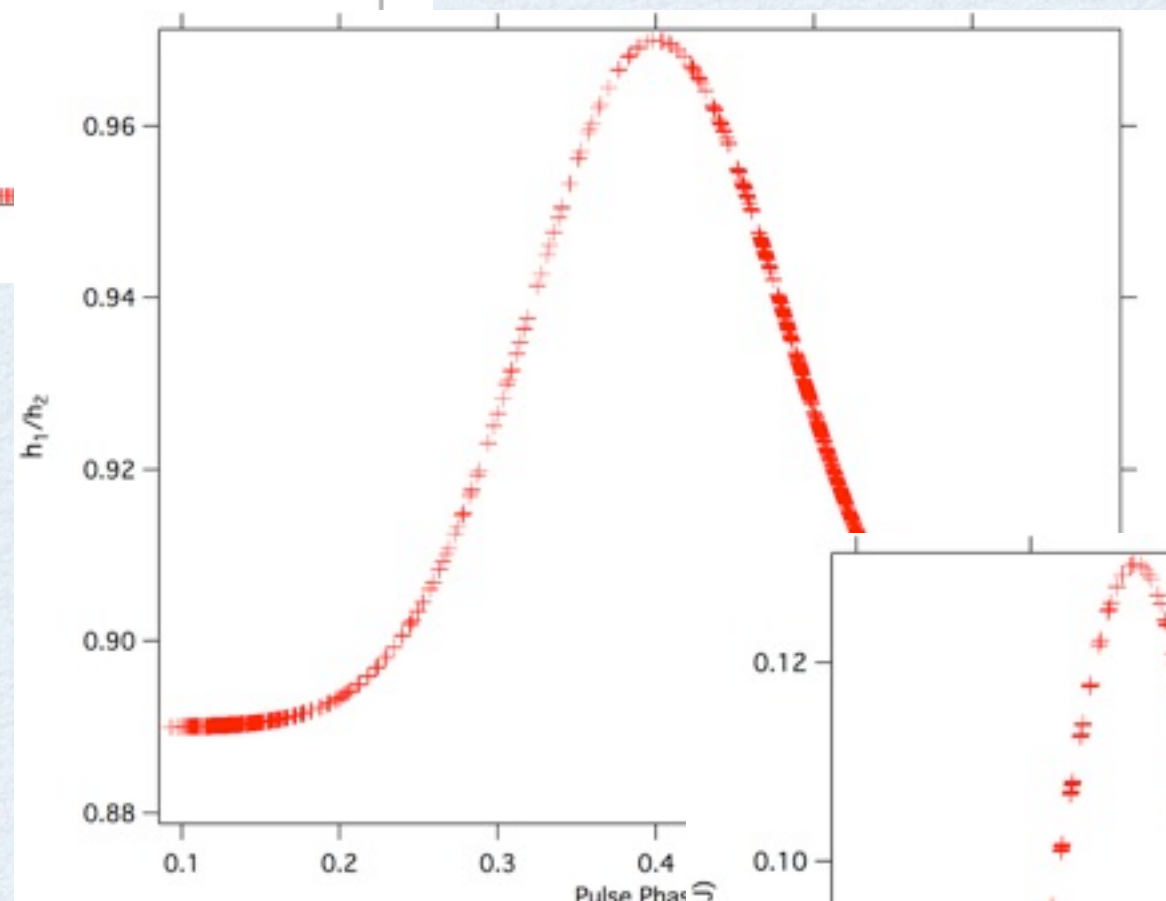
h1/h2
0.96
0.94
0.92
0.90
0.88
0.1
0.2
0.3
0.4
Pulse Phas

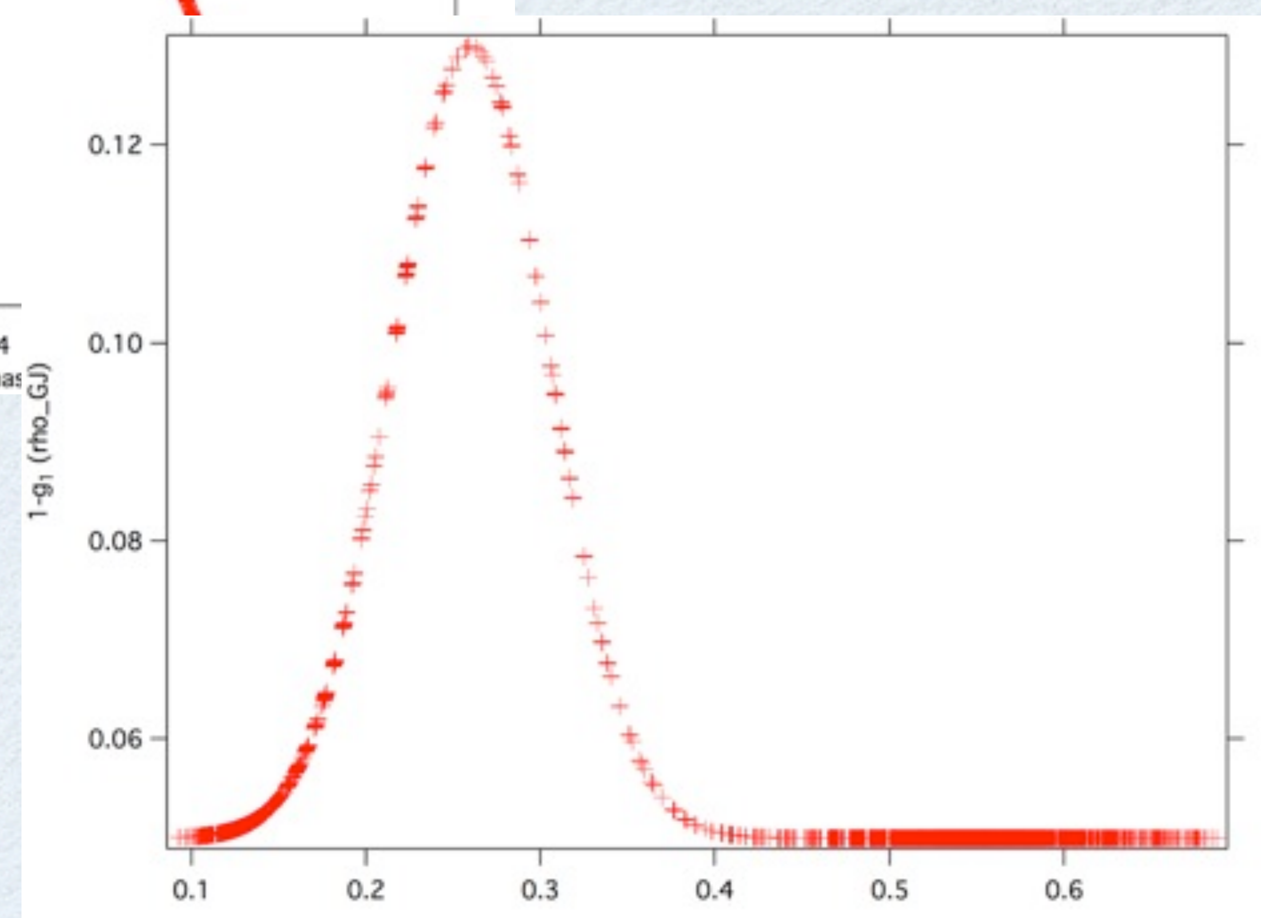
1-g1 (rho_GJ)
0.12
0.10
0.08
0.06
0.1
0.2
0.3
0.4
0.5
0.6

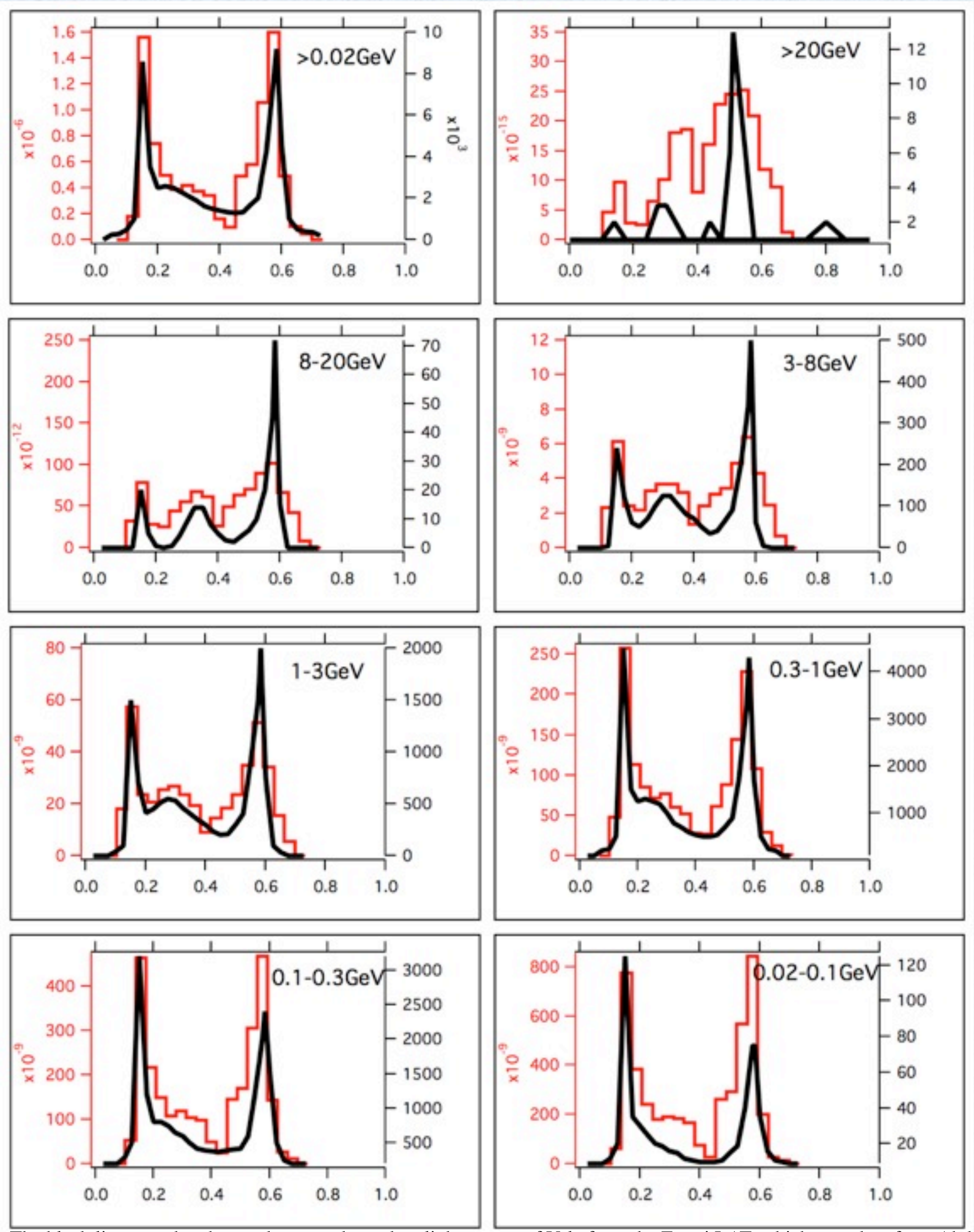

The black lines are the observed energy dependent light curves of Vela from the Fermi LAT, which are taken from Abdo et al. (2009)

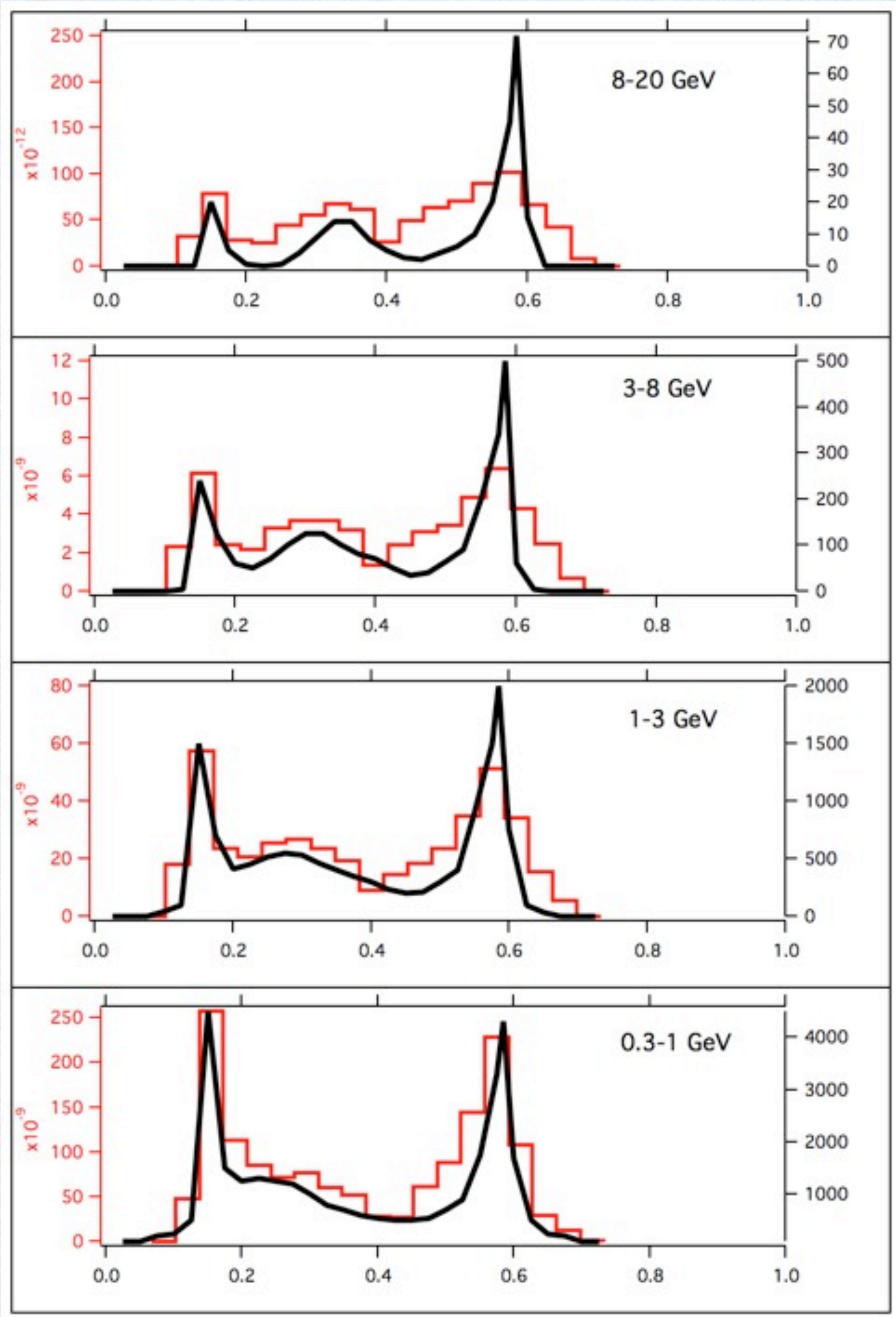

The black lines are the observed energy dependent light curves of Vela from the Fermi LAT, which are taken from Abdo et al. (2009)

The reason is clear:

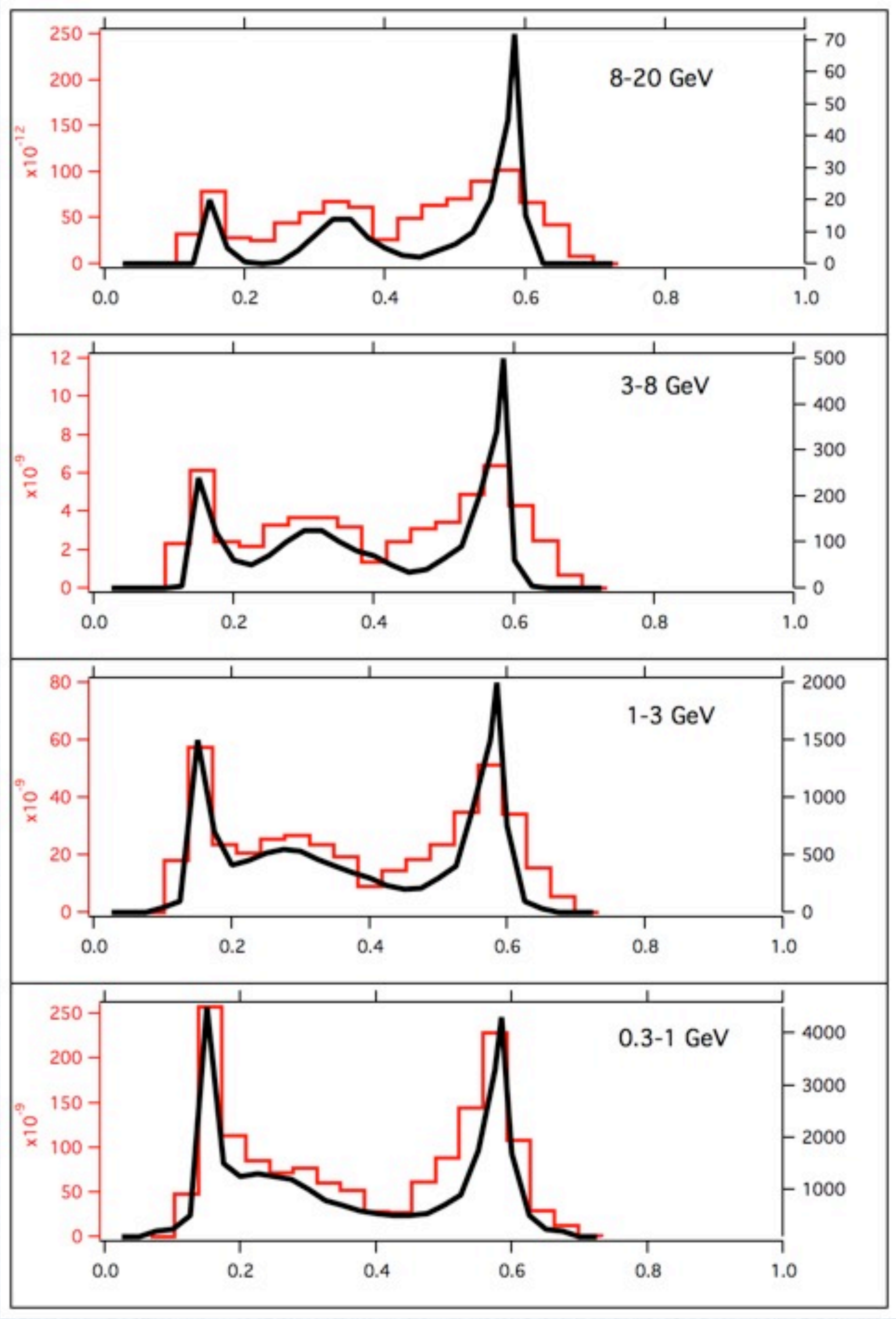

The black lines are the observed energy dependent light curves of Vela from the Fermi LAT, which are taken from Abdo et al. (2009)

The reason is clear:

The Peak3 is a combination of two peaks: a peak caused by the distribution of current and a peak caused by the distribution of the “f”.

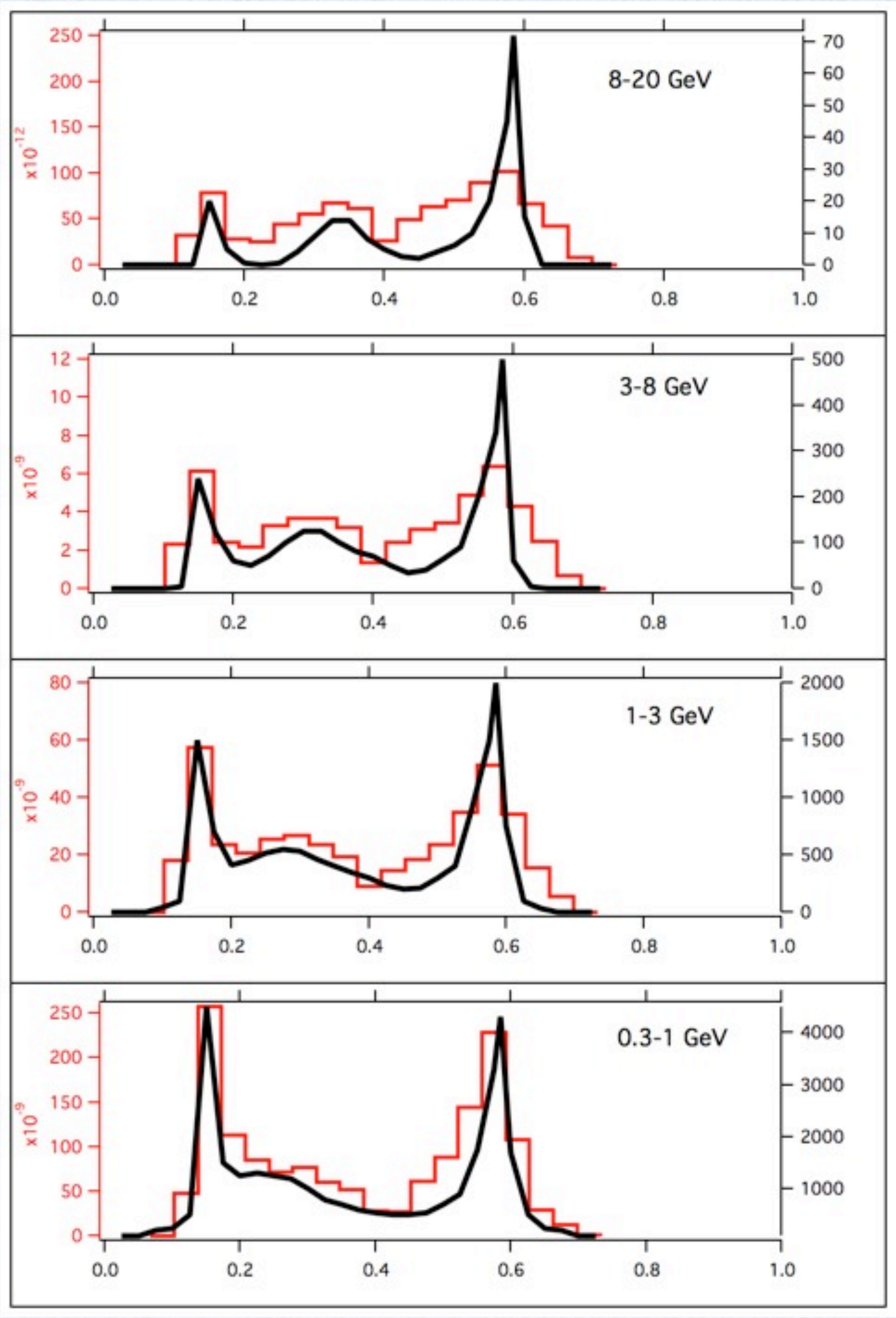

The black lines are the observed energy dependent light curves of Vela from the Fermi LAT, which are taken from Abdo et al. (2009)

The reason is clear:

The Peak3 is a combination of two peaks: a peak caused by the distribution of current and a peak caused by the distribution of the “f”.

The two peaks are at different places.

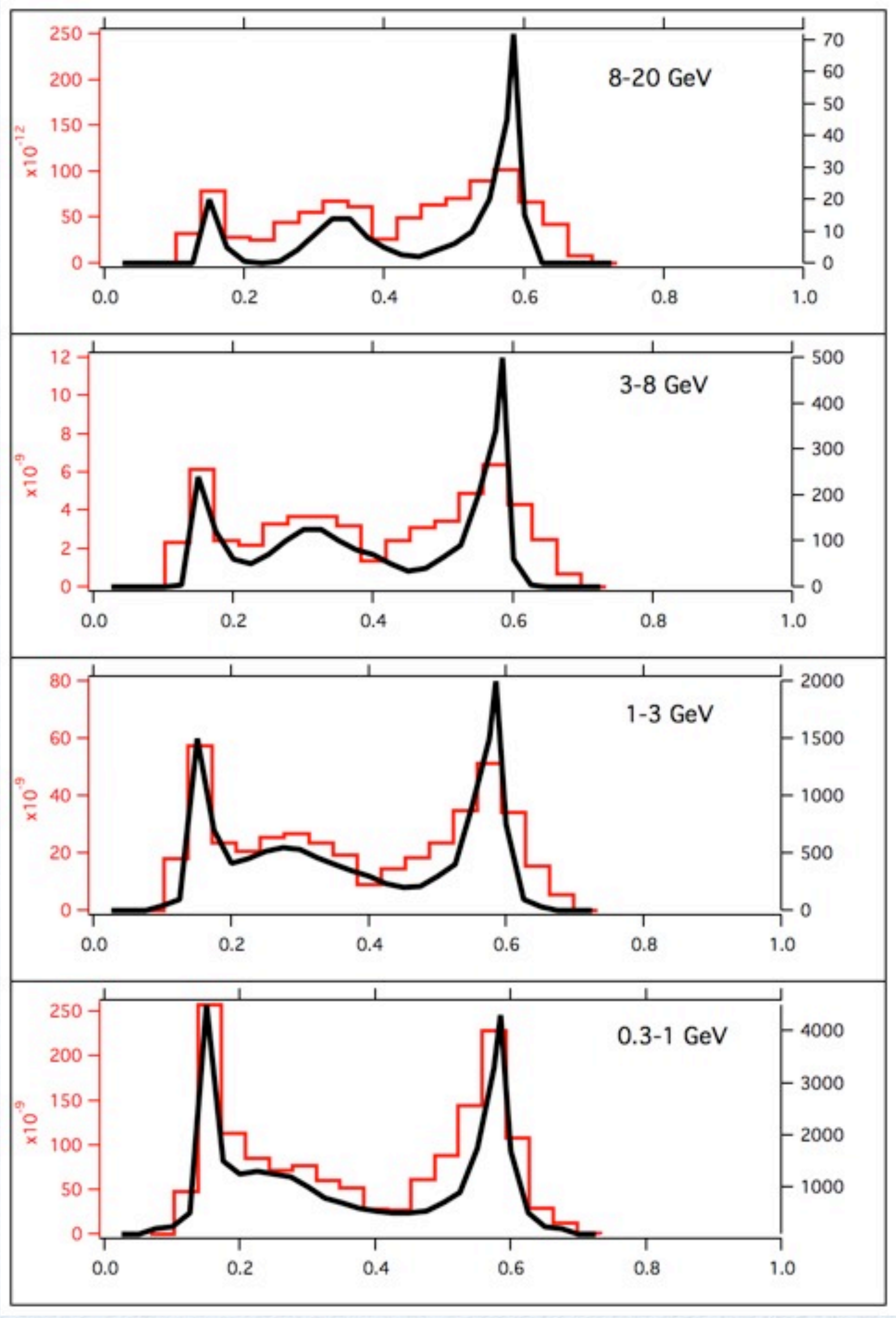

The black lines are the observed energy dependent light curves of Vela from the Fermi LAT, which are taken from Abdo et al. (2009)

The reason is clear:

The Peak3 is a combination of two peaks: a peak caused by the distribution of current and a peak caused by the distribution of the "f".

The two peaks are at different places.

As the energy increases, the peak caused by the "f" becomes more important than that caused by the distribution of the current.

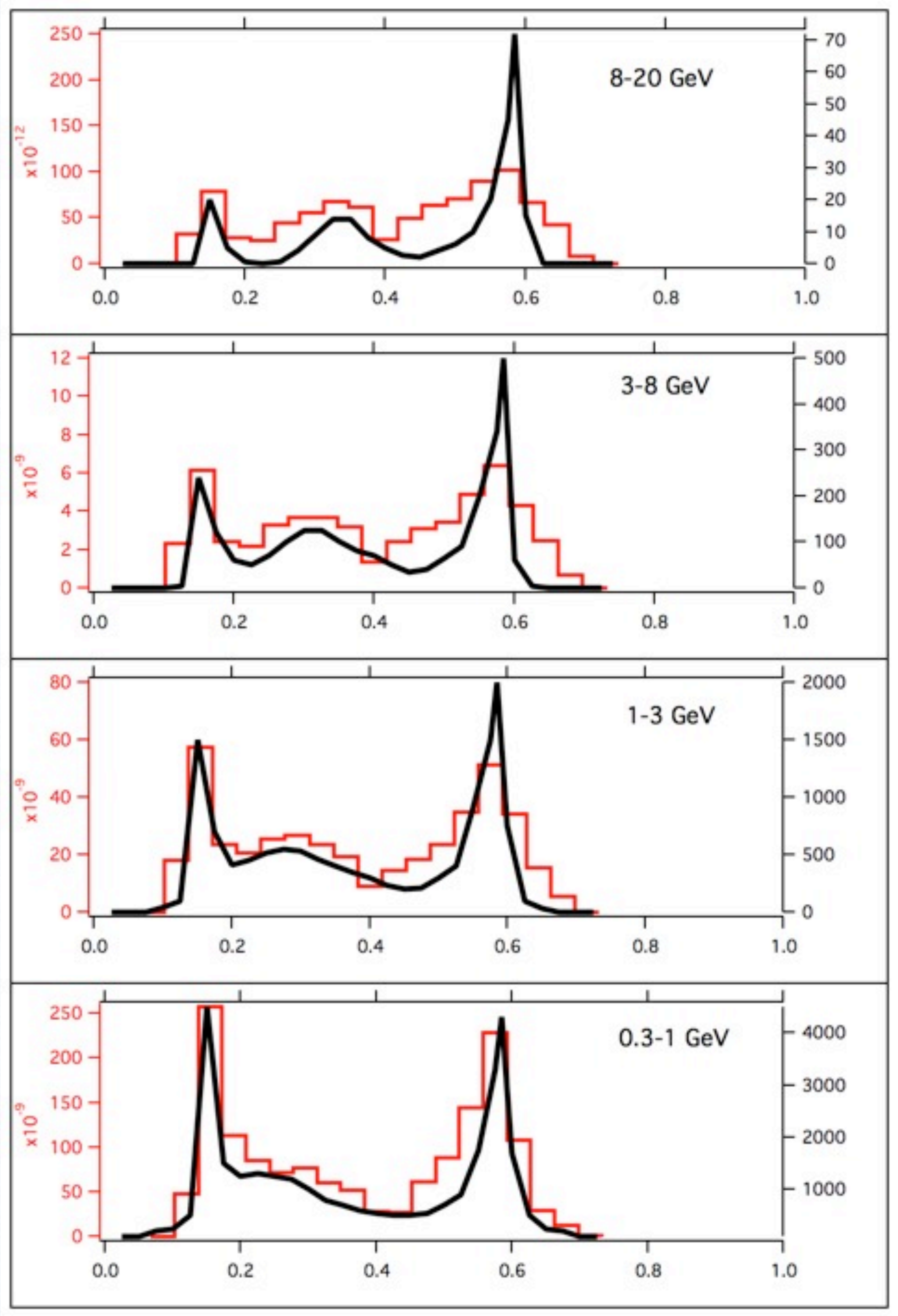

The black lines are the observed energy dependent light curves of Vela from the Fermi LAT, which are taken from Abdo et al. (2009)

The reason is clear:

The Peak3 is a combination of two peaks: a peak caused by the distribution of current and a peak caused by the distribution of the “f”.

The two peaks are at different places.

As the energy increases, the peak caused by the “f” becomes more important than that caused by the distribution of the current.

The the Peak3 moves.

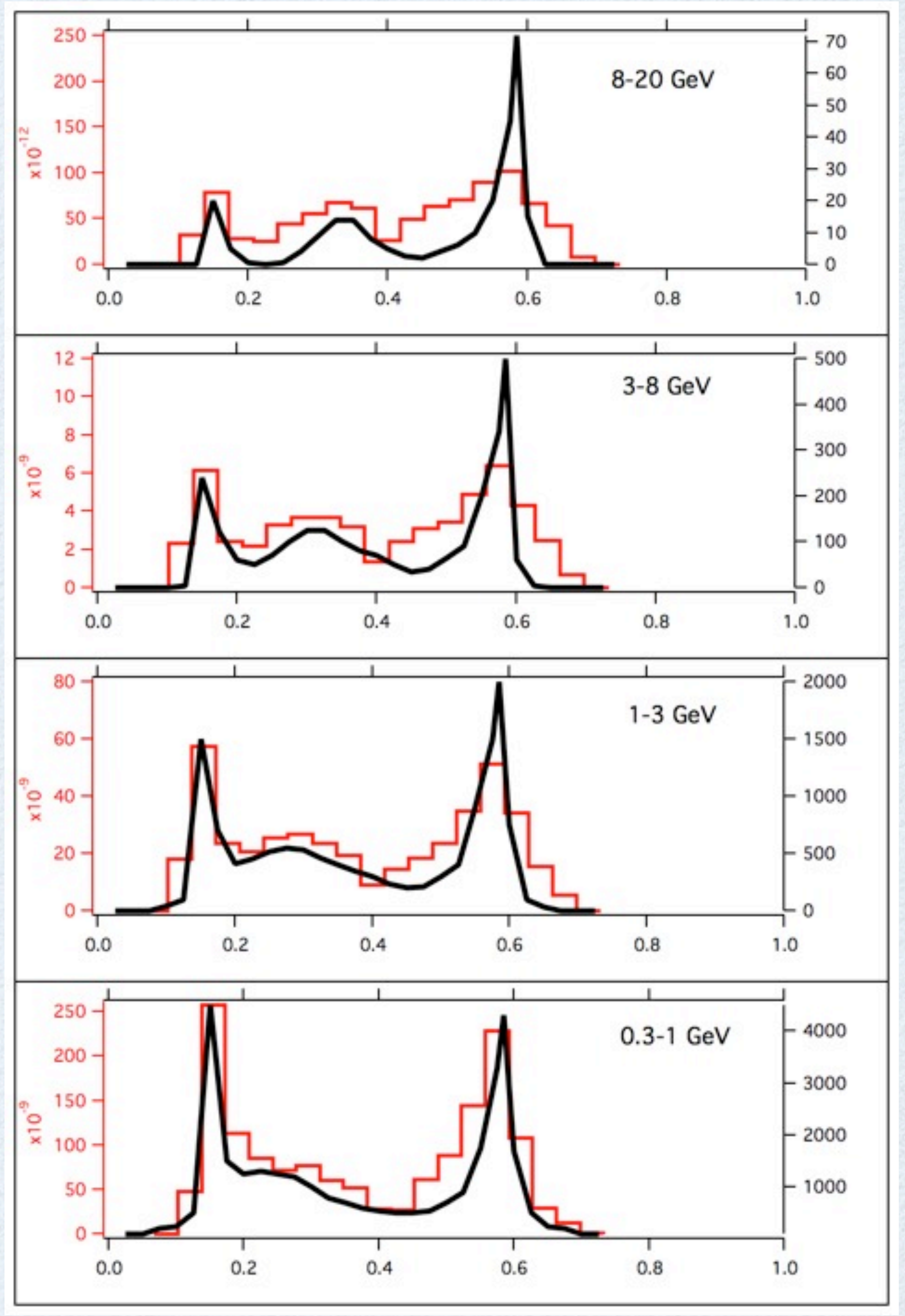

The black lines are the observed energy dependent light curves of Vela from the Fermi LAT, which are taken from Abdo et al. (2009)

Summary

SUMMARY

1. In the magnetic pair creation controlled outer gap model, the main source of the pairs, which screen out the accelerating electric field in the gap, are created near the stellar surface by the strong multipole magnetic field.

SUMMARY

1. In the magnetic pair creation controlled outer gap model, the main source of the pairs, which screen out the accelerating electric field in the gap, are created near the stellar surface by the strong multipole magnetic field.

2. The two-layer model, which is a simplification of the magnetic pair creation controlled outer gap model , can be used to fit most of the phase-averaged spectra of the gamma-ray pulsars observed by Fermi-LAT.

SUMMARY

1. In the magnetic pair creation controlled outer gap model, the main source of the pairs, which screen out the accelerating electric field in the gap, are created near the stellar surface by the strong multipole magnetic field.

2. The two-layer model, which is a simplification of the magnetic pair creation controlled outer gap model , can be used to fit most of the phase-averaged spectra of the gamma-ray pulsars observed by Fermi-LAT.

3. The 3-D model, which is an extension of the two-layer model to a 3-D field structure, can explain the energy-dependent light curves of the Vela Pulsar. But some distributions are necessary.

SUMMARY

1. In the magnetic pair creation controlled outer gap model, the main source of the pairs, which screen out the accelerating electric field in the gap, are created near the stellar surface by the strong multipole magnetic field.

2. The two-layer model, which is a simplification of the magnetic pair creation controlled outer gap model , can be used to fit most of the phase-averaged spectra of the gamma-ray pulsars observed by Fermi-LAT.

3. The 3-D model, which is an extension of the two-layer model to a 3-D field structure, can explain the energy-dependent light curves of the Vela Pulsar. But some distributions are necessary.

4. The third peak of Vela cannot be provided by the structure of the magnetic field lines, it is caused by the distributions of the current and the thickness of the gap in the outer gap.

Thank you!